Title
Plants on the move: the biogeography of dispersal and persistence under climate change

Author
Kling, Matthew

Publication Date
2020

Peer reviewed|Thesis/dissertation

Plants on the move:
the biogeography of dispersal and persistence under climate change

by

Matthew M. Kling

A dissertation submitted in partial satisfaction of the

requirements for the degree of

Doctor of Philosophy

in

Integrative Biology

in the

Graduate Division

of the

University of California, Berkeley

Committee in charge:

Professor David Ackerly, Chair
Professor Paul Fine
Professor Ian Wang

Summer 2020

Plants on the move:
the biogeography of dispersal and persistence under climate change

Abstract

Plants on the move:
the biogeography of dispersal and persistence under climate change

by

Matthew M. Kling

Doctor of Philosophy in Integrative Biology

University of California, Berkeley

Professor David Ackerly, Chair

This dissertation explores how climate shapes plant biogeography, and the implications for plant vulnerability in the face of ongoing climate change. Climate structures plant biodiversity patterns across biotic scales ranging from genes to species to biomes, not only by influencing plant physiology and its many downstream effects, but also by influencing plant movement through the transport of seeds, pollen, and spores by wind. Understanding these phenomena is a core goal in plant ecology, and has become an increasingly urgent societal priority as accelerating anthropogenic climate change threatens biodiversity and ecosystem services across the world. Focusing on large spatial scales, this dissertation research investigates three connected facets of climate biogeography. The three chapters proceed down a hierarchy of concepts, each focusing more narrowly and deeply on one aspect of the preceding chapter; the focal level of biotic organization narrows in tandem, beginning with a study of vegetation formations in the first chapter and ending with an analysis of genetic loci in the third. Chapter 1 begins broadly, developing a framework for integrating three previously separate paradigms of ecological vulnerability to climate change, and using this framework in a large-scale spatial analysis of vegetation vulnerability across the western US. Chapter 2 focuses on one of these three paradigms, spatial novelty, which addresses dispersal limitation under climate change. Many plant species disperse by wind, and this new conceptual and modeling work provides the first global assessment of how wind patterns may shape range shifts and gene flow as climate warms. In chapter 3, this focus on wind dispersal is further narrowed to an investigation of wind's role in shaping landscape genetic patterns in trees. This study reanalyzes population genetic data from more than a hundred tree species worldwide using the wind connectivity models developed in chapter 2, and shows for the first time that wind shapes directional gene flow, genetic differentiation, and genetic diversity. In sum, these analyses each advance our understanding of how climate influences basic spatial ecology, while also developing concepts and tools that may help land managers and conservation practitioners hone strategies for adaptation to global environmental change.

To my four grandparents, for bringing me home into the wild,
and to my two dogs, for bringing the wild into my home.

Contents

List of Figures

List of Tables

Acknowledgments

Neither this dissertation research, nor my own personal growth and fulfillment over these years or indeed my sanity (such that it is), would have been be possible without the support of many wonderful people. I am grateful to my advisor David Ackerly for always pushing me to produce science with more integrity and relevance, for giving me the trust and freedom pursue the research questions that motivated me, and for cultivating such an intellectually engaging and supportive lab community. I am grateful to every member of the Ackerly lab with whom I had the real pleasure of sharing this time, for their insight and skepticism and levity. I am grateful to the many generous and inspiring senior scientists I was fortunate to connect with in ways that substantively shaped my PhD research and enriched my academic experience—collaborators, mentors, committee members, and teachers including Bruce Baldwin, Steve Beissinger, Carl Boettiger, Paul Fine, Patrick Gonzalez, Healy Hamilton, Lara Keuppers, Brent Mishler, Wayne Sousa, Perry de Valpine, Ian Wang, and Caroline Williams, among others. I am grateful to the amazing undergraduate student apprentices Hudson Northrop and Yiwen Shi for their tireless work advancing my research over multiple semesters and for their patience with my learning curve as a supervisor. I am grateful to the anonymous souls at the National Science Foundation and the Berkeley Graduate School who in leaps of faith provided the generous fellowship funding that supported me as a PhD student. I am grateful for the unreasonably good fortune that has given me a lifelong series of opportunities that countless equally deserving but less privileged people never had. I am grateful to my family and friends for inspiring and supporting me along the way. And above all I am grateful to my partner Zoë and our son Wylie, whose mindfulness and humanity propelled me forward, kept me from straying too far into the weeds, and reminded me daily what is important in life.

Introduction

Plants are on the move. Driven by accelerating rates of contemporary climate change and other human environmental modifications, shifts in the geographic distribution of biodiversity at every level, from genes to species to biomes, are becoming pervasive (Parmesan & Yohe, 2003; Scheffers et al., 2016; Wiens, 2016). There is broad agreement that the global biodiversity landscape will look dramatically different in a century's time, but much less agreement on the ways in which those differences will manifest. To date, available models explain only a small fraction of the variation in observed biogeographic responses to climate change (Buckley & Kingsolver, 2012; Rumpf et al., 2019). There is much room for improvement in our understanding of the spatial ecology of climate change, and narrowing this uncertainty is important not just for basic science but for guiding applied efforts to manage and mitigate biodiversity loss. This dissertation explores a series of new concepts about how global climate dynamics shape large-scale biodiversity patterns in plants.

All biodiversity dynamics result from the interplay of four fundamental processes: mutation, selection, migration, and drift. The study of these processes and their interactions is the heart of disciplines across all of ecology and evolution (Vellend, 2020), including the field of global change biology. Global change biology in plants is shaped particularly strongly by selection and migration, which correspond to the two main ways that climate influences plants: by shaping fitness through its effects on plant physiology, and by shaping dispersal through wind transport of pollen and seeds.

Each of the three chapters in this dissertation examines a different aspect of the balance between selection and migration. Each study is focused on large-scale spatial ecology, and thus on higher-level patterns that emerge from fine-scale eco-evolutionary processes. While the spatial scale of all these studies is large, the three chapters span a range of conceptual scopes from broad to narrow, and a range of levels of biotic organization from biomes to genotypes.

Chapter 1 (Kling et al., 2020) focuses on three conceptual models—niche novelty, temporal novelty, and spatial novelty—that each make different assumptions about the relative importance of selection versus migration in shaping contemporary patterns of species distributions and their responses to climate change. These three paradigms have developed largely separately in the literature, and they are integrated and compared here for the first time in a framework for understanding how multidimensional novelty space shapes vulnerability to climate change. In a large spatial data analysis of roughly a hundred vegetation types across

the western United States, these three axes of climate novelty are shown to yield distinct predictions of vulnerability based on recent climate change patterns. It is proposed that considering these three novelty axes jointly could help to guide climate adaptation efforts by land managers, and could help to explain variation in observed ecological responses to climate change.

Chapter 2 (Kling & Ackerly, 2020) focuses more narrowly on one of these three paradigms, spatial novelty. The spatial novelty concept represents dispersal limitation under climate change. While migration of genes and species is an essential component of adaptation to climate change, most biogeographic forecasts of climate change vulnerability in plants focus entirely on selection landscapes using tools like climatic niche models, ignoring their interactions with migration landscapes. Many plants have seeds and pollen dispersed by wind, but few tools have been available to model spatially explicit wind migration landscapes. This study introduces a new method for using meteorological data to model migration potential via wind dispersal, and integrates it with data on future climate change to assess how wind patterns will affect the ability of wind-dispersed organisms in different places to track suitable conditions as climate warms. This analysis is one of the first to explore the potential implications of wind geography for patterns of dispersal limitation under climate change, and predicts that strong and distinct patterns in selection and migration landscapes will interact to shape the global redistribution of biodiversity over the next century.

Chapter 3 maintains this focus on wind, narrowing further in scope and scale to an investigation of how wind shapes landscape genetic patterns in trees. While wind plays a huge role in the movement of pollen and seeds in many trees, it is unknown whether and how it affects large-scale landscape genetic patterns. This new work aims to fill that gap, reanalyzing population genetic data from more than 100 tree species across the globe using the wind connectivity models developed in chapter 2. The results show that wind connectivity predicts patterns of directional gene flow, genetic differentiation, and genetic diversity. This study provides the first large-scale evidence of wind's role in landscape genetics, serves as an empirical validation of wind connectivity models, and highlights the potential importance of global wind patterns for the vulnerability of plants to ongoing climate change. It also highlights how wind dispersal shapes the balance between selection and migration, demonstrating that wind-dispersed and wind-pollinated species have higher rates of migration and lower levels of isolation by environment compared to species that rely on animal movement.

Chapter 1

Multiple axes of ecological vulnerability to climate change

This chapter is a reproduction of the following published manuscript, included here with the permission of my co-authors and in acknowledgement of their contributions to this research:

Kling MM, Auer SL, Comer PJ, Ackerly DD, & Hamilton H (2020). Multiple axes of ecological vulnerability to climate change. Global Change Biology 26:2798–2813. https://doi.org/10.1111/gcb.15008

1.1 Abstract

Observed ecological responses to climate change are highly individualistic across species and locations, and understanding the drivers of this variability is essential for management and conservation efforts. While it is clear that differences in exposure, sensitivity, and adaptive capacity all contribute to heterogeneity in climate change vulnerability, predicting these features at macroecological scales remains a critical challenge. We explore multiple drivers of heterogeneous vulnerability across the distributions of 96 vegetation types of the ecologically diverse western US, using data on observed climate trends from 1948 to 2014 to highlight emerging patterns of change. We ask three novel questions about factors potentially shaping vulnerability across the region: (a) How does sensitivity to different climate variables vary geographically and across vegetation classes? (b) How do multivariate climate exposure patterns interact with these sensitivities to shape vulnerability patterns? (c) How different are these vulnerability patterns according to three widely implemented vulnerability paradigms—niche novelty (decline in modeled suitability), temporal novelty (standardized

anomaly), and spatial novelty (inbound climate velocity)—each of which uses a distinct frame of reference to quantify climate departure? We propose that considering these three novelty paradigms in combination could help improve our understanding and prediction of heterogeneous climate change responses, and we discuss the distinct climate adaptation strategies connected with different combinations of high and low novelty across the three metrics. Our results reveal a diverse mosaic of climate change vulnerability signatures across the region's plant communities. Each of the above factors contributes strongly to this heterogeneity: climate variable sensitivity exhibits clear patterns across vegetation types, multivariate climate change data reveal highly diverse exposure signatures across locations, and the three novelty paradigms diverge widely in their climate change vulnerability predictions. Together, these results shed light on potential drivers of individualistic climate change responses and may help to inform effective management strategies.

1.2 Introduction

Biotic responses to climate change are characterized as much by their individuality as by their generality. Contemporary and paleoecological records show that the impacts of changing climate are widespread but highly varied, with novel ecological communities emerging as species range edges expand and contract individualistically in direction and degree (Jackson & Overpeck, 2000; Nolan et al., 2018; Rapacciuolo et al., 2014). These realities present both a puzzle to ecological understanding and a grave challenge to future resource management, which requires scientifically sound vulnerability predictions to guide local and regional climate change adaptation efforts. Improving our understanding of the many factors that underlie this variation is an important priority. Here we use terrestrial vegetation types of the western US as a case study to explore several layers of spatial and ecological variation that underlie emerging patterns of vulnerability to climate change over recent decades.

Climate change vulnerability is defined as the degree of threat to a population, species, or ecosystem in response to changing climate, and differences in vulnerability across systems are often conceived of as resulting from their differing levels of exposure, sensitivity, and adaptive capacity (Dawson et al., 2011). Developed originally to describe climate vulnerability of human systems, this framework has now been widely applied in the ecological realm, though operational definitions and metrics for the three components have been inconsistent across studies. Similarly to prior studies (Dawson et al., 2011), we define exposure as the magnitude of extrinsic change in climate itself, sensitivity as the amount of detrimental change that will result from a given amount of exposure, and adaptive capacity as the intrinsic ability of an individual, population, or ecosystem to naturally reorganize without collapse and maintain function given particular levels of exposure and sensitivity. While obtaining detailed measurements of these vulnerability components is infeasible at the macroecological scales needed for applications such as regional conservation planning, recent studies have begun to explore how proxies for these components may explain the variability in observed climate change impacts across species. Species-level ecological or phylogenetic traits offer one category of

proxies: range shifts have been found in some systems to correlate with sensitivity-related traits such as ecological generalization (Angert et al., 2011), adaptive capacity-related life history traits connected to growth, reproduction, and dispersal (Beever et al., 2016; Lenoir et al., 2008; Wolf et al., 2016), and phylogenetic relationships that likely capture covariance among many such traits (Willis et al., 2008). But meta-analyses have repeatedly found that these ecological and taxonomic traits have low explanatory power, accounting for at best a small proportion of the observed variation in recent climate change responses (Buckley & Kingsolver, 2012; MacLean & Beissinger, 2017; Rapacciuolo et al., 2014; Wiens, 2016).

Ecological responses have also been shown to correlate with exposure, though most studies have focused on changes in individual climate variables such as mean annual temperature, which tends to significantly but only weakly predict observed shifts in species distributions (Rumpf et al., 2019). Recent work has noted the likely importance of concurrent but differing changes in multiple climate variables in driving geographic variation in ecological responses (Dobrowski et al., 2013; Hamann et al., 2015; Nadeau & Fuller, 2015; Rapacciuolo et al., 2014). If climate variables exhibit different spatial patterns of change, then biogeographic responses have the potential to be complex, with species shifting in different directions and non-analog communities emerging (Jackson & Overpeck, 2000; Ordonez et al., 2016; Tingley et al., 2012). This will be particularly true if species differ in the variables to which they are most sensitive.

Biogeographic patterns of climate sensitivity have, like exposure, been studied primarily in a univariate context focused on temperature. Temperature sensitivity patterns are thought to underlie fundamental biogeographic patterns such as the latitudinal range size gradient (Ghalambor et al., 2006) and predicted to strongly shape patterns of vulnerability to contemporary climate change (Dillon et al., 2010; Tewksbury et al., 2008). But since climate change exposure clearly encompasses much more than mean temperatures, a broader, multivariate understanding of sensitivity to different aspects of climate is essential to predicting vulnerability. While it is common practice in species distribution modeling to evaluate variable importance, this is typically done on a case-by-case basis. Patterns of multivariate climate variable importance at a macroecological scale have remained largely unexplored. Several recent studies have begun to address this gap (Barbet-Massin & Jetz, 2014; Bradie & Leung, 2017; Schuetz et al., 2019), though few have explored potential trends in variable importance among locations, environments, or biomes. In this study, we quantify patterns of climate variable importance across vegetation types and across spatial and climatic gradients, and assess how these sensitivities intersect with patterns of multivariate climate exposure to shape predicted vulnerability at landscape to regional scales.

Beyond geographic patterns of climate exposure and biotic patterns of sensitivity to those variables, a third consideration is that geographies and biotas may experience different dimensions of climate novelty. The literature is full of indices used to estimate ecological vulnerability from multivariate climate exposure patterns, including climatic niche modeling (Elith & Leathwick, 2009), climate change velocity (Hamann et al., 2015; Loarie et al., 2009), standardized anomalies (Mahony & Cannon, 2018; "Projected distributions of novel and disappearing climates by 2100 AD", n.d.), expanding and contracting climates (D. Ackerly

et al., 2010), and numerous others (Garcia et al., 2014). We argue that most of these approaches relate to one of three basic vulnerability paradigms—the 'niche', 'temporal', and 'spatial' paradigms—each of which provides one answer to the question of how novel a new climate regime is to the group of organisms living at a given site. (Note that the term 'novel climate' has sometimes been used in narrower reference to spatiotemporal climate novelty metrics (Mahony et al., 2017; "Projected distributions of novel and disappearing climates by 2100 AD", n.d.), which are not neatly categorized in this framework since they combine two of the three novelty paradigms in a single index.) Each of these three novelty paradigms takes the same climate exposure value (difference in climate between two time periods) and combines it with a different proxy for sensitivity and/or adaptive capacity to generate a distinct estimate of vulnerability (Figure 1.1), as detailed below. Our terms for the three paradigms refer to these distinct proxies, though all are of course 'temporal' in relating to climate change over time.

The niche novelty paradigm predicts high vulnerability to conditions that are outside the range of long-term average climates across the geographic distribution of a focal species or ecosystem type, employing space-for-time substitution to predict local responses to climate change (Figure 1.1a). This ecological niche modeling approach has been widely applied both to species (Elith & Leathwick, 2009) and to vegetation types (D. D. Ackerly et al., 2015; Comer et al., 2013; Thorne et al., 2016; Thorne et al., 2018). It hinges on the assumption that populations of a 'species' or plant communities of a vegetation 'type' share a niche if they share a name, as well as the assumption that realized climatic niches reflect fundamental climatic niches. These assumptions are often violated by ecological realities such as local adaptation, dispersal limitation, spatially non-stationary biotic interactions, soil specialization, and rare historical climate events that have shaped geographic distributions. Empirical challenges such as limitation and bias in the quantity, accuracy, and scale of spatial biological and environmental data further strain the ability of climate niche models to accurately reflect climate change vulnerability. It is thus unsurprising that niche models often fail to predict observed biotic responses to climate change—or perhaps more generously, surprising that they succeed as often as they do. Challenging at the species level, niche models present additional problems at the scale of communities like vegetation types whose ecology may be determined less by classical species niche evolution than by the contingent intersections of individual species.

The temporal novelty paradigm instead predicts high vulnerability to conditions that are outside the range of local year-to-year climate variability at the focal site (Figure 1.1b), a proxy for the known survived experience of local populations (Klausmeyer et al., 2011; "Projected distributions of novel and disappearing climates by 2100 AD", n.d.). Temporal novelty assumes that the climatic tolerance of a local biota is connected to local historical temporal variability in climate, with ecological and evolutionary processes in sites with high climate variability selecting for species and genotypes with broader individual or collective tolerances. High temporal variability could select for resilient individuals in long-lived species, and for adaptive genetic variation in populations of short-lived species. Connections between climate variability and tolerance have roots in long-standing macroecological

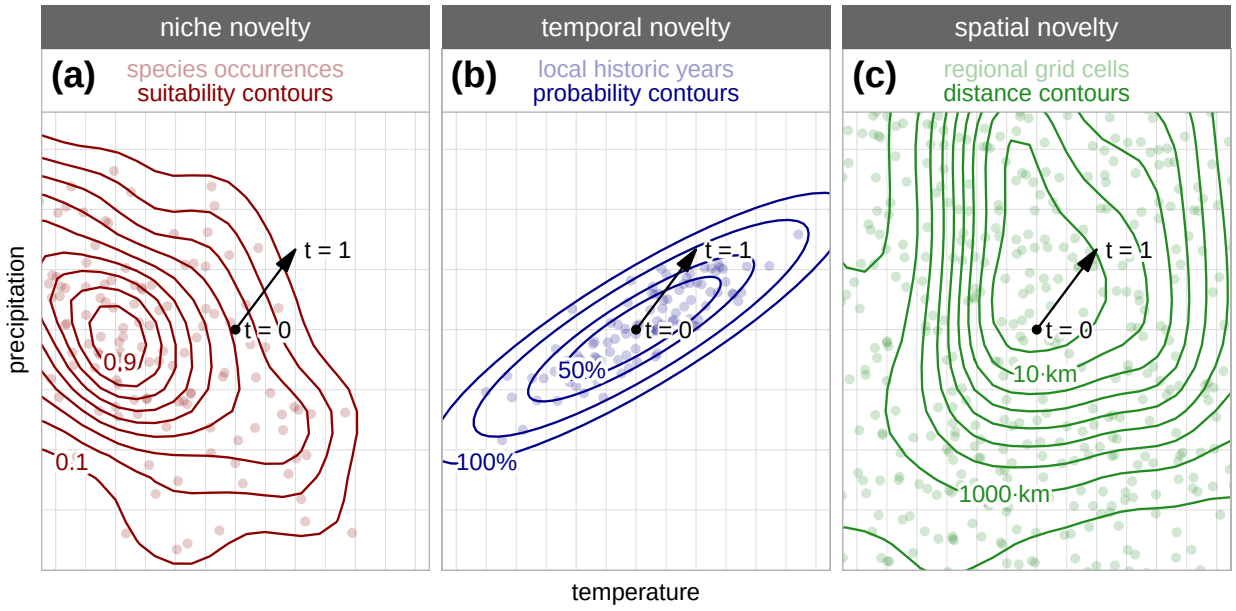

Figure 1.1: Conceptual diagram of the three dimensions of climate novelty explored in this paper, illustrated for a single focal site for two climate variables. The site has a historic mean climate (t = 0) that shifts as climate changes (t = 1), defining an exposure vector in multivariate climate space (black arrow). While the climate axes and climate exposure vector are identical across the three novelty metrics, each novelty paradigm evaluates this exposure against a different reference probability distribution (colored points). These distributions represent proxies for sensitivity and/or adaptive capacity, and each generates a distinct assessment of climate change vulnerability (contour lines) that increases as climate moves away from the center of the distribution. (a) The niche paradigm uses mean historic climates across all occurrences of a species or vegetation type to define suitability, and measures novelty as the decrease in suitability with climate change. (b) The temporal paradigm defines novelty as the degree of departure from year-to-year historic climate variability at the site, which we quantify as a Mahalanobis distance percentile. (c) The spatial paradigm defines novelty as the geographic distance to locations with historic climates similar to the site's new climate, which we quantify using inbound climate velocity. The three reference distributions, the exposure vector, and the most appropriate climate axes will differ across sites and across focal taxa or ecosystems, yielding different combinations of high and low vulnerability values across the three metrics; each of these drivers of predicted vulnerability patterns is explored in this paper.

hypotheses such as Janzen's treatise on high tropical mountain passes (Janzen, 1967) and Rapoport's rule about latitudinal gradients in niche breadth (Stevens, 1989), and have gained renewed attention in recent work on climate change vulnerability (Klausmeyer et al., 2011; Li et al., 2018; Mahony & Cannon, 2018; Mora et al., 2013; Sandel et al., 2011; Tewksbury et al., 2008). In cases where it is suspected that local adaptation, extreme climate events, or range limitation by non-climatic factors are important, or where the idea of an evolutionarily coherent climatic niche seems inappropriate due to the nature of the focal system, local historic variability may provide a better proxy for sensitivity than do range-wide niche models.

Finally, the spatial novelty paradigm predicts high vulnerability to conditions that are outside the range of historic mean climates across locations in the geographic region around the focal site (Figure 1.1c) (Hamann et al., 2015), emphasizing an aspect of vulnerability more connected to adaptive capacity than to sensitivity. The ability of a local population or ecosystem to maintain function through reorganization (i.e., its adaptive capacity) will depend in many systems on the rate of arrival of novel genes or species better suited to the new climate regime, replacing those with declining fitness *in situ* (Beever et al., 2016). This adaptive genetic and community turnover will, in turn, depend on the proximity of source areas with suitable migrants; when climate warms, sites that are close to historically warmer areas will be more likely than sites isolated from warmer areas to receive new genes and species that are evolutionarily adapted to the new climate. A full characterization of propagule availability and adaptive gene flow would be a function of the frequency distributions of climate conditions at increasing distances from a focal site, together with the dispersal capacity of the organisms. This can be approximated with backward climate velocity (Hamann et al., 2015), which measures the distance from a site to the nearest location with a historic climate similar to the site's new climate. Rather than 'backward' and 'forward' velocity, here we use the terms 'inbound' and 'outbound' velocity, which we believe are more intuitive and will facilitate future discussion.

Given their distinct approaches, each of these novelty paradigms potentially has an important place in holistic vulnerability assessments at the macroecological scale, and each approach will have strengths and weaknesses for particular study systems. While each metric will predict higher vulnerability given higher exposure, these vulnerability magnitudes also have the potential to differ substantially. However, it remains largely unexplored how they compare empirically in terms of vulnerability patterns across landscapes and ecosystem types (though see Garcia et al. (2016) for a study on African vertebrates). If these alternative novelty metrics are positively correlated, as might be expected since all are based on the same strongly patterned climate exposure values, then their conceptual distinctions are unlikely to result in contrasting ecological patterns and they can be considered redundant in conservation applications. But if they diverge in their vulnerability estimates, then it raises important questions about what metrics to consider in which ecological contexts, and about what management strategies to pursue in relation to intersecting measures of climate novelty.

In this study, we address three broad questions about emerging patterns of vulnerabil-

ity to recent climate change across the distributions of 96 vegetation types covering more than two million square kilometers of relatively intact landscapes in the western US. (a) How does sensitivity to different climate variables, measured as predictive importance in distribution models, vary across vegetation types and geographic gradients? (b) How do these sensitivity patterns interact with multivariate climate change exposure patterns to shape predicted vulnerability across ecosystems in the region? (c) How correlated are niche, temporal, and spatial novelty dimensions, and what are the management implications for ecosystems considered to have different combinations of high and low vulnerability on these three axes?

1.3 Methods

Study area

Our study focused on terrestrial vegetation of the conterminous US west of 95°W longitude, an area selected for having high-quality data on vegetation and climate, a high degree of ecological diversity, and relatively high intactness of native vegetation. This region encompasses hot and cold desert shrublands, diverse grassland habitats, and forests ranging from coastal temperate rainforest to oak savannah to subalpine coniferous forest, as well as various important alpine, lowland, and substrate-driven sparsely vegetated types.

Vegetation data

Our analysis is based on the NatureServe Terrestrial Ecological Systems, a classification of 642 vegetation 'types' that have been extensively described and mapped at high resolution by resource managers in the conterminous US through a combination of remote sensing and extensive ground surveys (Comer et al., 2003; Gergely & McKerrow, 2013; Rollins, 2009) and widely used in ecological assessments (Aycrigg et al., 2013; Comer et al., 2013; Thorne et al., 2018). Each of these vegetation types represents a recurring natural plant community defined by dominant and diagnostic plant species and their characteristic environment (Comer et al., 2003). Each type also equates to a Group or Alliance within the hierarchically structured US National Vegetation Classification (USNVC) (Faber-Langendoen et al., 2014), and types can thus be aggregated to broader classification levels (Macrogroup, Division, Formation, Subclass, Class).

We used existing data on the distributions of each type across the conterminous US from the LANDFIRE dataset (Rollins, 2009) as well as corresponding data from Canada and Mexico (P. Comer, unpublished data) which are based on hundreds of thousands of georeferenced ground-based vegetation samples in combination with satellite imagery, climate, and landform data. These 90 m resolution gridded spatial data include both existing vegetation type (EVT) maps representing contemporary distributions and biophysical setting (BPS) maps representing the estimated pre-Columbian extent of each type (Rollins, 2009).

To select types for analysis, we first eliminated anthropogenic cover types and vegetation types with less than 50% of their range falling within the western US study area. Next, we ranked types in descending order of land area within the study area, and selected the first n types that cumulatively covered 90% of natural land area. Several riparian and wetland vegetation types were removed to limit the analysis to upland vegetation deemed likely to be climate-limited. This resulted in a final set of n = 96 vegetation types (Figure S1.1) that collectively represent the vast majority of natural lands in the western US. To match the scale of the climate data described below, the 90 m resolution grid of each vegetation type distribution was converted to a coarser 810 m resolution grid, with values representing the fraction of 90 m cells occupied by a type. This was done for both the EVT and BPS datasets.

Climate data

Gridded historic climate data interpolated from weather station measurements were obtained from TopoWx (Oyler, Ballantyne, et al., 2015), PRISM (Daly et al., 2008), and ClimateNA (T. Wang et al., 2012). TopoWx was considered most robust due to its use of remote sensing data and algorithms to correct weather station inhomogeneities that can confound climate trends, but it only includes temperature variables and is limited to the United States. We supplemented this with monthly precipitation data from PRISM, which uses the same spatial grid and extent and a nearly identical set of input weather station data as TopoWx. Data for Canada and Mexico, which are outside our study area and used only for a small portion of the analysis, were obtained from ClimateNA. These datasets all comprise four monthly climate variables (average daily mean temperature, average daily maximum temperature, average nightly minimum temperature, and total precipitation) for each month of each year from 1948 to 2014.

For each year in these time series, we derived 19 bioclimatic variables (Table S1.1) from the 48 monthly variables following the methods of O'Donnell and Ignizio (O'Donnell & Ignizio, 2012). We then calculated multidecadal means of these bioclimatic variables for baseline (1948–1980) and recent (1981–2014) periods. 1980 was chosen as a breakpoint since global temperatures were already trending steadily upward in the 1980s (Pachauri et al., 2014) and we wanted to avoid these trends biasing estimates of baseline climates.

Climate variable sensitivity

To evaluate the relative importance of the 19 climate variables for each of the 96 vegetation types, we trained niche models using different combinations of climate variables, and tested their performance in predicting the distributions of each vegetation type. Niche models were fit using BPS data to avoid bias from human land use change, and were fit based on the entire Mexico–US–Canada range of each type, including areas outside the main study area. Models were trained within the rectangular bounding box encompassing each type, to emphasize climate gradients that differentiate neighboring vegetation types at landscape

scales. They were fit using presence–absence as the dependent variable, with presence defined as one or more 90 m occurrences within an 810 m grid cell.

Our model testing framework used recursive feature elimination (RFE) to rank the climate variables for each type, based on a combination of spatial block cross-validation (SBCV) and pairwise distance sampling (PWDS) used to evaluate model performance in the presence of spatial autocorrelation. We performed this process for each of five niche modeling algorithms (GAM, GLM, Mahalanobis distance [MD], MaxEnt (Phillips & Dudık, 2008), and random forest), including multiple specifications and tuning parameter values for each algorithm. The random forest classification algorithm performed best on average across vegetation types, and was used in the final analysis (with parameters ntree = 10,000, nodesize = 8, and mtry = 1 tuned to optimize performance). The final variable importance analysis using the random forest algorithm involved fitting and evaluating a total of 2,903,040 separate niche models: 96 vegetation types x 189 RFE variable sets x 8 SBCV folds x 20 randomized repetitions per fold.

Recursive feature elimination variable selection for each vegetation type begins with all 19 variables, tests the predictive performance of 19 sub-models each with a single variable removed, and then eliminates the variable that least negatively impacted predictive performance. It then repeats this process for the remaining 18 variables, and so on until only one variable remains, deriving a ranking of variable importance based on elimination order. Uninformative variables removed at each step may be ecologically unimportant and/ or may be statistically redundant with other variables due to high correlations.

For each vegetation type, this RFE process involves hundreds of evaluations of model performance. When testing predictive performance, it is critical to test models on data that are independent from the training data used to fit them. Because both climate and the ranges of vegetation types are spatially autocorrelated, randomly selected training and testing points will be non-independent. We thus used SBCV to measure performance in predicting to a spatially separate domain (Bahn & McGill, 2013), by dividing the range of each vegetation type into four north–south strips each containing 25% of presence localities, and iteratively using three of these blocks for training and one for testing, and then repeating the process using four east–west strips. For each of these eight 'folds', we selected testing presence and absence points using PWDS (Hijmans, 2012) to further control the bias from spatial autocorrelation near the boundaries of spatial blocks, and measured predictive performance using the area under the receiver-operator curve (AUC) statistic. For each fold, 20 randomized models were fit, each using a random sample of 1,000 presences and 1,000 absences. Mean AUC across the eight folds and 20 randomizations was used to identify the least informative variable at each step of the RFE progression.

This analysis generated variable importance rankings for each of the 96 vegetation types (Figure S1.2), which we used in two ways. First, for each type, we selected the four most important variables for use in the niche, temporal, and spatial novelty analyses as detailed below. The choice to use four variables was based on observed model performance during RFE—mean AUC began declining rapidly with fewer than four variables but barely improved with more than four, making this a reasonable tradeoff between parsimony and information

content (Figure S1.3). Second, we used these data to quantify similarity among vegetation types in the variables most important in shaping their distributions, by performing a principal component analysis (PCA) ordination of the 19 by 96 matrix of variable importance values; in this analysis, a climate variable that for example loads positively onto PC1 will tend to have relatively high importance for the vegetation types with positive PC1 values, and relatively low importance for types with negative PC1 values.

Niche novelty

To calculate niche-based vulnerability, we quantified departure from the realized range-wide climate niche of a vegetation type. For each vegetation type, a final random forest niche model was fit as described above, using the full distribution of the type and using the baseline mean climate data for the four most important variables for that type. Models were then used to predict suitability across the existing (EVT) distribution of each vegetation type for both the baseline and recent time periods. Niche novelty in each cell was calculated as recent minus baseline suitability, with all negative values coded as zero. Positive values thus represent declining suitability (with a maximum possible value of one), whereas zero values represent stable or increasing suitability.

Temporal novelty

We used standardized anomalies (Mahony & Cannon, 2018) to calculate the degree of climatic departure from local baseline year-to-year variability. Specifically, we calculated the MD of the recent mean with respect to the baseline time series. Separately for each grid cell occupied by each vegetation type, the four variables most important to the type were reduced to their first two principal components based on a PCA of their local temporal covariance structure, and then the MD of the recent mean was calculated relative to these principal components. This dimension reduction was done to avoid overemphasizing the biological significance of high-dimensional climatic covariance. We report these MD values as percentiles for communication purposes, by computing MD for each individual year in the baseline and calculating the fraction of baseline years whose MD value is exceeded by the recent mean; these percentile values work well for the moderate recent trends assessed here but would saturate with continued future climate change. MD values and percentiles are most interpretable when data are relatively multivariate normal, which we confirm is indeed the case for our analysis (Figure S1.4).

Spatial novelty

To calculate vulnerability defined by climates being new to the geographic neighborhood around each grid cell, we calculated multivariate inbound (backward) climate velocity (Hamann et al., 2015) for each grid cell occupied by each vegetation type. The four variables most important to a given type were de-skewed using a Yeo-Johnson power transformation to

produce a relatively normal distribution across the continent. Following closely the methods of Hamann et al. (2015), we converted the climate data to a Lambert conformal conic projection, used a PCA to reduce the dataset to two dimensions, split each dimension into 100 equal-interval bins, and finally calculated multivariate inbound climate velocity. We ignored extreme outliers (the top and bottom 0.1% of data) when setting bin widths. The algorithm generates distances to climate analogs; in keeping with Hamann et al. (2015), we redefined distances of zero as half the smallest possible non-zero distance and redefined non-analog distances as 10,000 km, before dividing distances by 33.5 years (the time between the midpoints of the two time periods) to derive velocities. Converting distances to velocities does not change the resulting spatial patterns, and was done for consistency with the literature. To minimize the effect of discrete bin boundaries, we evaluated velocity under four variants of the binning scheme each offset slightly in climate space and then averaged the results for each grid cell. Finally, velocities were log-transformed to support plotting and summarization.

Summary analyses

Downstream analyses used EVT-based vegetation cover values in each grid cell when summarizing vulnerability metrics across types within a cell, or across cells within a single type's range. To summarize range-wide vulnerability of higher-level USNVC categories, we calculated mean vulnerability of grid cells occupied by any vegetation type within a category, weighted by percent cover within a cell. To explore how novelty varied within the geographic range of the average type, we converted climate and geographic coordinates into deciles within each type's range and then summarized these deciles across types.

All analysis was done in R version 3.5.1 (R Core Team, 2017), with geospatial and statistical tools from the raster (Hijmans, 2019), caret (Kuhn, 2018), and dismo (Hijmans et al., 2017) packages.

1.4 Results

Climate variable importance

The relative importance of different climate variables differed across the 96 vegetation types (Figure 1.2; Figure S1.2). In the variable importance PCA (Figure 1.2a), PC1 primarily distinguished vegetation types influenced by summertime climate (five of the six variables with the largest positive PC1 loadings relate to climate in the warmest or driest times of year) versus vegetation types influenced by wintertime climate (seven of the eight variables with the largest negative PC1 values relate to cold-season variables or to variables describing seasonality, which indirectly reflects winter extremes). PC2 primarily distinguished temperature versus precipitation-influenced vegetation types (9 of 12 temperature variables loaded positively onto PC2, while all strong PC2 loadings for precipitation variables were negative).

These PC scores indicate strong geographic and ecological patterns of climate sensitivity. Variable importance was hierarchically clustered across vegetation types, with similar types tending to share sensitivity to similar climate variables (Figure 1.2b). Desert and semi-desert vegetation tended to be most influenced by winter seasonality-related variables, whereas shrub and herb vegetation tended to be most limited by precipitation and summer temperature gradients; forests and woodlands were less consistent in their climate sensitivities (Figure 1.2b). Across geographic space and climate gradients, vegetation types in the Intermountain West and in colder and/or drier regions tended to be delimited by temperature-related and winter-seasonality-related variables; vegetation along the Pacific coast, the cordilleras, and the Great Plains—regions with relatively warmer and/or wetter mean annual climates—tended to be informed by gradients of precipitation and summer temperatures (Figure 1.2c,d).

Climate change exposure

Rates of recent multidecadal climate change varied geographically, including across nearby locations, generating a mosaic of exposure patterns (Figure 1.3a–c). For example, mean annual precipitation changes varied from -10% to +20% across the region, and changes in minimum temperature of the coldest month varied from near zero to more than +2°C. Furthermore, these geographic exposure patterns differed substantially among climate variables: in a PCA of exposure values for the 19 bioclimatic variables across the western US, 10 principal components were required to capture 95% of the total variance. This variation is further illustrated by bivariate correlations among exposure values for the 19 variables (Figure 1.3d), which show that most variables are changing relatively independently of one another across the region, although some subsets of variables did have highly correlated exposure patterns. These bivariate correlations between exposure values were only modestly predictable from correlations between baseline means ($r^2 = .40$), indicating that spatial associations among climate variables are being restructured with climate change. In sum, these results show that locations across this region experienced a highly diverse, individualistic set of climate change signatures that cannot be effectively summarized by a small number of representative climate variables.

Vulnerability dimensions

The three metrics of climate change vulnerability—niche novelty (decline in suitability), temporal novelty (standardized climate anomaly), and spatial novelty (inbound climate velocity)—yielded distinct vulnerability estimates across various dimensions of the dataset (Figure 1.4; Figures S1.5 and S1.6). Grid cells of individual vegetation types had a mean (minimum/median/maximum) niche novelty of 0.09 (0.00/0.03/0.99) across the region, with the largest possible value of 1 representing a change from maximum suitability to zero suitability. Average temporal novelty was 0.23 (0.00/0.18/1.00), with the largest possible value of 1 indicating that the recent multivariate mean was more extreme than any individual year

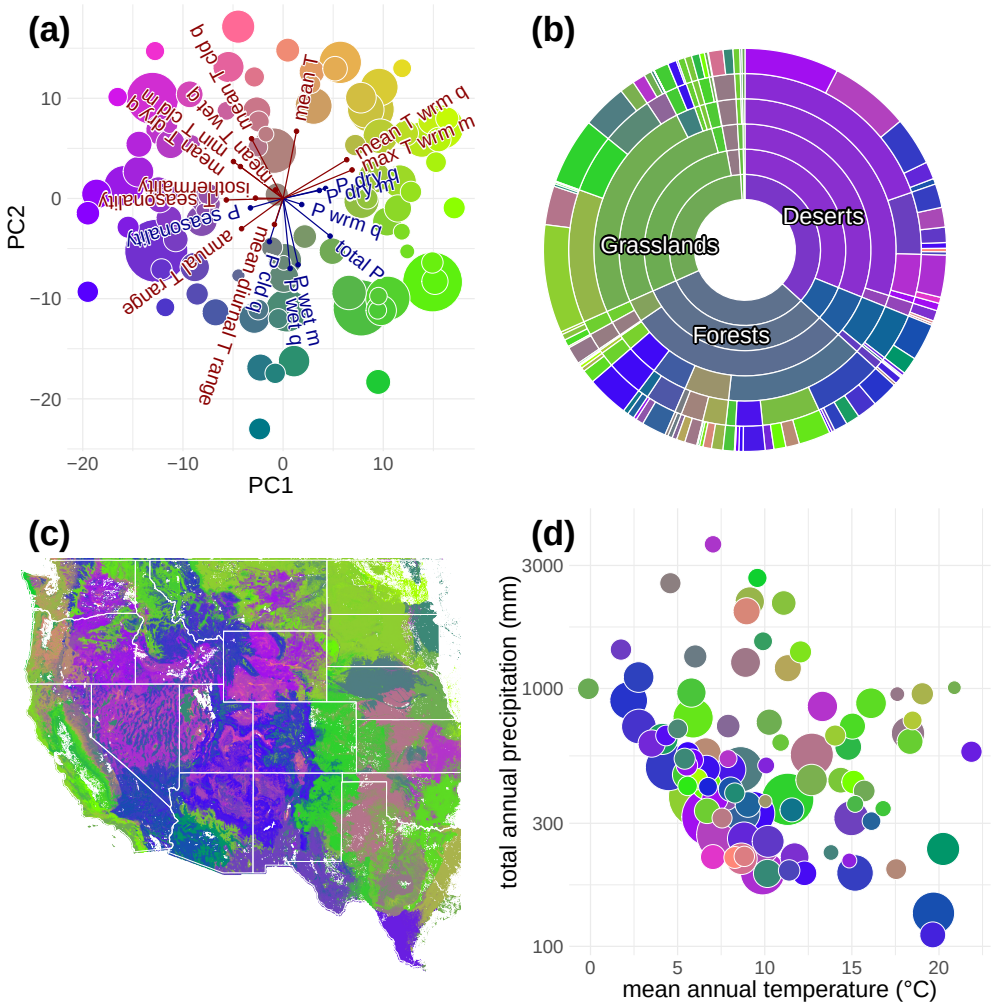

Figure 1.2: Geographic and ecological patterns in the climate variables most important to each vegetation type. (a) Vegetation types in variable importance space, based on ordination of the variable importance matrix—vectors indicate input variable importance loadings (m, month; P, precipitation; q, quarter; T, temperature; full definitions in Table S1.1), while points indicate vegetation types, with nearby types having distributions shaped by similar suites of variables; colors on this panel serve as the legend for other panels. (b) Variable importance across the vegetation classification (see Figure S1.1 for a labeled key); internal values are means of results for constituent vegetation types. (c) Geographic patterns of variable importance; grid cell values are means of local vegetation type PC scores, weighted by percent cover. (d) Variable importance across climate space, with points representing the mean annual temperature and precipitation across the range of each vegetation type. In all panels, color represents the set of climate variables important to each vegetation type as illustrated in (a). In (a), (b), and (d), point size and slice size are proportional to land area covered by a vegetation type within the study area.

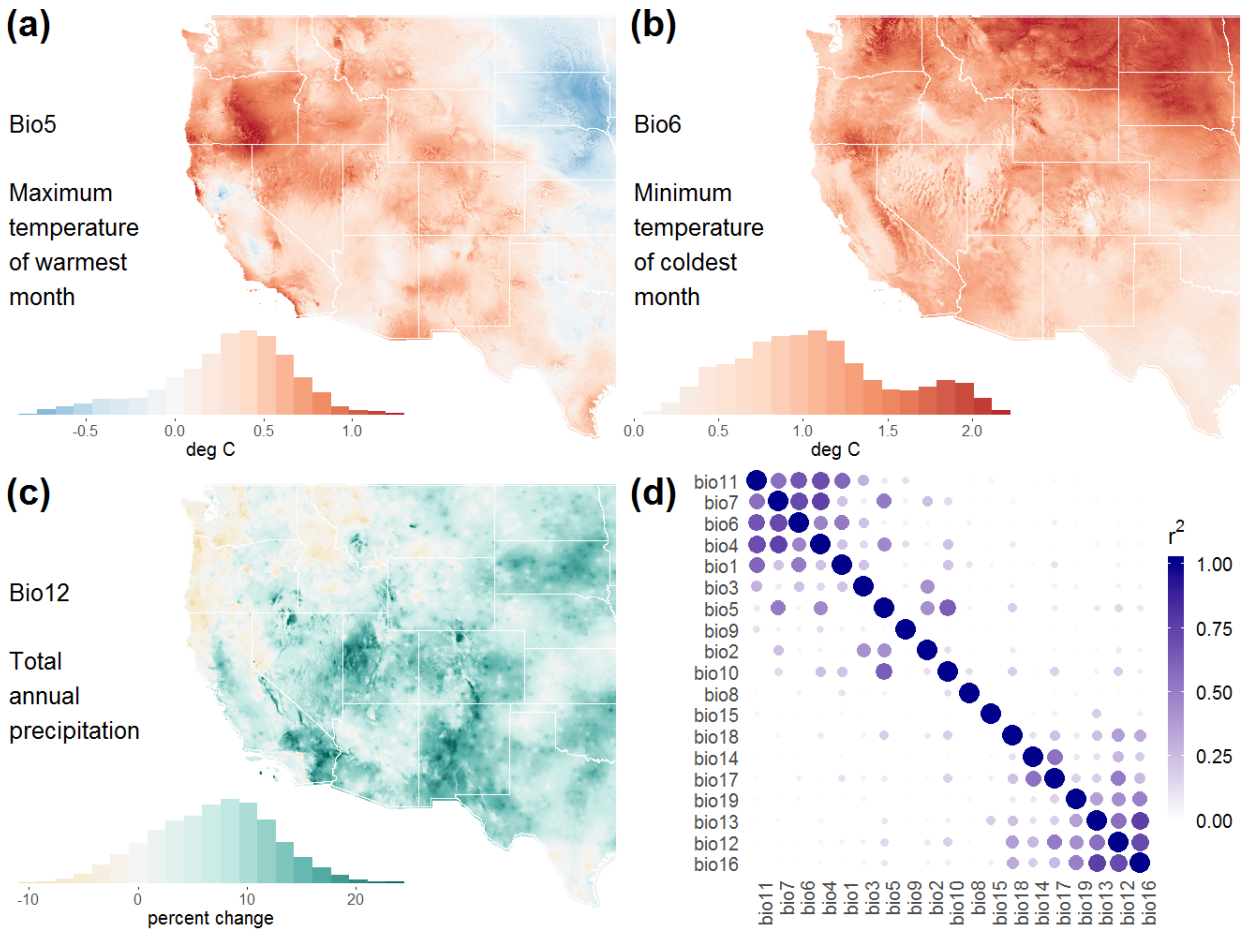

Figure 1.3: Geographic variation in climate change exposure, defined as the difference in mean climates between the 1948–1980 baseline and 1981–2014 recent time periods. (a–c) Geographic variation in exposure for maximum temperature of the warmest month, minimum temperature of the coldest month, and total annual precipitation, respectively. (d) Pairwise correlations in exposure for the 19 bioclimate variables (defined in Table S1.1), illustrated as a heat map of the squared bivariate Pearson's correlations of exposure values across grid cells in the study area; point size and opacity indicate r^2.

in the baseline. Mean spatial novelty (calculated after converting infinite distances to 10,000 km) was 2.77 (0.00/0.28/infinite) km/year, with infinite values indicating locations with no analog climate in North America.

When we ranked grid cells according to the mean vulnerability of local vegetation for each of the three metrics, we found that most three-dimensional combinations of high and low vulnerability quantiles were present across some portion of the western US (Figure 1.4; Figure S1.5), indicating that these novelty dimensions are non-redundant and ecosystems are likely to experience diverse regimes of departure from baseline climate patterns. While most locations had some combination of high and low novelty values across the three measures, pockets of the Great Plains and Madrean Desert were among areas ranked as relatively highly vulnerable according to all three measures, whereas areas including parts of central Oregon, northeastern Colorado, and central Texas had relatively low exposure for all measures (Figure 1.4a). Niche and spatial novelty tended to be greatest in the east, whereas temporal novelty tended to be greatest in the central and southwest regions of the study area, though all regions exhibited major variation at finer scales.

Across the 96 vegetation types, mean range-wide vulnerability scores were relatively independent for the three metrics, with niche novelty and temporal novelty very weakly negatively correlated and both very weakly positively correlated with temporal novelty (Figure S1.6). These mean vulnerability values were clustered on the vegetation classification hierarchy, with similar types often exhibiting similar vulnerability for a given metric. Spatial novelty was most extreme among shrub and herb vegetation types (which are primarily grasslands), whereas temporal novelty was most extreme among forest and desert vegetation types; niche novelty exhibited little hierarchical structure (Figure S1.6).

We also found vulnerability trends across geographic and climate gradients at multiple scales (Figure 1.4). At broad scales comparing the mean vulnerabilities of vegetation types (Figure 1.4b), no novelty metric had clear relationships with latitude, but niche and spatial novelty were highest in lower-elevation vegetation types while temporal novelty was highest in higher-elevation types. Niche and spatial novelty also tended to be higher in warm-wet and cold-dry regions than in warm-dry or cold-wet regions. Patterns also emerged at smaller scales within the range of the typical vegetation type (Figure 1.4c). Niche vulnerability tended to be highest at the warm, wet edge of a type's distribution along the low elevation and low latitude margins, whereas temporal vulnerability was higher in colder high-elevation and low-latitude portions of a type's range; spatial vulnerability exhibited indistinct patterns with respect to within-range spatial gradients but tended to be lowest at warm, cool, and/or dry range edges.

The trend toward higher temporal novelty at higher elevations is consistent across 14 of the 19 climate variables, as measured by correlations between univariate standardized anomalies and altitude (Figure S1.7). This was a function of lower interannual climate variability at higher elevations for almost every variable (17 of 19) as well as higher exposure magnitudes at higher elevations for a subset of the variables (8 of 19, including the broadly important temperature variables Bio1, Bio5, and Bio6).

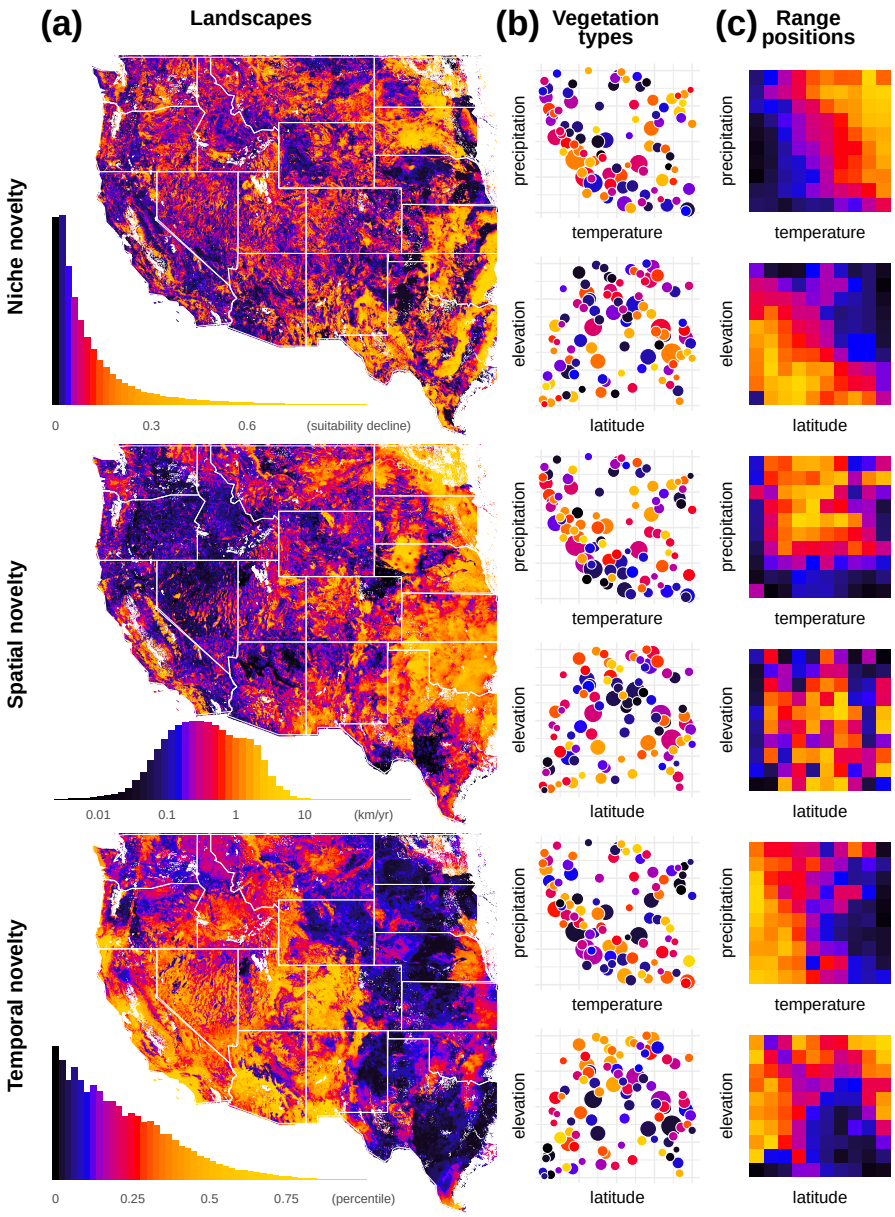

Figure 1.4: Vegetation climate change vulnerability across the western US according to three metrics of vulnerability: niche novelty, spatial novelty, and temporal novelty. (a) Mean novelty across all vegetation types in each grid cell, with histograms indicating frequencies of novelty values. (b) Mean range-wide novelty of vegetation types in climate and geographic spaces, with point size indicating the range size of each type. (c) Novelty as a function of a site's position within the geographic or climatic range of a vegetation type, averaged across all types. All colors represent percentiles within a sub-panel, with warmer colors indicating higher relative vulnerability. Figure S1.5 shows the multivariate combinations of these novelty metrics.

1.5 Discussion

In this study, we examined multiple aspects of climate change vulnerability across the geographic ranges of more than ninety vegetation types of the western US. This represents to our knowledge the first systematic comparison of niche-, spatial-, and temporal-based novelty paradigms, as well as an important advance in inferring patterns of climate variable importance and their influence on projected vulnerability patterns. Our findings offer new lessons about the relative climate vulnerability of vegetation communities and the landscapes they occupy, and highlight a range of vulnerability signatures that have distinct management implications for climate adaptation across these sites. Our focus on observed recent climate change helps to highlight the finescale spatial heterogeneity of multivariate climate trends and their potential implications for biodiversity in ways that future models cannot, though future models of course remain critical tools for ecological forecasting. While our analysis was focused on vegetation types, we stress that many of our findings should apply at other scales of the biotic hierarchy, from genes to species to biomes.

We identified a surprisingly diverse mosaic of climate change vulnerability profiles across the region's plant communities (Figure 1.4). This spatial heterogeneity was a function of three key underlying drivers: (a) highly variable rates of climate change itself, (b) differences among locations and vegetation types in the importance of different climate variables, and (c) relatively independent vulnerability patterns across the three metrics.

Rates of climate change are highly heterogeneous

The first of these three drivers is largely extrinsic to vegetation and instead simply reflects the complex geophysics of climate change. Our results add to those of other studies (Rapacciuolo et al., 2014) in showing that different climate variables are changing at very different rates in different places (Figure 1.3), a phenomenon likely driven by interactions among nested macro-, meso-, and topo-scale climate feedbacks. Spatial heterogeneity in even a single variable can generate large exposure differences across landscapes (e.g., minimum temperature of the coldest month has increased more than 2°C since the mid-20th century in some landscapes but barely at all in others), and has been invoked as an explanation for diverse ecological responses to recent climate change (Chen et al., 2011). Add to this our finding that such exposure patterns are largely uncorrelated among climate variables, likely driven by their contrasting relationships with geophysical gradients and their influences on one other, and a picture emerges of a high-dimensional exposure space in which each landscape is experiencing a relatively unique manifestation of climate change, with exposure signatures often differing strongly even among nearby sites.

One definition of a climate change refugium is a location in which climate changes less quickly than the surrounding region, helping buffer the local biota against the most rapid rates of change (Ashcroft et al., 2009; Morelli et al., 2016). Our results corroborate previous studies in highlighting that such refugia tend to occur at multiple scales, and in different locations for different climate variables. These patterns highlight the importance of landscape-

scale heterogeneity (Ashcroft et al., 2009) that would be masked by the low spatial resolution and significant uncertainties inherent in future GCM simulations. This reinforces the value of studying observed recent climate trends at relatively high spatial resolution as a complement to coarser future model predictions. Whether emerging fine-scale spatial patterns in recent climate change magnitudes will increase or decrease in the future as global climate change progresses remains an open and critically important question (Maclean et al., 2017).

Strong climate variable importance trends shape vulnerability

The second major driver of heterogeneous climate vulnerability was spatial and ecological variation in the importance of different climate variables. Variable importance patterns are an aspect of the 'sensitivity' component of climate change vulnerability, shaping how vegetation types are projected to respond to a given magnitude of climate exposure. Broad-scale patterns in the importance of different climate variables have been underexplored, and while several recent studies have begun to examine variation in the importance of different climate variables across species (Barbet-Massin & Jetz, 2014; Bradie & Leung, 2017; Schuetz et al., 2019), ours is the first to our knowledge to assess how such variation is structured spatially and ecologically. Our results present a first systematic look at broad-scale variable importance patterns for terrestrial vegetation, revealing patterns relevant both to basic ecology and to global change.

We found strong patterns of variable importance across geographic space, climatic gradients, and vegetation classes (Figure 1.2). The PCA of importance scores suggested that vegetation types can be primarily characterized as limited by either summer or winter conditions, and as limited by either temperature or precipitation variables. Desert shrubland vegetation types occupying the cool, dry Intermountain region at the center of the study area tended to be most sensitive to temperature and winter climate, whereas grasslands were more sensitive to precipitation and summer climate, with forest vegetation types having a more diverse set of limiting factors. These results imply that the key climatic variables relevant to vulnerability assessments differ across contexts, and offer a first look at factors predicting these differences.

Even if all locations experienced identical climate exposure, variable sensitivity patterns would generate heterogeneous ecological impacts because some species will be more sensitive to the variables that are changing fastest. In reality, we found that these variable importance patterns interacted with the highly non-uniform exposure patterns described above to generate even more spatially heterogeneous vulnerability patterns. This implies that tailoring climate vulnerability assessments to locally important variables can strongly influence results, and underscores the importance of ecological knowledge about the sensitivity of local ecosystems to different aspects of climate. These results stress that refugia are likely to differ among vegetation types and among species, depending on overlap between climate variables changing most slowly in different locations and those that are important influences on each vegetation type.

Vulnerability estimates differ markedly by novelty paradigm

The third aspect of heterogeneous vulnerability was differences among the three novelty paradigms, each of which is based on a different reference distribution for what is considered the historical and normative baseline for a given ecosystem. All three metrics are based on the same exposure and variable importance inputs for a given vegetation type in a given site, and novelty for all three metrics is thus expected to correlate positively with the exposure magnitude of locally important variables. Given the strong patterns in exposure and variable importance common to all three metrics, and given a prior study that found concordance between niche models and future climate change metrics for African vertebrates (Garcia et al., 2016), we expected that our vulnerability metrics might also be strongly correlated and that any differences among them might emerge only as second-order distinctions. Instead, we found that the three metrics were highly divergent, each identifying distinct landscapes and vegetation types as most and least vulnerable to climate change. Niche-based vulnerability and spatially based vulnerability exhibited a weak negative correlation across vegetation types, and both were only weakly positively correlated with temporal-based vulnerability. This multidimensionality of vulnerability metrics based on relatively finescale regional patterns of observed recent climate change adds empirical weight to similar patterns that have been forecast based on modeled coarser-resolution global data for the future (Garcia et al., 2014).

Detailed patterns of vulnerability across the three novelty metrics included both confirmations of common narratives as well as unexpected patterns. The three metrics showed striking differences in which edges of a given vegetation type's realized niche and geographic range they implicated as most threatened on average, as well as in which vegetation types they implicated as most threatened overall. Niche novelty was highest at warm, wet climate edges for the typical type, corresponding to the low-elevation, low-latitude margins of the type's distribution—an expected pattern that is in keeping with the narrative of upwardand poleward-shifting ranges in warming climates, which has been widely though inconsistently observed in field studies over recent decades (Rumpf et al., 2019; Wiens, 2016). Interestingly and more unexpectedly, we also found that low-elevation vegetation types had higher average niche novelty overall across their ranges. This broader-scale pattern represents a second relatively independent aspect of niche-based vulnerability in lower-elevation terrestrial ecosystems.

Spatial novelty, measured as inbound climate velocity, was generally highest for vegetation types in relatively low-elevation sites in the eastern portion of the study area and lowest for types inhabiting cool, dry landscapes of the intermountain region; these broad patterns largely agree with prior studies (Belote et al., 2018; Dobrowski et al., 2013). Within the geographic range of the typical vegetation type, inbound climate velocities were also low in dry areas and relatively high on the wet range edge, an expected pattern when climates are becoming wetter: all else equal, locations whose climate is more extreme in the direction that climate is changing (e.g., relatively wetter locations when precipitation is increasing) will tend to have higher inbound velocities. Velocities also tended to be lowest near both

the warm and cool range margins, which could be driven by the tendency of climatically marginal populations to occur in isolated microclimates nested in topographically complex landscapes with low climate velocities.

In contrast to these metrics, temporal novelty was typically highest in colder, higher-elevation portions of a type's distribution, as well as in higher-elevation vegetation types overall. While temporal novelty is a function of both exposure magnitude and year-to-year variability, the data suggest that the latter component is the primary cause of the observed higher novelty at higher elevations. While higher elevations had higher exposure for many important temperature variables, in keeping with prior studies showing modest positive relationships between elevation and temperature trend magnitudes after carefully controlling biases (Oyler, Dobrowski, et al., 2015), precipitation variables tended to change faster at lower elevations. However, the large majority of both temperature and precipitation variables exhibited lower year-to-year variability at higher elevations, ultimately leading to a clear pattern of higher temporal novelty at higher elevations. It remains uncertain whether this result is driven by an elevation-mediated climate dynamic *per se*—it could also result from higher-elevation areas tending to occur in regions that have high temporal novelty across all elevations, or could be an artifact of climate interpolation (if higher-elevation sites have lower spatial autocorrelation in their temporal climate anomalies, then climate surfaces interpolated from high-elevation stations could exhibit artificially dampened temporal variation). Further study is needed addressing mountain climate change dynamics, including at scales finer than the broad patterns reported here.

Novelty signatures suggest distinct management approaches

Each of these conceptually and empirically distinct novelty paradigms offers a hypothesis about the vulnerability of a given local population or ecosystem based on a particular model of resilience to climate change. While the metrics can be considered additive in the sense that higher vulnerability on any axis may mean a higher likelihood of ecosystem change or collapse under climate change, a richer management perspective may come from considering the three metrics jointly. A given site will fall somewhere in the three-dimensional vulnerability space defined by these novelty metrics (Figure S1.5), different regions of which we argue are associated with distinct management strategies for climate adaptation (Figure 1.5).

When novelty is low in all three dimensions, intervention is not a priority and a relatively hands-off strategy of protecting and monitoring local populations may be warranted. The vegetation types most exemplifying this pattern across their ranges were certain coniferous forest types of the Sierra Nevada and Cascade mountains and shrubland types of the Intermountain Basin, though pockets of low vulnerability were present in many landscapes across the study area. Sites with this vulnerability signature may be important as climate refugia due to low rates of climate change, steep spatial climate gradients, or resilient vegetation.

When novelty is high in some dimensions but not others, different forms of intermediate-intensity intervention may be required to facilitate climate adaptation in the local ecosystem. If climate novelty for a site is high on the spatial and temporal dimensions but remains within

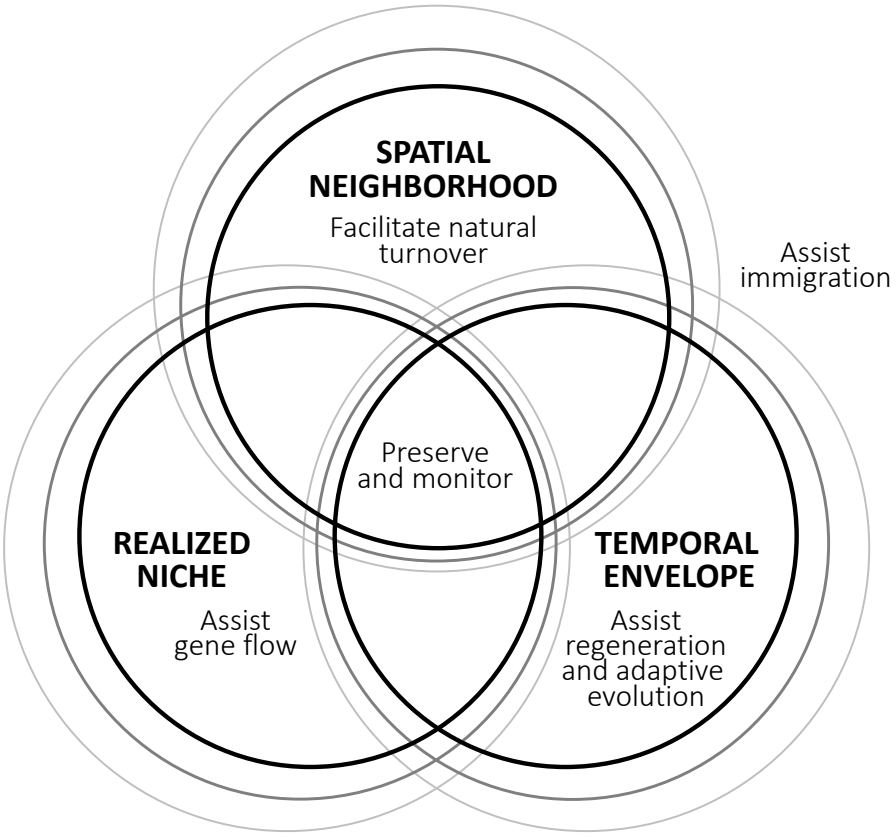

Figure 1.5: Potential management approaches to climate change adaptation for populations or ecosystems with different combinations of climate novelty values across the three metrics. High novelty or vulnerability for a given dimension is represented as a site's new climate being outside the circle encompassing the baseline climate distribution that defines a given vulnerability metric. For example, a population with low niche novelty but high spatial and temporal novelty would be located within the species realized niche but outside the local spatial neighborhood and the historic temporal envelope, and could be a target for assisted gene flow. Management strategies for the empty two-way intersections could represent more subtle combinations of the approaches listed for adjacent regions. Concentric circles reflect the notion that these novelty metrics are continuous rather than binary designations.

the realized range-wide niche of the species or vegetation type, it raises the possibility that local genotypes or community members may be ill-adapted to the new climate and that future movement of adapted genes from nearby sites (or *in situ* adaptive variation from historic local gene flow) is unlikely. In this scenario, assisted gene flow from other parts of focal species' ranges may be warranted as a way to maintain population fitness in the locally novel climate (Aitken & Whitlock, 2013). While the rationale for assisted gene flow often assumes that plant populations are evolutionarily adapted to their local historic environments—a pattern that is common but not ubiquitous (Hereford, 2009)—assisted gene flow can also help facilitate evolutionary adaptation even in the absence of local adaptation by increasing genetic diversity (Aitken & Whitlock, 2013). High levels of historical gene flow could also lead to maintenance of adaptive genetic variation within populations (Sork et al., 2010), even if conditions depart from the historical climate distribution. Field studies are needed to determine the degree of local adaptation and levels of adaptive genetic variation within populations. Where niche and spatial novelty are both high but temporal novelty remains relatively low, gene flow or natural turnover are unlikely to maintain ecological function but local populations have some demonstrated ability to survive the new mean climate. This scenario is common at low-elevation range limits and across large tracts of the Great Plains in the eastern portion of the study area, both geographies that tend to have relatively high year-to-year climatic variation that may have facilitated local adaptation to a wider range of climates. Under these conditions, the management priority may be to bolster the fitness of local populations by facilitating adaptive evolution and assisting with regeneration, which is often the limiting demographic stage if the juvenile recruitment niche is more restrictive than the adult tolerance niche (Grubb, 1977; Jackson et al., 2009). Interventions in this scenario might include seeding and artificial selection, as well as more broadly applicable strategies like reducing non-climatic ecological stressors such as grazing and invasive species that are widespread across the study area.

If spatial novelty is low but both niche and temporal novelty are high, local populations of the focal species may be unsustainable but nearby sites are likely to contain climatically suitable species that could disperse and establish in the focal site, adaptively maintaining ecosystem function by filling ecological roles left by extirpated species. Managers in such cases may wish to facilitate this natural turnover using approaches such as maintaining or restoring connectivity among natural vegetation patches, employing prescribed fire where appropriate to reduce competition and speed establishment of newly suitable species, or performing localized assisted migration to jumpstart populations. In these situations, assisted migration may involve only local-scale movement of propagules, reducing concerns about introduction of exotic species. However, facilitating vegetation change may still raise concerns that historical baselines are being lost unnecessarily, challenging long-established norms for priority setting in conservation (Hobbs et al., 2014).

High vulnerability in all three novelty dimensions indicates that intensive management intervention may be required to prevent ecosystem collapse. This novelty signature was found across pockets of the Great Plains, the Madrean desert, the Rocky Mountains, and the Pacific coast. With the new mean climate outside the range of historic variation experienced by

the local population, outside the range of mean climates across the entire distribution of the type, and outside the range of climates found in the nearby area surrounding the focal site, local populations may be unsustainable and viable alternatives may be lacking from nearby communities. Longer-distance assisted immigration—importing species that have desirable ecological attributes and are adapted to current or future climates—has been recommended under such circumstances as a means to maintain ecosystem structure and function (Hoegh-Guldberg et al., 2008). While controversial, assisted migration may play an increasing role in the adaptation toolkit as climate exposure and its ecological impacts continue to grow (Richardson et al., 2009).

It is important to carefully consider the concepts and assumptions that underlie each novelty metric when evaluating vulnerability, as the dimensions may be more or less relevant for a given species or vegetation type. For example, temporal novelty may provide more insight than niche novelty where local adaptation or non-climatic distributional constraints are thought to be important, and spatial novelty may be less relevant than other metrics in highly dispersal-limited systems where natural immigration is unlikely. Thus, while phylogenetic or ecological traits may be imperfect as direct predictors of climate vulnerability as discussed above (Buckley & Kingsolver, 2012), they could prove much more informative in determining the relevance of different vulnerability paradigms. For instance, niche model success in predicting range shifts is associated with plant species traits (Dobrowski et al., 2011), and characteristics like dispersal ability shape the influence of spatial novelty on paleoclimatic range shifts (Sandel et al., 2011).

Integrating these multiple vulnerability paradigms with additional ecological knowledge may thus offer a way forward in understanding and predicting individualistic responses to climate change. Macroecological-scale data are now widely available on ecological traits and on recent trends in population sizes and range limits. We call for further studies to assess which of the niche, temporal, and spatial novelty paradigms best explain observed biodiversity trends under what ecological circumstances, and to do so using frameworks that consider the high-dimensional nature of climate exposure and incorporate variation in sensitivity to these climate dimensions.

Chapter 2

Global wind patterns and the vulnerability of wind-dispersed species to climate change

This chapter is a reproduction of the following published manuscript, included here with the permission of my co-author and in acknowledgement of his contributions to this research:

Kling MM & Ackerly DD (2020). Global wind patterns and the vulnerability of wind-dispersed species to climate change. Nature Climate Change, https://doi.org/10.1111/gcb.15008

2.1 Abstract

The resilience of biodiversity in the face of climate change depends on gene flow and range shifts. For diverse wind-dispersed and wind-pollinated organisms, regional wind patterns could either facilitate or hinder these movements, depending on alignment of winds with spatial climate patterns. We map global variation in terrestrial wind regimes, and model how 'windscape' connectivity will shape inbound and outbound dispersal between sites and their predicted future climate analogs. This model predicts that wind-accessible, climatically analogous sites will be scarcer in locations such as the tropics and on the leeward sides of mountain ranges, implying that the wind-dispersed biota in these landscapes may be more vulnerable to future climate change. A case study of *Pinus contorta* illustrates species-specific patterns of predicted genetic rescue and range expansion facilitated by wind. This framework has implications across fields ranging from historical biogeography and landscape genetics to ecological forecasting and conservation planning.

2.2 Introduction

For biodiversity, resilience to climate change eventually requires either range shifts or in situ adaptation (Bellard et al., 2012). Both rely on dispersal. Species survival depends on outbound dispersal to track suitable conditions and resources through range expansion (Hampe, 2011), whereas the adaptation of local populations and ecosystems depends largely on the inbound dispersal of novel genes and species better suited to the new environment (Kremer et al., 2012). Already widespread, climate-induced biogeographical shifts are predicted to become a race against time as the pace of climate change accelerates, with major consequences for global biodiversity and human society (Pecl et al., 2017).

Although some organisms can actively track suitable climates, many passive dispersers are subject to the whim of the winds. Wind is the essential dispersal vector for a substantial fraction of species across all life forms. Wind regimes (speed, direction and directional consistency) help explain the transoceanic dispersal of birds (Felicısimo et al., 2008), arthropods (Gillespie et al., 2012), plants (Munoz et al., 2004) and microorganisms (Austerlitz et al., 2007; Bullock & Clarke, 2000; Gassmann & Pérez, 2006; Skarpaas & Shea, 2007; Z.-F. Wang et al., 2016) and fungi (Soubeyrand et al., 2007); the landscape genetics of diverse plants (Austerlitz et al., 2007; Born et al., 2012; Geremew et al., 2018; Z.-F. Wang et al., 2016) and pathogens (Brown & Hovmøller, 2002); and the overland dispersal of aquatic species (Vanschoenwinkel et al., 2008). Wind influences on insect pollinators can even drive directional pollen dispersal in non-wind-pollinated plants (Ahmed et al., 2009).

Wind regimes could thus strongly influence the range expansion and gene flow required for climate tracking at landscape to regional scales (Larson-Johnson, 2016; Nathan et al., 2011; Sorte, 2013). Under warming conditions, adaptation and range shifts require the dispersal of genes and species down geographical temperature gradients towards historically cooler sites (for example, towards higher latitudes and elevations) (Loarie et al., 2009). Wind may facilitate this migration in landscapes where it flows strongly from warmer to cooler sites, and hinder it where the flow is from cooler to warmer sites or blows weakly overall (Larson-Johnson, 2016; Sorte, 2013). Alignment with precipitation gradients will also be important for many species, but we focus mainly on temperature in this article because future rainfall projections are more heterogeneous and uncertain, and wind has important causal links with temperature gradients.

The direction of currents is a well-established factor in determining the success of climate-driven range shifts in marine systems (Molinos et al., 2017), but the corresponding role of wind currents in terrestrial systems has received less attention, in spite of studies that identify wind direction as a key open question for modelling range shifts (Higgins et al., 2003; Nathan et al., 2011). Although studies using wind-speed data have assessed future range-expansion potentials (Bullock et al., 2012; Kuparinen et al., 2009; Nathan et al., 2011) and concluded that dispersal could limit future climate responses in many species, we are unaware of studies that account for wind direction or spatial variation in wind regimes. Studies on wind direction's role in historical climate tracking are also scarce, although it has been implicated in shaping local (Davis et al., 2004; Dullinger et al., 2003) and regional

(Payette, 1993) climate-driven range expansion. Observations that some wind-dispersed trees and grasses have failed to keep pace with high palaeoclimate velocities (Sandel et al., 2017; Svenning & Skov, 2007) and that incomplete range filling is related to seed aerodynamics (Schurr et al., 2007) further suggest that wind conditions can limit range expansion even when climate change is much slower than that predicted for the coming decades.

In this study, we model the predicted global patterns of climate adaptation tailwinds and headwinds. We begin by characterizing the geography of key dispersal-relevant features of local wind regimes. Next, we offer a conceptual introduction that examines climatic drivers of alignment (tailwinds) and misalignment (headwinds) between prevailing winds and temperature gradients. In our main analysis assessing the potential for wind to facilitate climate tracking, we then implement a global 'windscape' connectivity model to compare upwind and downwind dispersal catchments with patterns of shifting climate analogues. Finally, we demonstrate how species-specific wind connectivity modelling can inform predicted patterns of genetic rescue and range expansion under climate change, using lodgepole pine (*Pinus contorta*) as a case study.

2.3 A typology of global wind regimes

The geography of wind regimes will determine potential impacts on climate change biogeography. Wind dispersal patterns depend on the long-term distribution of instantaneous wind conditions at a site (Bullock & Clarke, 2000), and these wind regimes can be characterized by three key properties. Average wind speed represents the total wind dispersal potential for a site. Prevailing wind direction represents the expected bearing of wind dispersal to or from a site, quantified as the circular mean of hourly wind angles weighted by wind speed. And wind anisotropy reflects how unidirectional wind dispersal is expected to be for a site, quantified as one minus the circular standard deviation of hourly wind directions weighted by wind speed. Vertical turbulence also plays a critical role in wind dispersal, although we are unable to assess it in detail due to data and space limitations. Diurnal and seasonal patterns in these factors are also important, depending on the dispersal phenology of individual species (Z.-F. Wang et al., 2016).

We characterized global patterns in these wind regime properties using 30 years (1980–2009) of hourly resolution near-surface wind data from the gridded (35 km pixels) Climate Forecast System Reanalysis (CFSR) dataset (Saha et al., 2010), which we used for all the analyses in this article. Each of the three variables exhibits strong and relatively independent spatial trends (figure 2.1), with important implications for the biogeography of wind dispersal. Globally, the prevailing wind direction is structured in latitudinal bands associated with Hadley, Ferrel and polar atmospheric circulation cells. Equatorial regions have weak westward and equatorward surface flow, which makes the tropics a relative wind trap (known to sailors as the doldrums); tropical winds tend to be more anisotropic near coasts. At temperate latitudes, winds are stronger and tend to flow eastward and poleward, although the strength and direction are more variable. Polar latitudes exhibit strong anisotropic

winds that flow westward and equatorward, although this is more consistent in the Southern Hemisphere. Smaller-scale geography also shapes wind regimes, with wind strength often increasing near coasts and both strength and anisotropy increasing with elevation.

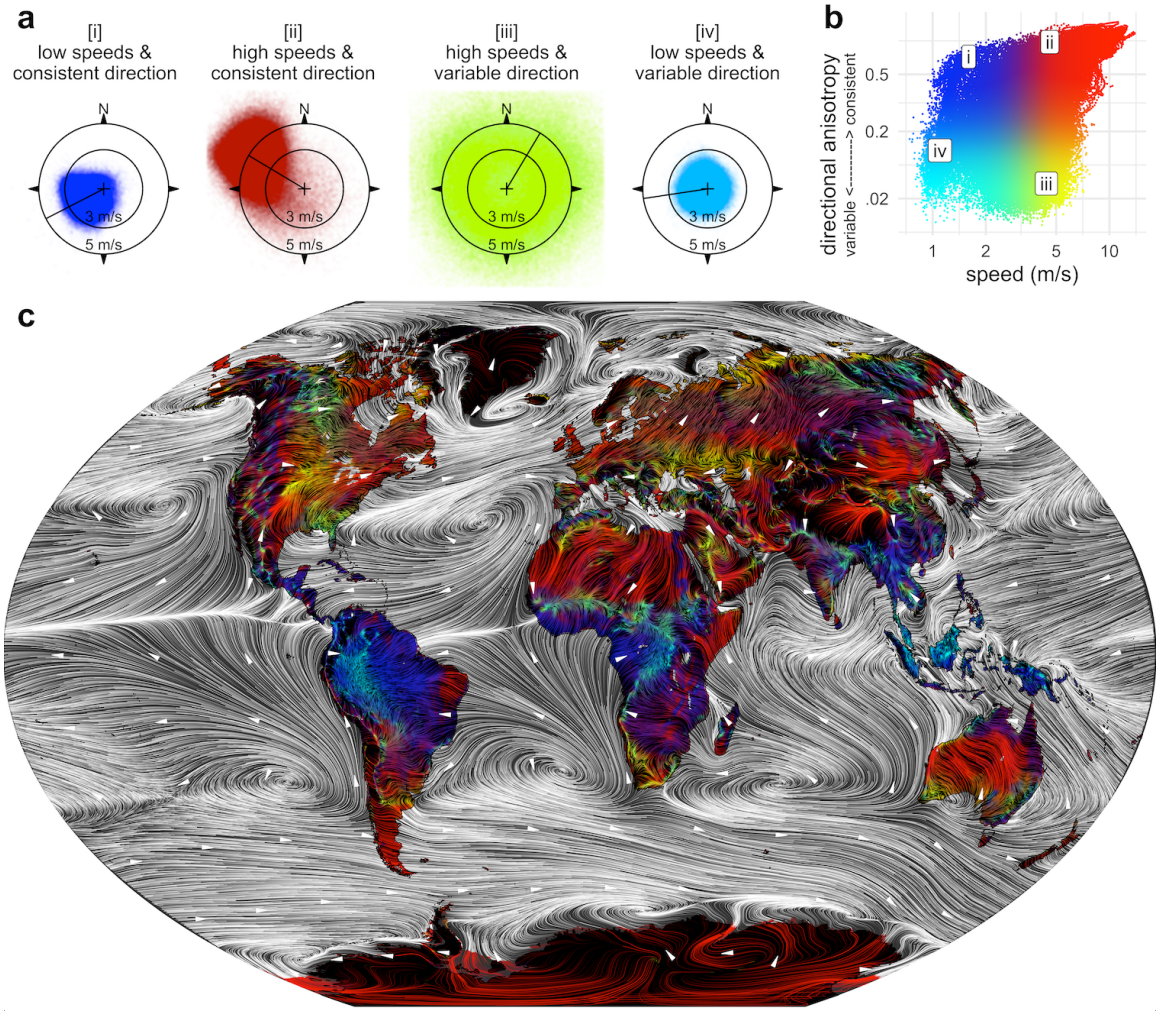

Figure 2.1: Global wind patterns as characterized by three drivers of dispersal: prevailing wind direction, average wind speed and anisotropy. (a) Examples of local wind regimes; point clouds represent speed and direction for every hour from 1980 to 2009, and radial lines indicate the prevailing direction. (b) Wind speed and anisotropy across terrestrial grid cells ($r^2 = 0.25$); the examples in *a* are shown. (c) Geographical patterns of wind regimes; the prevailing wind direction is indicated by wind paths and arrows, and the speed and anisotropy correspond to the colours in *b*.

2.4 Prevailing wind alignment with temperature gradients

Global wind patterns will influence the direction and speed of movement for wind dispersers in relation to spatial temperature gradients and warming temperatures. Importantly, wind and temperature are mechanistically coupled. The very temperature gradients that biodiversity must traverse to offset climate change are directly responsible for generating wind across these landscapes. Generally, the prevailing surface winds tend to flow from cooler towards warmer locations due to the pressure differential between areas of sinking cool air and rising warm air—the opposite direction that genes and species must migrate in a warming world. Although this is a generality, it is also a simplification, and important exceptions exist. In this section we explore general spatial patterns in the alignment ('tailwinds') and misalignment ('headwinds') between prevailing winds and temperature gradients at various geographical scales. We set aside temporal variation in wind speed and direction for this conceptual introduction, and return to it in the subsequent section.

The largest-scale temperature gradient on the planet is latitudinal, and poleward range shifts are a key component of biodiversity migration under climate change. The latitudinal temperature gradient drives equatorward-flowing headwinds in the Hadley and polar cells that cover about two-thirds of the Earth's surface, whereas poleward-flowing tailwinds are the norm in the temperate-latitude Ferrel cells between 30 and 60°N and between 30 and 60°S. Global data indicate that the mean terrestrial winds follow these expectations across 94% of latitudinal zones outside the Arctic (figure 2.2a,b). Deviations occur in the Arctic and other northern areas where large landmasses interrupt the idealized circulation.

Temperature gradients also drive prevailing winds at regional to landscape scales. Examples include 'thermal lows' pulling wind toward hot deserts, 'katabatic winds' pushing air off of ice caps and high mountains and 'sea breezes' pulling wind from cool waters towards warm landmasses (figure 2.2e,g,h), all of which flow opposite the direction needed to facilitate temperature tracking. In other locations, the prevailing winds flow across landscapes that encompass heterogeneous temperature gradients. Where winds blow across deserts or mountain ranges, they may facilitate migration on one side and hinder it on the other (figure 2.2c,d). The windward side of mountain ranges (generally the west side in temperate regions) will experience tailwinds, which will help move species to higher elevations; on the leeward side, headwinds will push dispersers downhill towards higher temperatures.

Alignment can be extended to two dimensions by quantifying the angle between the prevailing wind direction and the orientation of the local temperature gradient (figure S2.1), and similar metrics for oceanic currents have been shown to explain observed range shifts in marine systems (Molinos et al., 2017). However, although prevailing winds offer important insights, winds vary across time and space, and biodiversity must track climates across complex temperature landscapes, which necessitates a more realistic landscape-scale modelling approach.

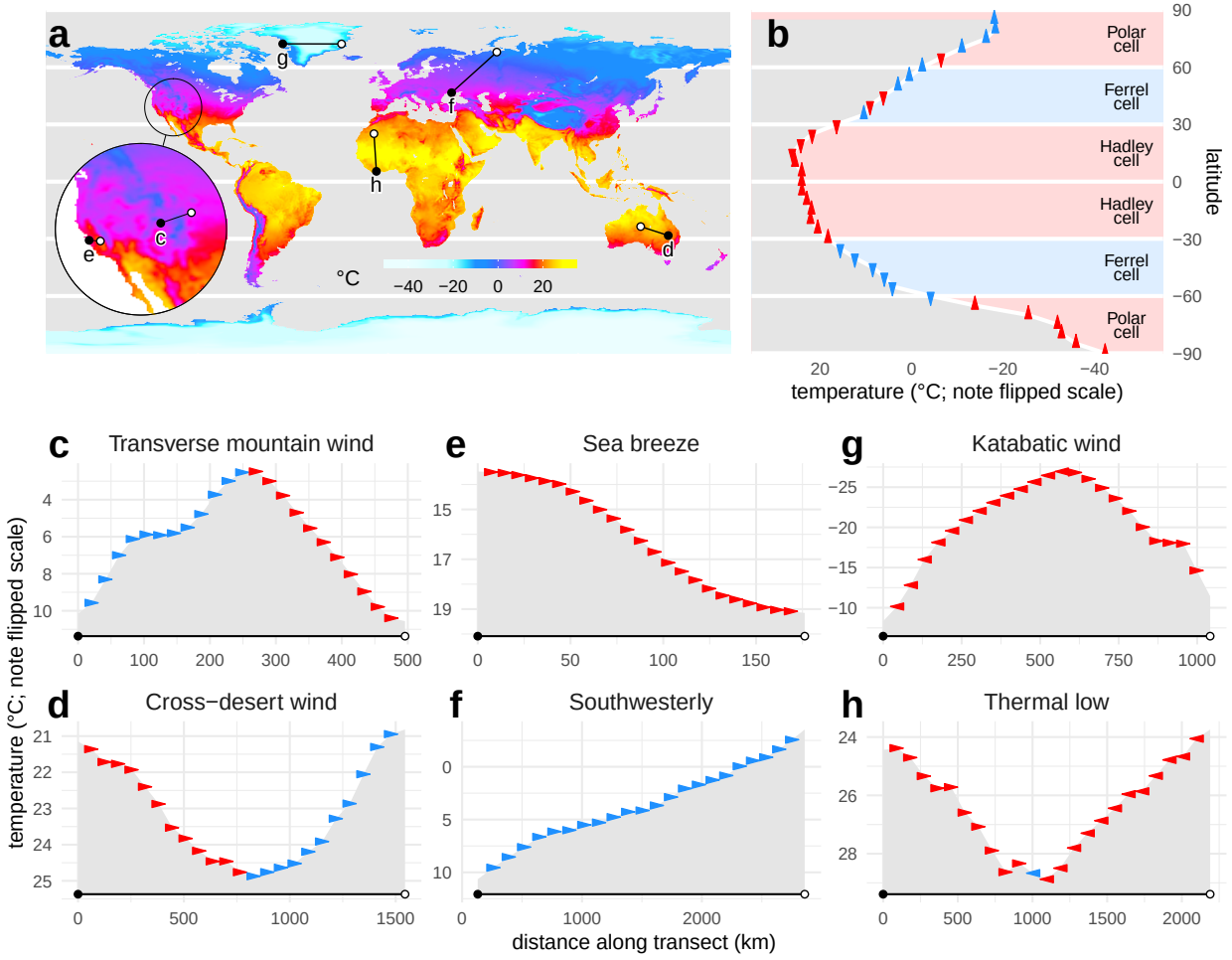

Figure 2.2: Prevailing wind alignment with temperature gradients. (a) Global temperatures and locations of examples displayed in panels *c*–*h*. (b–h) Characteristic wind-temperature patterns likely to influence climate tracking. Axes show temperature against distance, with the temperature flipped to resemble mountains that are colder at higher elevations. Arrows indicate the prevailing wind direction with respect to the transect—blue for wind that blows towards cooler locations (facilitation) and red where it blows towards warmer locations (hindrance). (b) Terrestrial meridional winds versus the latitudinal temperature gradient, averaged across 5° latitudinal bins; the coloured rectangles represent hypotheses based on idealized atmospheric cells. (c–h) Examples of local wind-temperature relationships: transverse mountain wind (c), cross-desert wind (d), sea breeze (e), southwesterly wind (f), katabatic wind (g) and thermal low (h); these transects were selected to roughly parallel prevailing winds.

2.5 Upwind and downwind connectivity to analog climates

Under a given climate change scenario, a focal site will have a particular spatial distribution of climate analogues: outbound analogues represent attractive emigration targets with future climates similar to the site's historic climate, whereas inbound analogues represent attractive immigration sources with historic climates similar to the focal site's future condition (Hamann et al., 2015) (figure 2.3a-d). (Although originally termed forward and backward analogues (Hamann et al., 2015), we find the outbound and inbound terms (Kling et al., 2020) more intuitive and use them here.) In contrast to previous studies, we calculated a continuous metric of inbound or outbound climatic similarity (figure S2.12) rather than a discrete classification of analogues. Mapping landscape connectivity to analogue climates has become a major topic of conservation planning, but has focused on actively dispersing terrestrial organisms (Keeley et al., 2018). Here we report an analysis of climate change connectivity by wind.

Unlike atmospheric plume models, which represent a single wind-dispersal event associated with a specific weather episode (Nathan et al., 2005; Savage et al., 2010), a dispersal model aimed at capturing long-term biogeographical shifts should integrate over time (which encompasses the long-term distribution of local weather patterns) and over space (which encompasses numerous short dispersal events that link an origin and destination over multiple generations). Landscape connectivity models that represent conductance between neighbouring grid cells are well-suited to model spatial diffusion, and have been used to study terrestrial dispersal (Zeller et al., 2012), marine dispersal (Treml et al., 2008) and wind dispersal using individual wind fields that represent average or instantaneous wind conditions (Fernández-López & Schliep, 2018; Munoz et al., 2004). We extended this landscape wind-connectivity ('windscape') approach to allow multidirectional connectivity parameterized using decades-long time series of hourly wind fields. For a given site, this model predicts the relative accessibility of downwind and upwind dispersal landscapes, which represents the potential for outbound emigration and inbound immigration, respectively (figure 2.3e,f).

The expected time for wind to travel between two points, given the full spatiotemporal distribution of wind regimes across a landscape, is measured in wind-hours. Conceptually, this offers a more realistic alternative to geographical distance for predicting the actual time for genes or species to reach a site. As a simple illustration, for a species with a one-year generation time and propagules that spend one hour aloft per dispersal event, the mean spread rate would be one wind-hour per year and the expected years until colonization would equal the wind-hours between sites. Although this example does not reflect the complexity of a species-specific demography, propagule aerodynamics or vertical uplift (Nathan et al., 2011; Nathan et al., 2005; S. Thompson & Katul, 2008), we propose that relative rates of spread for given genes or species should be roughly proportional to the wind-hours to sites across the region. To validate these model predictions with empirical data and to integrate windscape models with biologically explicit range-expansion models (Nathan et al., 2005;

Savage et al., 2011) are important areas for future research. For our purposes, we quantify wind accessibility as the inverse of wind-hours between points (figure 2.3g,h). This inverse function resembles the long-tailed wind dispersal kernels used in many studies (Bullock & Clarke, 2000; Bullock et al., 2012; Nathan et al., 2011), which reflect the non-linear probability of dispersal at increasing distances.

Comparing a site's climate analogue and wind-accessibility landscapes (figure 2.3c–h) shows how wind patterns are predicted to affect the dispersal accessibility of climatically suitable sites. Wind–climate overlap maps (figure 2.3i,j), calculated by multiplying wind accessibility by climatic similarity, represent areas with the highest predicted potential for successful natural migration. Using the 30-year hourly wind data and baseline and future temperature data (1979–2013 versus 2060–2080 under the Representative Concentration Pathway 8.5 emissions scenario), we modelled wind-accessibility and temperature-similarity surfaces for every terrestrial grid cell in a circular landscape 500 km in diameter, in both the inbound and outbound directions. For each landscape we summarized these surfaces by calculating the mean climate similarity, mean wind accessibility and mean wind–climate overlap across cells. The ratio of overlap to climate similarity gives a normalized metric that we call 'wind facilitation', which indicates the degree to which wind is expected to facilitate versus hinder connectivity to the available climate analogues.

Globally, we found that these models predict strong geographical patterns in the wind facilitation of climate tracking. Facilitation is higher in temperate latitudes and on the windward sides of mountain ranges (figures 2.4, S2.2, S2.2, S2.2). Relationships between facilitation and coastal or elevational gradients are also prominent in some regions, and often differ between the inbound and outbound directions; for example, along the immediate eastern coast of North America, winds that flow offshore are expected to facilitate inbound migration from warmer inland areas, but hinder outbound migration. For cases in which climate analogues are abundant but facilitation is low, wind could hinder range shifts either because it blows in the wrong direction (headwinds) or because it blows too weakly, syndromes that exhibit strong global patterns (figure S2.5).

Patterns in the underlying wind and climate change components are also notable. Wind-dispersal potential itself is much higher at high absolute latitudes, and exhibits strong but regionally variable relationships with elevation (figure S2.6). Prior studies hypothesized that the latitudinal wind-speed gradient may be responsible for the higher prevalence of wind-pollinated and wind-dispersed plants at higher latitudes (Regal, 1982). Whether this is due to evolution towards wind dispersal at higher latitudes or to greater colonization of temperate regions by wind dispersers, it illustrates the potentially profound role of global wind geography in shaping biodiversity patterns. It also means our results will be relevant to a larger fraction of the flora in temperate than in tropical areas.

Contrasts between inbound and outbound climate tracking have important ecological and conservation implications. The outbound direction emphasizes the resilience of the taxonomic or genetic diversity currently present at a site, whereas the inbound direction emphasizes the site's ability to sustain diversity and function through immigration of new genes and species; the concepts are therefore most relevant to species-based versus place-

based conservation perspectives, respectively (Carroll et al., 2015; Hamann et al., 2015). Where inbound and outbound migration are balanced, temporal turnover is expected, in which genes and species replace each other as all move up a common gradient; where they diverge, transient ecological states of extinction debt or immigration credit may persist for extended periods of time (Jackson & Sax, 2010). We found weak correlations between wind-analogue overlap area in the outbound versus inbound directions (figure S2.2), which suggests that ecological disequilibria may become widespread, and that the areas of greatest conservation concern may differ by management perspective. This result is driven not by wind, but by climate analogue availability; for example, outbound availability is higher than inbound at low elevations, but this reverses at high elevations (figure S2.7) and the two metrics exhibit a triangular relationship in which they are never both high (figure S2.2d). Such patterns are broadly consequential for both wind- and non-wind-dispersed taxa (D. Ackerly et al., 2010; Carroll et al., 2015; Hamann et al., 2015).

We stress that these model predictions are hypotheses that should be tested and refined by future empirical work. We expect wind-speed-based connectivity to correlate positively with dispersal potential on average, but there is substantial uncertainty in this average, and in the translation from relative to absolute measures of wind accessibility, due to the simple nature of our model. There will also be major variation around the average in the application to different species. In Supplementary Appendix 1 we discuss a number of these uncertainties in more detail, and present a set of sensitivity analyses (figure S2.8– S2.14) related to different model assumptions and parameters. Notably, our overall conclusions are relatively robust under a range of alternative parameterizations. Beyond dispersal dynamics, our focus on the mean annual temperature for the climate change component also adds uncertainty. Sensitivity analyses indicate that wind facilitation patterns based on seasonal temperature and annual precipitation are similar to those for mean annual temperature, whereas patterns based on seasonal precipitation differ substantially (figure S2.13); our results will therefore be less relevant for species whose climate suitability is highly dependent on precipitation seasonality.

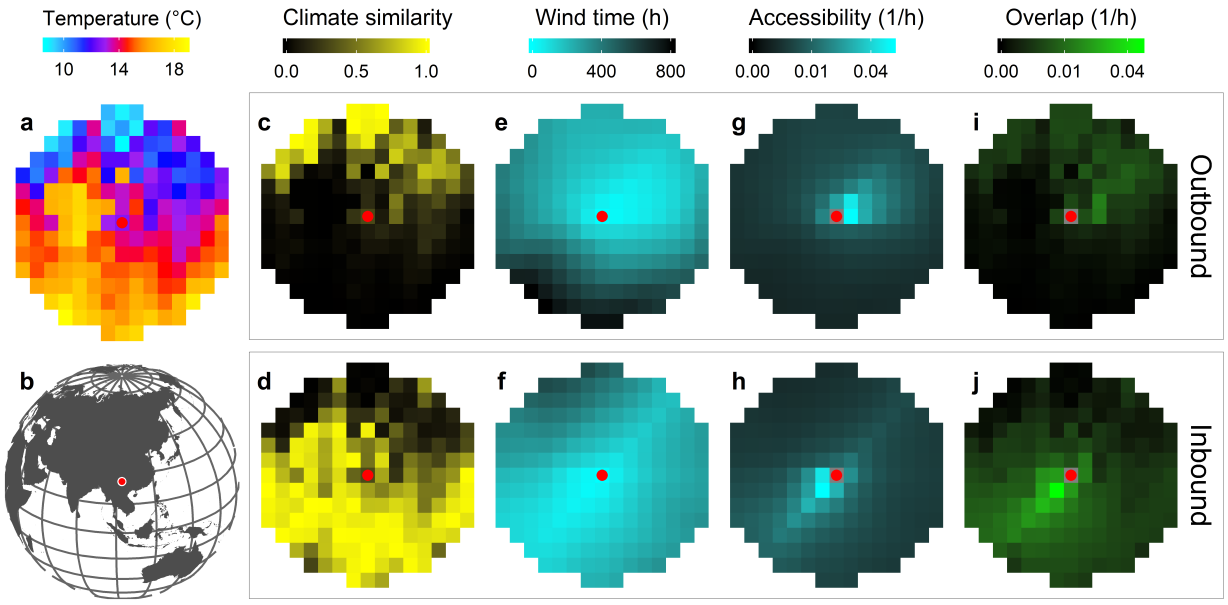

Figure 2.3: Example wind and climate change landscapes for one focal site. (a–d) For the location in *b*, twentieth century temperature patterns (a) combined with future climate change generates patterns of outbound (top row) and inbound (bottom row) climate similarity (c,d), which represent emigration and immigration targets for the site. (e-h) Wind time–distance estimates (e,f) that represent the travel time from and to the site are converted into wind accessibility surfaces (g,h). (i,j) The product of wind accessibility and climate similarity is a wind–climate overlap surface, which represents areas that are both accessible and suitable, and are predicted to be the most likely destinations and origins for migrant genes and species associated with this site.

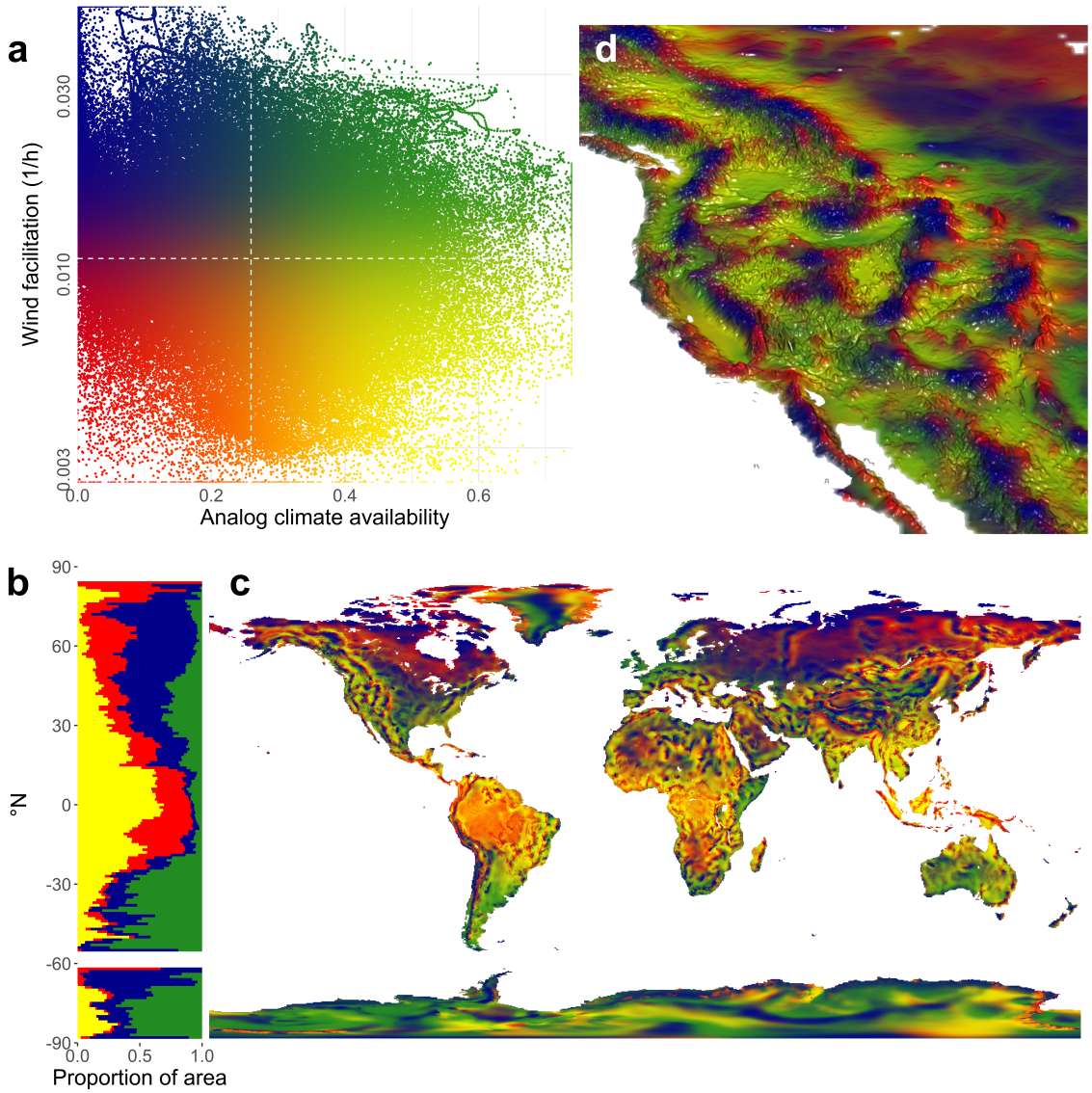

Figure 2.4: Modelled global patterns of downwind accessibility to outbound climate analogs. (a) Relationship between outbound climate analogue availability and wind facilitation; colours represent combinations of the two variables and extreme outliers were rescaled for visualization. (b) Latitudinal trends in the relative prevalence of the four categorical combinations of these metrics, which are delineated by the dashed median lines in *a*. (c) Global geographical patterns in the two metrics. (d) Regional perspective highlighting the mountain ranges of western North America, where the dominant temperature gradients are elevational and prevailing winds flow towards the east-northeast. Colours in all the panels correspond to those in *a*. See figure S2.2 for the inbound results that correspond to these outbound results.

2.6 Case study of genetic rescue and range expansion in *Pinus contorta*

Windscape models can be used to assess the potential for genetic rescue and species range expansion for particular focal species, incorporating additional geographical and biological features. We demonstrate this for lodgepole pine (*P. contorta*), a wind-dispersed, wind-pollinated tree of major ecological and commercial importance in western North America. In this species, pollination occurs in late spring and seed release occurs mainly during late summer and autumn (Owens, 2006); we thus used wind data from these seasons for the gene flow and range-expansion models, respectively. Also, as pine seeds (unlike pollen) probably have higher rates of abscission and uplift under higher wind speeds, we modelled connectivity for range expansion and gene flow as quadratic and linear functions of wind speed, respectively.

Genetic rescue entails gene flow that bolsters a population's declining fitness under warming climates (Bontrager & Angert, 2019; Sexton et al., 2011). We modelled this by calculating inbound wind conductance between all the population pairs within the current species range, and comparing their current and predicted future climates in light of published population-level thermal performance curves (Rehfeldt et al., 1999; T. Wang et al., 2010), which reflect patterns of niche breadth and local adaptation in *P. contorta*. The highest potential for genetic rescue occurs in populations in northeastern portions of the species range that are downwind from numerous substantially warmer populations; greater vulnerability is predicted for populations near the warm edge of the range and for populations in cooler areas but with poor inbound wind connectivity to warmer populations (figure 2.5a–c). Although long generation times limit evolutionary rates, these results may reflect not just future gene flow, but also existing in situ adaptive genetic variation from historic gene flow.

To assess the role of winds in range-expansion potential, we used an environmental niche model based on multiple temperature and precipitation variables to predict future suitability across the region, and modelled outbound wind connectivity from every location in the current range to the surrounding region. Sites with a high future suitability that are downwind from many occupied sites are most likely to be colonized, whereas areas with low suitability or poor wind connectivity to the current range have a lower predicted colonization potential (figure 2.5d–f). For lodgepole pine, most newly suitable habitat is predicted to be northwest of the current species range, whereas wind-dispersal potential is predicted to be strongest towards the east. This suggests that wind is less likely to facilitate a rapid natural expansion to the northwest, whereas higher-elevation areas encircled by the species range are more likely to be both suitable and wind accessible.

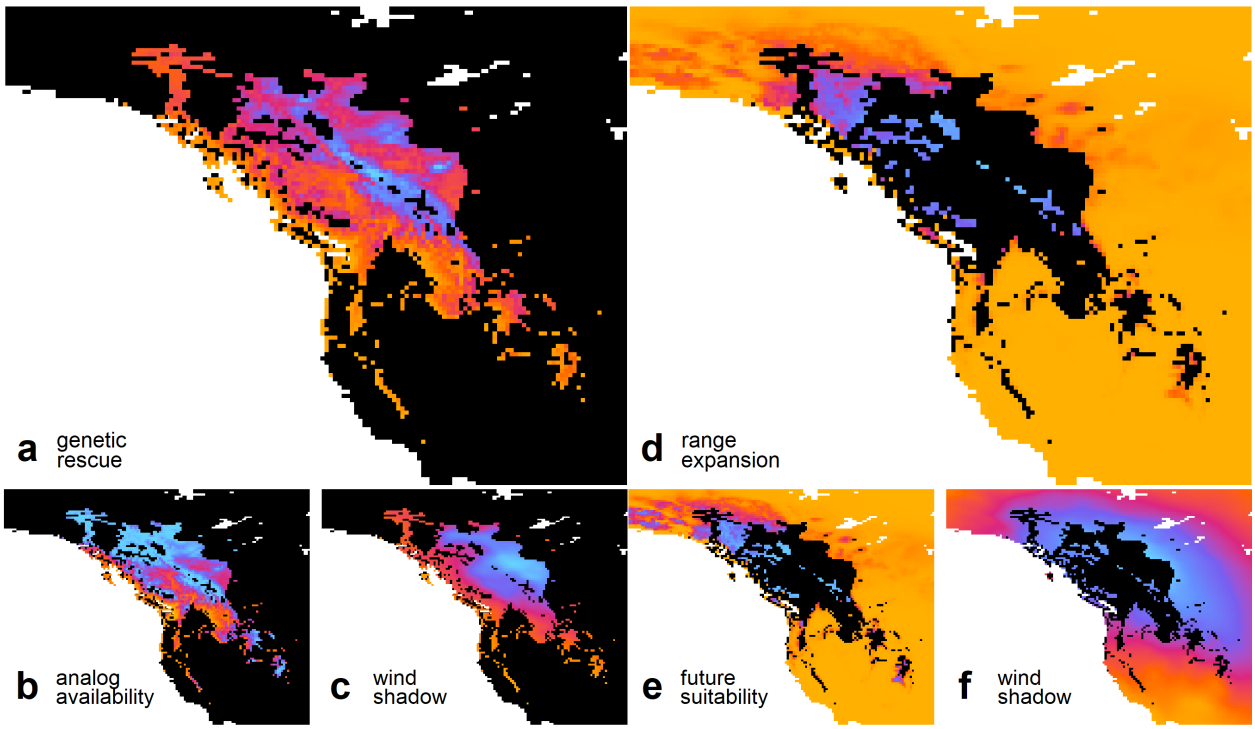

Figure 2.5: Case study of wind connectivity and climate resilience for lodgepole pine in western North America. (a–c), Potential for wind-mediated genetic rescue (a) within the current species range; higher values indicate upwind accessibility to many populations (b) with high inbound climate similarity (c). (d–f) Potential for wind-mediated range expansion (d), with sites outside the current species range (shown in black) coloured by the product of future suitability (e) and wind dispersal pressure (f). Gold–red–blue colours represent continua from relative vulnerability to resilience in all the maps; units are h^{-1}, except in *b* and *e*, which are unitless.

2.7 Discussion

In this study, we explored the possibility that global wind patterns may influence the ability of wind-dispersed genes and species to keep up with climate change. Combining a novel wind-connectivity model with future temperature data, we generated hypotheses about the sorts of patterns that could result from this phenomenon, such as the facilitation of upward elevational migration on the windward mountain slopes and poleward migration in temperate regions. The wind-dispersed biota in these regions may be able to naturally adapt to future temperature increases through genetic rescue and range shifts, whereas areas characterized by wind hindrance may have less capacity to adapt and could be higher priorities for management intervention. At the level of the individual species range, we also projected how wind could influence range expansion and adaptive gene flow, and so facilitate climate change resilience in some landscapes but hinder it elsewhere. Testing these hypotheses with empirical data and refining windscape-modelling methods to increase their biological and meteorological realism are important priorities for future studies. If winds do shape future climate vulnerability patterns as predicted here, it could have profound ecological consequences, not just for wind-dispersed species, but also indirectly for entire ecosystems in which they play important roles, such as temperate forests with the majority of trees are wind-dispersed, wind pollinated or both. Our results are also relevant in cases when the goal is to prevent range expansion, such as for pathogens and invasive species.

Although there is a long history of wind-dispersal modelling, the role of wind geography has been underexplored at the landscape-to-regional scales important for the dynamics of species ranges, metacommunities and population genetics, including responses to climate change. The connectivity modelling approach we utilize here helps address this gap and offers hypotheses about the relative ease of wind dispersal between locations. Here we combined these predictions with data on future climate change to predict where wind may facilitate versus hinder climate adaptation. Windscape models also generate predictions about historical patterns—predictions that will be useful to both improve dispersal models and climate vulnerability forecasts and also to understand historical ecological patterns. Windscape models hold promise for integration with climate-change-focused studies on simulated range expansion, incomplete range filling, palaeoclimatic range shifts and long-distance gene flow, as well as diverse areas of spatial ecology and biogeography not explicitly connected to climate change.

2.8 Methods

Climate data

Our analysis is based on wind data from the CFSR (Saha et al., 2010), a gridded global climate reanalysis dataset with a temporal resolution of 1 h and a spatial resolution of 35 km. The CFSR is a weather model continually parameterized with empirical hourly data

from meteorological stations worldwide, and is considered the best-available representation of the actual state of the Earth's atmosphere over recent decades (Saha et al., 2010). We used hourly mean near-surface (10 m) zonal (u, that is the east-west component) and meridional (v, that is the north-south component) wind speeds from 1980 through 2009 (n = 262,800 hourly time steps), which we converted from the native Gaussian grid format into latitude-longitude raster grids with a spatial resolution of 0.312°. Data from other atmospheric heights were also compared with winds 10 m above ground in a sensitivity analysis (figure S2.9) and found to yield similar global patterns of wind facilitation.

We used gridded climate surfaces for historical (1979–2013 mean) and projected future (2060–2080 mean) time periods from the CHELSA (climatologies at high resolution for the Earth's land surface areas) downscaled climate dataset (Karger et al., 2017), aggregated to the CFSR spatial grid. Future data were the mean of an ensemble of ten Coupled Model Intercomparison Project 5 (CMIP5) models (ACCESS1-0, CESM1-BGC, CESM1-CAM5, CMCC-CM, FIO-ESM, GISS-E2-H, inmcm4, IPSL-CM5A-MR, MIROC5, MPI-ESM-MR) for the Representative Concentration Pathway 8.5 emissions scenario. The primary analyses were done using mean annual temperature, with the exception of the *P. contorta* species distribution model, for which we used a total of 12 climate variables (monthly minimum and maximum temperatures and monthly total precipitation for January, April, July and October).

Wind regimes

To characterize the wind regime of each grid cell, we calculated three summary statistics based on the 30-year time series of hourly u and v wind speeds: mean speed, prevailing direction and anisotropy. Hourly u and v components were first converted into hourly speed ($sqrt(u^2+v^2)$) and direction ($arctan(v/u)$). The mean speed was calculated as the average of the hourly speeds. The prevailing direction was calculated as the circular mean of the hourly direction, weighted by speed. Anisotropy was calculated as 1 minus the circular standard deviation of the hourly wind direction, weighted by speed, and can theoretically range from 0 for a location with a perfectly uniform circular distribution to 1 for a location with no variation in wind direction.

Wind–temperature alignment

To illustrate the spatial patterns of climate change headwinds and tailwinds, we compared local prevailing wind direction with local temperature gradients. For a one-dimensional analysis along a transect across a sequence of grid cells (figure 2.2c–h) or along a global sequence of latitudinal bins (figure 2.2b), the wind–temperature alignment at each point is a binary variable that indicates whether the sign of the prevailing wind matches the sign of the temperature gradient. The wind sign at each point is positive if the angle between the prevailing local wind bearing and the transect bearing is acute, or negative if it is obtuse; this is most relevant if transects run parallel to the prevailing winds, and we chose examples

accordingly (figure 2.2). The sign of the temperature gradient at each point is positive if its leading neighbour is colder than its lagging neighbour, and negative if it is warmer.

For a two-dimensional analysis (figure S2.1), alignment is an angle between 0 and 180° that represents the difference between the prevailing wind direction and the angle of the local temperature gradient. This temperature gradient angle is calculated by fitting a plane across the temperature values for a focal cell and its eight closest neighbours, as described by Dobrowski et al. (2013).

Wind connectivity

We used graph-theory-based methods from landscape connectivity modelling to estimate wind connectivity between pairs of grid cells. In our model, each grid cell ('node') in a global graph has 16 connections ('edges'), which include an inbound and outbound connection with each of its 8 'queen' neighbours. Conductance along each of these edges represents the frequency and speed of wind flowing in that direction, averaged over the long-term distribution of hourly wind conditions at both nodes. Note that although our main analysis uses wind speed directly in these conductance calculations, wind speeds can also be transformed first to represent the non-linear relationships between wind speed and dispersal expected for particular species, implemented for seed dispersal in the *P. contorta* case study and explored in figure S2.10.

For a given hourly timestep at a given node, conductance was allocated to four edges based on wind speed and direction at that node. A wind blowing towards the east-northeast contributes conductance to its eastern and northeastern neighbours, and also conductance from its western and southwestern neighbours. Conductance (s^{-1}) is calculated as wind speed (ms^{-1}) divided by intercell distance (m), and is allocated across these edges in proportion to the difference between the wind direction and the bearing to the centre of each neighbouring cell. For example, a wind blowing at 81° is 80% of the way between its northeastern neighbour at 45° and its eastern neighbour at 90°, and would thus contribute 80% of its speed to the former edge and 20% to the latter. Angles and distances between nodes were calculated to reflect the distortion of a square latitude–longitude grid wrapped on a geodesic spheroid, and edge-conductance values were averaged over many hourly wind values to develop a final global connectivity graph. As our focus was on terrestrial organisms, we downweighted conductance over water by 90%, which makes dispersing over large lakes and oceans difficult but not impossible. Finally, edge-conductance values were inverted to derive resistance (s) to represent the expected wind travel time along every edge of the graph, and the results were converted into units of hours for ease of interpretation.

Based on this connectivity graph, cumulative resistance between a given pair of grid cells can be calculated in either direction using a variety of algorithms from graph theory; we used a least-cost-path algorithm (implemented in the R package gdistance (Etten, 2017)), which identifies cumulative travel time along the shortest path that connects two locations (figure 2.3e–f). Our focal metric, wind accessibility, is calculated as the inverse of cumulative wind-hours (figure 2.3g,h). Alternatives to this inverse function for wind accessibility yield

similar results, which indicates that our qualitative results are not especially sensitive to this modelling choice (figure S2.11). For every terrestrial grid cell, we calculated wind accessibility both to and from all the other terrestrial cells within 250 km, which generates a distinct upwind and downwind accessibility surface or 'windshed' that represents the ease of inbound or outbound wind dispersal, respectively. A sensitivity analysis using alternative landscape sizes in the range 50–2500 km in radius (figure S2.14) indicates that the final modelled wind facilitation patterns are relatively insensitive to the size of the landscape considered.

Climate similarity

In addition to inbound and outbound wind accessibility surfaces, we calculated inbound and outbound climate similarity surfaces for each grid cell across the same 250-km-radius landscapes. For a given grid cell, we calculated the difference between its historical climate and the future climates of all cells across the landscape (outbound) and also between its future climate and the historical climates of all cells across the landscape (inbound). 'Climate' here refers to mean annual temperature, although we compared this with alternative climate variables in a sensitivity analysis (figure S2.13). Climate differences were converted to unitless similarity values between 0 and 1 (figure 2.3c,d), based on a Gaussian decay function with a standard deviation of $\sigma = 2°C$. This σ value yields a similarity function (figure S2.12) that falls off steeply beyond 1.5°C, a range considered to be a critical threshold for many terrestrial ecosystems (*IPCC Special Report on Global Warming of 1.5 C*, n.d.; Schleussner et al., 2016). Under this function, absolute temperature differences of 0, 1, 2, 3 and 4°C translate to similarity values of 1.00, 0.88, 0.61, 0.32, 0.14 and 0.04, respectively. A sensitivity analysis to evaluate alternative forms and breadths of the climate similarity function (figure S2.12) found that the predicted global wind facilitation patterns are not highly sensitive to this modelling choice.

Wind facilitation

Climate similarity surfaces were multiplied by wind accessibility surfaces to represent areas of overlap that are accessible and climatically similar to a given grid cell (figure 2.3i,j). This yielded a total of six surfaces associated with each grid cell: wind accessibility, climate similarity and wind–climate overlap, each in the inbound and outbound directions. Next, we calculated the mean value across each of these surfaces to derive landscape summaries, which gave the amounts of wind-accessible area, analogue climate availability and wind–climate overlap area in the moving window around each grid cell. Finally, we divided the mean wind–climate overlap for each cell by its mean climate analogue availability to calculate the proportion of climatically similar area that is accessible by wind, a variable we call outbound or inbound wind facilitation, which indicates the extent to which wind is projected to facilitate or hinder the dispersal of genes and species to or from suitable sites.

We also characterized the degree to which cells fall into one of four relative wind-facilitation syndromes based on how they ranked globally in terms of climate analogue avail-

ability, wind facilitation and windshed anisotropy across their surrounding landscapes. Sites were considered 'climate limited' if they ranked low for climate availability. Non-climate-limited sites were considered wind facilitated if they ranked high for the facilitation ratio, or wind hindered otherwise. Wind-hindered sites were considered 'direction hindered' if they ranked high for directional divergence (with winds consistently blowing away from climate analogues) and 'speed hindered' if they had a low directional divergence. Directional divergence was measured as the product of windshed anisotropy (calculated as one minus the circular standard deviation of the bearings to all cells in a site's 500-km-diameter landscape, weighted by their wind accessibility) and divergence angle (calculated as the angle between bearings to the centroids of the windshed and climate surfaces, with centroids defined as the weighted mean coordinates of all the cells in a site's 500-km-diameter landscape, weighted by accessibility or climate similarity).

P. contorta case study

To model how wind patterns are predicted to shape genetic rescue and species range expansion in lodgepole pine, we transferred an expert range map that represents the current distribution (Little Jr, 1971) to the CFSR raster grid. For the gene flow analysis, to model the genetic rescue potential for a given population in the species range, we calculated both upwind accessibility and inbound climate similarity to every other cell in the range, and then summed the product of these two values across all cells in the species range. This process was repeated for every grid cell in the species range. To calculate the climatic similarity, the mean annual temperature was used with a niche standard deviation of 2°C, to approximately match the estimated thermal niche breadth of individual populations of *P. contorta* (Rehfeldt et al., 1999; T. Wang et al., 2006; T. Wang et al., 2010).

To model the species range expansion, we fitted a MaxEnt climatic niche model (Phillips et al., 2006) based on the 12 temperature and precipitation variables listed above, using the species current range as presences and the surrounding region as background. We then estimated future climatic suitability by projecting the model using future climate data. To estimate the wind-dispersal potential outside the current range, we generated a region-wide downwind accessibility surface for every grid cell in the current range and took the sum of these surfaces to represent the estimated dispersal shadow of the entire species range. We used a quadratic wind conductance function because the dispersal of heavier seeds often exhibits exponential relationships with windspeed. The summed wind-shadow surface was multiplied by the climatic suitability surface to identify areas outside the current range that are predicted to be both suitable and accessible.

CMIP5 analysis

To assess the long-term stability of prevailing winds over periods of climate change, we compared wind between the Last Glacial Maximum, twentieth century and late twenty-first century, based on general circulation model simulations (Taylor et al., 2012). To derive wind

climatologies for an ensemble of four CMIP5 models that had simulations available for all three time periods (CNRM-CM5, IPSL-CM5A-LR, MIROC-ESM and MRI-CGCM3), we calculated mean u and v windspeeds across years for each model run, averaged these across runs for each model and finally averaged these across models to derive a final ensemble mean. Both u and v values were then compared across time periods for each grid cell.

R code

All data analysis was done in R version 3.5.1 (R Core Team, 2017). The code is available online (Kling, 2020a, 2020b).

2.9 Extended discussion: uncertainty and sensitivity

As with any modeling exercise, our data and methods contain uncertainty. In this supplement we discuss several sources of uncertainty in the underlying wind data and their relevance for this study, and in the aspects of wind dispersal dynamics that are and are not captured by our modeling approach. In addition, we present the results of a set of sensitivity analyses comparing global wind facilitation patterns as reported in the main manuscript to a variety of alternative parameterizations including winds at different seasons of year (figure S2.8) and different atmospheric heights (figure S2.9); different functional forms of the wind conductance function (figure S2.10) and the wind accessibility function (figure S2.11); different forms and breadths of the climate similarity function (figure S2.12) and different climate variables (figure S2.13); and dispersal landscapes of different sizes (figure S2.14). We also explore changes in wind patterns between the Last Glacial Maximum (LGM), 20th century, and late 21st century (figure S2.15 & S2.16).

Trends in wind conditions

It is important to consider whether the 20th century wind regimes analyzed here are reasonable proxies for future Anthropocene wind conditions; changes since the mid-Plestocene are also of interest for questions of historic biogeography, though those are not directly relevant to the present study. The extent to which climate change may alter wind regimes and dispersal patterns is an important and active area of research, and there remains significant uncertainty about this topic. While global mean windspeeds appear to have declined in recent decades (McVicar et al., 2012; S. E. Thompson & Katul, 2013) and some studies suggest future changes in windspeeds over the next century could be quite substantial in places (Bullock et al., 2012), other large-scale analyses predict that future mean windspeeds will change on the order of only +/-10% over most of the globe during the 21st century (Kulkarni & Huang, 2014; Ma et al., 2016; Pryor & Barthelmie, 2010, 2011), a relatively modest effect in the context of our analysis.

Prevailing wind direction is important in addition to wind velocity, and we used data from global circulation models to explore changes in prevailing winds between the LGM, the 20th century, and the late 21st century. We found that patterns were predicted to be broadly consistent across these periods (figure S2.15 & S2.16), with the notable exception of large historic changes in wind conditions over regions that were glaciated during the LGM. As the resolution of future regional and global climate models increases, and as the dynamics of these models grow more realistic, it will become possible to directly incorporate predicted wind changes into wind connectivity models. In the meantime, potential future wind trends represent an important priority for future research and an important source of uncertainty in our analysis.

Spatial and temporal scale

Compared to many analyses in spatial ecology, the Climate Forecast System Reanalysis data used in our analyses (Saha et al., 2010) have fairly high temporal resolution (one hour), but relatively coarse spatial resolution (35 km), which smooths over fine-scale spatial variation within landscapes and second to minute scale temporal variance in wind conditions. Spatial averaging means that individual localities within grid cells will vary in their wind regime properties; uncertainty from within-pixel variance is presumably higher in areas with complex terrain, as suggested by higher observed between-pixel variance in mountainous areas (main manuscript figures 2.1 & 2.3). Temporal averaging will mean that many places experience brief wind gusts far stronger than indicated by hourly means. High-frequency windspeeds tend to be highly autocorrelated at sub-hourly timescales, particularly under conditions with strong winds (Ren et al., 2018). This suggests that hourly means are likely a reasonable predictor of key spatial patterns in the timing, direction, and magnitude of wind dispersal, though as discussed below they may be less predictive of dispersal for low-terminal-velocity propagules that disperse in low winds and for locations with very weak winds. Hourly wind data have been found to be strong empirical predictors of dispersal patterns (Bullock & Clarke, 2000). These factors suggest that the resolution of the CFSR data is likely sufficient to capture the broad-scale patterns that are the focus of this paper, though further research on geographic patterns in the temporal scaling of windspeed would be valuable.

Climate data resolution is another important source of uncertainty in our results. Many of the grid cells used in our analysis will encompass substantial climate variation, particularly in heterogeneous landscapes like mountains. These microclimates will provide critical opportunities for inbound and outbound migration at shorter distances than illustrated with coarse grid cells. This contributes uncertainty to our analysis, but because climate velocity patterns are often relatively insensitive to resolution (Hamann et al., 2015) and because microrefugia can't be expected to shelter the full diversity and abundance of species found on a given landscape, coarse-grain analyses remain relevant.

It is also important to consider how the spatial and temporal scale of our analysis connects to the temporal scale of species range expansion and gene flow. Differences in spread rates

among species will depend on their generation time, fecundity, and degree of adaptation to wind dispersal (Nathan et al., 2011). Species with lighter dispersers, higher fecundity, and shorter generation times can spread at faster rates, making them less dispersal-limited under a given velocity of climate change. For example, fern species with highly-mobile spores and short generation times adapted relatively rapidly to Quaternary climatic changes and may experience little to no lag under rapid future climate change, while some tree species are still lagging behind climate changes since the last glacial maximum and are likely to be severely constrained over the next century (Nathan et al., 2011; Normand et al., 2011; Svenning & Skov, 2007). In aiming to be relevant for both slow and fast dispersers, our model takes a relative view of accessibility via wind dispersal: it makes no statement about how likely it is for a given species to colonize a location with a wind facilitation value of 0.01 by the year 2070, predicting only that it is relatively more likely to colonize a location with a higher vs. a lower value. The one aspect of the model that does impose an absolute limit on dispersal distances is the radius of the dispersal landscape considered for each location; we consider the 250 km radius to be a reasonable extent over which to evaluate range shifts and gene flow between now and 2070, but the reasonableness of this assumption will vary by species; in a sensitivity analysis comparing landscapes ranging from 50 km to 2500 km radius in size (figure S2.14), we found that predicted global wind facilitation patterns are fairly consistent across these scales.

The time scale of climatic change will also determine which portion of the wind frequency distribution and species dispersal kernel are most relevant. Dispersal kernels express the probability of dispersal over a range of distances, with high probabilities of dispersing short distances and increasingly low probabilities of dispersing increasingly longer distances. Vanishingly small probabilities of extremely long-distance dispersal can become near certainties when integrated over the timescales involved in paleoclimatic responses to climate change, such as range shifts over the 20,000 years since the Last Glacial Maximum. Colonization dynamics on these biogeographic timescales are likely driven by highly unusual extreme wind events that may have little relationship to common wind patterns (Clark et al., 1998; Nathan, 2006), and so a model like ours that is parameterized by wind conditions over a few decades may have limited use in these contexts. In contrast, gene flow and range shifts over the ecological timescales between now and 2070, which are the focus of this paper, will not have the opportunity to rely on extremely rare events. Newly-arrived species or genes take generations to become abundant after arriving in a location, particularly if the number of colonists is small. For many species, colonists will need to arrive at a site early and in large numbers in order to establish at levels that are ecologically relevant for adaptation to decadal climate change during this century (Koontz et al., 2018; Simberloff, 2009)—a process that will depend more heavily on the relatively common wind events and local connectivity emphasized in a model like ours. Our model is not designed to address slow historic processes dominated by rare dispersal events, and further work would be necessary to modify and validate wind connectivity analyses in the paleoecological context.

Dispersal unit release, uplift, and transport

Long-distance wind dispersal generally cannot occur without three essential processes: dispersal unit release (e.g. seed abscission or animal takeoff), uplift in the air column (e.g. by updrafts or active thrust), and horizontal transport (by wind). Our model only represents the horizontal transport component, and ignoring the other factors is an important source of uncertainty in our results.

If release and uplift occur randomly with respect to horizontal wind conditions, then our approach using time-integrated horizontal windspeed distributions should be a reasonable representation of long-term dispersal potential via near-surface winds. But release and uplift in any real-world species will of course be nonrandom, occurring at particular times of year and day and triggered by particular weather and wind conditions. In cases where these detailed predictors of dispersal timing are known for a specific study species (Greene, 2005; Maurer et al., 2013; S. J. Wright et al., 2008), that information would be straightforward to incorporate in wind connectivity models by filtering or weighting wind data according to these covariates, which should reduce uncertainty in the results. We show in figure S2.8 that global wind facilitation patterns are quite similar across different seasons of the year, which suggests that our generic conclusions may be relatively robust to differences in dispersal phenology among species and locations. Phenology aside, our generic model is likely to fit some species and locations better than others. One key species-level variable is the terminal velocity of the dispersal unit, which falls on a gradient from lower-terminal-velocity dispersers (e.g. pollen, spores, cottony seeds, small flying insects, and ballooning spiders) that can achieve long distance dispersal in light wind under gentle updrafts, to higher-terminal-velocity wind dispersers (e.g. large pollen grains and the seeds of many trees and grasses) that fall relatively rapidly and require substantial updrafts or very strong horizontal windspeeds to disperse long distances. For simplicity we refer to these as "light" and "heavy" dispersers, respectively, though terminal velocity is not perfectly correlated with mass. The updrafts required to lift passive wind dispersers are the result of atmospheric turbulence, which can be generated by wind shear, by thermal convection, or by a combination of the two; while thermal convection in the absence of much horizontal wind generates relatively weak uplift forces that are mainly capable of transporting light dispersers, wind shear is capable of generating strong updrafts near the ground that are important for uplifting heavy dispersers (Nathan et al., 2002).

For heavier dispersal units, horizontal windspeed is likely to be a key determinant of dispersal, because higher windspeeds are key drivers of release and uplift as well as of horizontal transport. The seeds of most wind-dispersed plants are abscised by aerodynamic drag, which is proportional to the square of windspeed. Both theoretical and empirical studies have shown rates of seed release increase as a function of windspeed, an effect that varies by species and can be a step function, a linear or quadratic function, or a mix thereof; it may also depend on material wear from wind conditions over time, in combination with wind at the time of release (Greene, 2005; Pazos et al., 2013; Savage et al., 2014; Schippers & Jongejans, 2005; Soons & Bullock, 2008). The strength of vertical uplift from wind shear also increases

as horizontal windspeeds increase (Nathan et al., 2002; Ren et al., 2018; Soons et al., 2004). And in addition to enabling uplift, strong updrafts can also promote seed abscission (Maurer et al., 2013; Savage et al., 2014; Skarpaas et al., 2006), in some cases further amplifying the effects of windspeed on seed dispersal. In a hypothetical species where propagule release rates, uplift by turbulence, and horizontal transport rates all increase linearly with windspeed, the probability of dispersing a given distance would be expected to increase as a power of windspeed—and indeed, empirical and modeling studies for many species have found that seed dispersal distances tend to follow exponential or power relationships with windspeed (Bullock & Clarke, 2000; Dorp et al., 1996; Hensen & Müller, 1997; Heydel et al., 2014; Soons & Bullock, 2008; Soons et al., 2004). Studies have found horizontal windspeed to be the dominant environmental predictor of variation in seed dispersal distance in tree and grass seeds (Nathan et al., 2011; Nathan et al., 2001; Sinha & Davidar, 1992).

In contrast, lighter dispersers are less dependent on strong winds to achieve long-distance dispersal, and the relative importance of release and uplift dynamics unrelated to windspeed may be higher for them, leading to greater uncertainty under our windspeed-focused analysis. Models incorporating these dynamics have predicted that decoupling between windspeed and dispersal distance will be greater in low-terminal-velocity propagules (Heydel et al., 2014), and empirical examples have found that long-distance dispersal for lightweight seeds may be unrelated to windspeed (Tackenberg et al., 2003) or may happen at reduced frequency under high windspeeds (Maurer et al., 2013).

One simple way to begin to account for these different relationships between windspeed and propagule release and uplift in our connectivity model is to alter the form of the wind conductance function, which converts instantaneous windspeeds into connectivity between neighboring grid cells. Implementing this in a sensitivity analysis (figure S2.10), we show that global wind facilitation patterns are relatively similar when using cubic, square, or linear functions of windspeed, but are more sensitive (as would be expected) when conductance is treated as invariant with respect to windspeed. While the linear relationship is straightforward and represents a middle ground, studies on individual taxa should consider which function makes the most sense. Conductance functions could also incorporate factors like threshold windspeeds for seed abscission or empirical relationships between windspeed and turbulence, for cases where those phenomena were known.

The uncertainty in our generic results will also vary by location. For locations with relatively anisotropic wind regimes (blue-purple-red in figure 2.1 of the main manuscript) the timing of release and uplift is less likely to cause dispersal direction to deviate from the generic results, whereas locations with highly variable wind direction regimes (cyan-green-yellow in the figure) have more potential for individual species responses to be decoupled from average wind patterns, due to diurnal or seasonal phenology of dispersal. Local climate and vegetation will also affect the turbulence regimes that lift propagules during wind dispersal (Heydel et al., 2014), with windspeed being a less dominant driver of dispersal of light dispersal units in places where convective turbulence dominates over shear-induced turbulence near the ground (i.e. under conditions with strong solar radiation to drive convection but low windspeeds that would drive wind shear). These conditions may be most

likely in the tropics where windspeeds are lowest (main manuscript figure 2.1) and in the subtropics where daytime high temperatures and the depth of the planetary boundary layer (one indicator of strong convective turbulence) are highest (von Engeln & Teixeira, 2013).

We also note that for propagules that achieve long-distance wind dispersal by uplifting far aboveground, higher-altitude winds will be relevant in addition to the 10 m wind data we used. A sensitivity analysis comparing several atmospheric layers (figure S2.9) shows that winds at hundreds or thousands of meters aboveground yield reasonably similar global patterns of climate tracking facilitation. The turbulent three-dimensional component of wind dispersal remains an important open modeling challenge (Nathan et al., 2005), and how best to incorporate it into wind connectivity models is a question requiring future work.

Climate variables

Our analysis focuses on mean annual temperature, for the reasons explained in the main text. Still, it is useful to explore how much the results change when alternative climate variables, or combinations of more than one climate variable, are used. A sensitivity analysis examining wind facilitation patterns for several additional climate variables (figure S2.13) indicates that wind facilitation patterns based on mean temperature remain relatively consistent when minimum temperature of the coldest month, maximum temperature of the warmest month, and total annual precipitation are considered in addition or instead. When precipitation of the driest and wettest months are considered, the patterns change substantially, and our results will therefore be less relevant for species whose climate suitability is highly dependent on precipitation seasonality.

Chapter 3

Isolation by wind: atmospheric currents shape genetic differentiation, asymmetric gene flow, and genetic diversity across the world's forests

3.1 Abstract

Wind disperses the pollen and seeds of many plants, but little is known about whether and how it shapes large-scale landscape genetic patterns. We address this question by a synthesis and reanalysis of genetic data from 1,900 populations of 103 tree species around the world, using a novel framework for modeling long-term landscape connectivity by wind currents. We show that wind shapes three independent aspects of landscape genetics: populations linked by stronger winds are more genetically similar, populations linked by directionally imbalanced winds exhibit asymmetric gene flow ratios, and downwind populations have higher genetic diversity. (A fourth metric, directional gene flow, is shaped by directional wind flows but is not independent of these other patterns.) Together, these phenomena suggest that both wind strength and wind directionality play significant roles in shaping large-scale genetic patterns across the world's forests. In a secondary analysis focused on isolation by distance and isolation by environment rather than wind connectivity, we show that genes transported by wind, as compared to by animals, have higher absolute rates of gene flow, diffuse more uniformly across space, and are more likely to swamp signals of local adaptation. These findings have important implications for our understanding of ecology and evolution in historical studies as well as biodiversity response to future global change.

3.2 Introduction

Wind is a driving force in plant ecology and evolution, dispersing the seeds, pollen, or spores of a large percentage of all plants. Strong geographic trends in wind speed and direction have shaped major patterns in plant biogeography, such as colonization of oceanic islands (Gillespie et al., 2012; Munoz et al., 2004) and latitudinal gradients in the prevalence of wind versus animal pollination (Regal 1992). While wind's role in these taxonomic and functional diversity patterns is well established, comparatively little is known about wind's possible role in shaping genetic diversity patterns within species ranges. While isolated case studies have hinted at wind's role in shaping directional gene flow in individual species (Ahmed et al., 2009; Born et al., 2012; Z.-F. Wang et al., 2016), others have concluded that prevailing wind direction has no meaningful relationship with gene flow (Ashley (2010) and references therein). It has not been shown whether wind speed and direction systematically shape landscape genetic patterns in species that are dispersed or pollinated by wind.

One reason for this knowledge gap is that long-distance wind transport of seed and pollen is difficult to directly observe, and is challenging to model given the chaotic variability of weather patterns. While wind dispersal modeling has a rich history in plant ecology, studies of long-term dispersal potential have focused mainly on temporal windspeed variability and vertical windspeed profiles and generally ignored geographic variation in wind speed and direction, while dispersal studies that do incorporate this real wind geography have generally focused on individual weather events rather than the long climatic timescales that shape landscape genetics and biogeography. (Note that for brevity we use "wind dispersal" throughout this paper as a generic term for wind transport of seeds, pollen, and spores.) Only recently have methods emerged to combine large-scale, spatially-explicit, high-resolution wind data with landscape connectivity algorithms to move beyond prevailing wind direction and more rigorously model the role of long-term wind variability in biogeography (Fernández-López & Schliep, 2018; Kling & Ackerly, 2020; Munoz et al., 2004). These wind connectivity models use the time-integrated speed of wind diffusion between origin and destination locations as estimates of relative dispersal potential, opening a range of important questions about the role of wind in biogeography and spatial ecology. In this study we employ wind connectivity modeling in landscape genetics for the first time, in a large-scale global analysis aimed at assessing how wind geography shapes gene flow in trees.

Landscape genetic patterns have multiple facets, including rates of directional gene flow, degrees of genetic differentiation, ratios of gene flow asymmetry, and levels of genetic diversity. We hypothesize that these genetic patterns are shaped by separate facets of wind patterns, and we refer to these as the "flow", "isolation", "asymmetry", and "diversity" hypotheses, respectively. As a useful example to illustrate these wind connectivity hypotheses (figure 3.1), we will consider the wind-dispersed, wind-pollinated tree species *Betula pendula*, or silver birch. In this example we reanalyze nuclear microsatellite data sampled from populations across this species' range in western Eursasia, originally collected by Tsuda et al. (2017) for a study unrelated to wind. We apply newly developed wind connectivity models (Kling & Ackerly, 2020) to quantify several measures of wind patterns across this region, and

relate these to pairwise genetic measures across these populations to assess each of the four hypotheses. Wind and genetic metrics have a natural correspondence, because both atmospheric circulation and propagule dispersal can be considered processes of spatial diffusion, and quantified as pairwise relationships among populations.

The flow hypothesis (figure 3.1a) predicts that gene flow across a species range, represented as separate rates of migration linking population pairs in each direction, should be higher along routes with higher rates of wind flow. Wind flow, like gene flow, is a rate. It is quantified here as the inverse of the time it takes an air parcel to diffuse from one location to another, averaged over spatial and temporal variation in wind speed and direction. In the birch example, winds in this region are variable but blow most frequently and strongly toward the east-northeast; for a focal population in the center of the species range, rates of outbound wind flow are thus highest to destinations toward the northeast, while rates of inbound wind flow are highest from origins toward the southwest. These wind flows are positively correlated with estimated empirical rates of directional gene flow in this species after controlling for distance and environment, which is consistent with the flow hypothesis.

Flow patterns like these are a composite of the speed and directionality of movement, and can be decomposed in to independent sub-patterns associated with the isolation and asymmetry hypotheses, respectively. Genetic isolation patterns are a longstanding focus in landscape genetics, and include common phenomena like isolation by distance (IBD) (S. Wright, 1943) and isolation by environment (IBE) (I. J. Wang & Bradburd, 2014). Our hypothesis of isolation by wind (figure 3.1b) posits that populations linked by higher wind speeds will be more genetically similar, after controlling for distance and environment. We can calculate a directionless measure of wind isolation for a given pair of populations by averaging over pairwise wind travel times in both directions, and compare this to genetic differentiation measures like F_{st} to test the isolation hypothesis. In the birch example we see that the central focal population is more wind-isolated from the northern portion of the species range than the southern portion. And across all population pairs of this species, we indeed see the hypothesized positive relationship between wind connectivity and genetic similarity.

Third, the asymmetry hypothesis (figure 3.1c) posits that population pairs linked by winds with higher asymmetry, calculated as the ratio of wind flow in one direction versus the other, will have higher corresponding gene flow asymmetry ratios. Asymmetric gene flow between populations can have important evolutionary and ecological consequences (Aguilée et al., 2016; Garcıa-Ramos & Kirkpatrick, 1997; Kawecki & Holt, 2002; Pringle et al., 2011; Savolainen et al., 2007), and has become an increasing area of focus in landscape genetics with the development of methods to estimate asymmetric gene flow from population genetic data (e.g. Beerli and Felsenstein (1999), Sundqvist et al. (2016)). In the birch example, wind flow asymmetry patterns for the focal population emphasize the prevailing northeastward flow of wind in this region. These correlate positively with estimated gene flow asymmetry across these populations, as expected under the asymmetry hypothesis.

Finally, the diversity hypothesis (figure 3.1d) predicts that downwind populations will tend to have higher genetic diversity. This hypothesis is based on the idea that populations

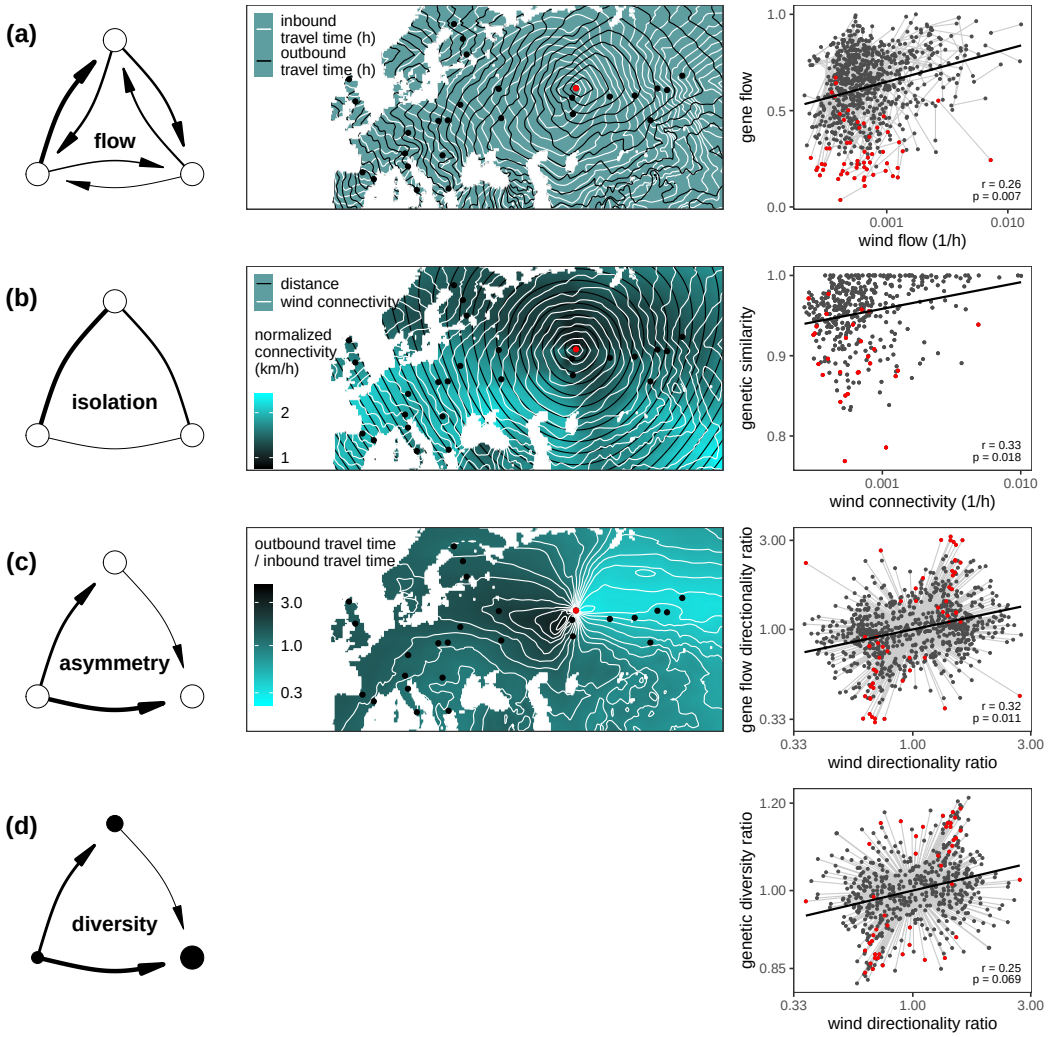

Figure 3.1: Examples of the four facets of landscape genetics and wind patterns explored in this study: (a) flow, (b) isolation, (c) asymmetry, and (d) diversity. This example shows the wind-dispersed, wind-pollinated birch *Betula pendula*, one of the 126 datasets reanalyzed in this study; these genetic data were collected across the species range in western Eurasia by Tsuda et al. (2017) at the populations shown in the maps, for a study unrelated to wind. The schematic diagrams illustrate the four metrics. Wind connectivity landscapes are different for every reference location, and the maps here show patterns in the three wind connectivity metrics for one focal population (red point). The scatterplots show relationships between the wind and genetic metrics, which are all hypothesized to be positive for wind-dispersed genomes, with red points indicating relationships involving the red reference population in the maps; plots show first-order relationships, while the r and p values listed indicate the magnitude and significance of partial correlations controlling for distance and climatic difference. Note that there are three wind metrics and four genetic metrics, since wind asymmetry is used as a predictor for both gene flow asymmetry and genetic diversity.

with higher rates of net immigration will accumulate genetic variation more rapidly than it is lost due to selection or drift, an effect that has been observed in empirical and modeling studies in river systems (Gornall et al., 1998; Lundqvist & Andersson, 2001; Morrissey & de Kerckhove, 2009). Standing genetic diversity influences a population's evolutionary potential and its conservation importance, and can vary widely across a species range. We can assess the downwind diversity hypothesis by calculating the ratio of allelic richness measures for a given population pair, and comparing this to the same measure of wind flow asymmetry as in the asymmetry hypothesis above. The prediction holds true in the silver birch example, in which downwind populations tend to have higher levels of allelic richness.

To summarize, a given pair of populations is linked by a pair of directional wind flows and a pair of directional gene flows. These can be compared directly to assess the flow hypothesis. To assess the asymmetry hypothesis, the pairwise ratio of these wind flows is compared to the pairwise ratio of gene flows. To assess the diversity hypothesis, this same pairwise ratio of wind flows is instead compared to the pairwise ratio of genetic diversities. And to assess the isolation hypothesis, the pairwise mean of wind flows is compared to genetic similarity. It is important to note that wind asymmetry and wind connectivity are entirely independent patterns—when pairwise directional wind flows linking populations are converted into ratios and means, the ratio and mean are by definition uncorrelated across population pairs. Whereas the mean emphasizes wind speed, the ratio emphasizes wind directionality.

Wind-genetic relationships like these in any individual dataset can be instructive, but they are also subject to numerous assumptions and uncertainties that could confound our ability to measure any genetic effect of wind. While it must be true, at some level, that winds shape gene flow patterns in wind-dispersed and wind-pollinated taxa, it is far from clear that these effects will be detectable using available methods. Wind dispersal dynamics and millennial metapopulation histories are far more complex than wind connectivity models and gene flow models can hope to represent, and a variety of assumptions are thus necessary on both the wind and genetic sides of the modeling equation. For instance, wind dispersal takes place in three dimensions (uplift and transport at high elevations can be very important) while wind connectivity models are based on two-dimensional near-surface wind conditions; also, important long-distance dispersal events may occur under rare extreme conditions that are poorly understood and poorly reflected by diffusion models that integrate over wind conditions across many decades, hours, and weather patterns. On the genetic side, inferring historic directional gene flow from static snapshots of population genetic patterns can be attempted using a range of approaches (Beerli & Felsenstein, 1999; Sundqvist et al., 2016; Wilson & Rannala, 2003), but all are subject to sampling uncertainty and make strong assumptions about evolutionary processes and metapopulation dynamics, and even in contrived situations when these assumptions are met there is substantial irreducible uncertainty in inferred gene flow patterns. The historical idiosyncrasies of population genetic dynamics help explain why IBD and IBE, standard concepts for understanding how dispersal and selection shape genetic differentiation among populations, often explain only a small fraction of the observed variance in genetic patterns in the typical tree species. The concept of

isolation by wind will advance our understanding of how wind patterns shape evolutionary ecology only if and when wind connectivity models can overcome these uncertainties enough to detect clear systematic signs of wind-genetic relationships after accounting for distance and environment.

Macroecological approaches that test broad hypotheses across many species offer a partial solution to this uncertainty, by averaging over the idiosyncratic metapopulation histories and assumption violations that in any individual species may be likely to confound the signal of the phenomenon of interest. In this study we used this approach to test whether wind shapes large-scale genetic patterns in trees. We reanalyzed published landscape genetic data for more than 1,900 populations of 103 tree species from around the globe 3.2a), integrating genetic metrics and wind connectivity models with functional trait data to test each of the four hypotheses described above.

The assembled datasets include a heterogeneous mix of nuclear and chloroplast DNA for species with varying reproductive ecology. For each species, the expected role of wind in shaping genetic patterns will depend on the combination of three traits: pollination syndrome, dispersal syndrome, and chloroplast DNA inheritance (figure 3.2b). We classify pollination and dispersal each as either wind or non-wind, a simplification that puts mixed wind-animal pollination or dispersal in the wind category. Chloroplast DNA is maternally inherited and dispersed through seeds in most angiosperms but paternally inherited and dispersed through pollen in most conifers, which sets up important differences in the landscape genetics of these two groups (Petit et al., 2005). By combining these three traits, we can classify each genetic dataset as falling into one of three "wind dispersal levels" indicating whether wind is expected to drive spatial genetic patterns fully, partially, or not at all (figure 3.2b). All partially-wind-dispersed datasets in this classification are diploid nuclear genomes in species that receive wind-dispersed genes from just one of their two parents, while fully-wind-dispersed or non-wind-dispersed datasets include haploid plastid genomes as well as diploid nuclear genomes.

Focusing on different facets of this multispecies dataset, three predictions can then be made about the ways wind should influence a given genetic metric (figure 3.2c). The first prediction is that for fully or partially wind-influenced genomes, wind and genetic patterns will be positively correlated after controlling for distance and environment. The second approach compares the three wind dispersal levels, predicting that increasingly wind-dispersed genomes will exhibit increasingly strong genetic correlations with wind. The third prediction focuses on the subset of datasets where nuclear and plastid DNA were both collected for the same individuals and populations; in our case these all happen to be oak species, in which plastid DNA is exclusively animal-dispersed while nuclear DNA is influenced by both wind and animal vectors. The plastid genome in these oak populations can be used as an in-vivo statistical control to isolate the wind-specific signal in the nuclear genome by removing the confounding effect of animal dispersal, holding everything else constant, with the prediction that the residual nuclear genetic signal will then be positively correlated with wind. We test each of these predictions for each of the four landscape genetic metrics described above (flow, isolation, asymmetry, diversity), for a total of 12 hypothesis tests.

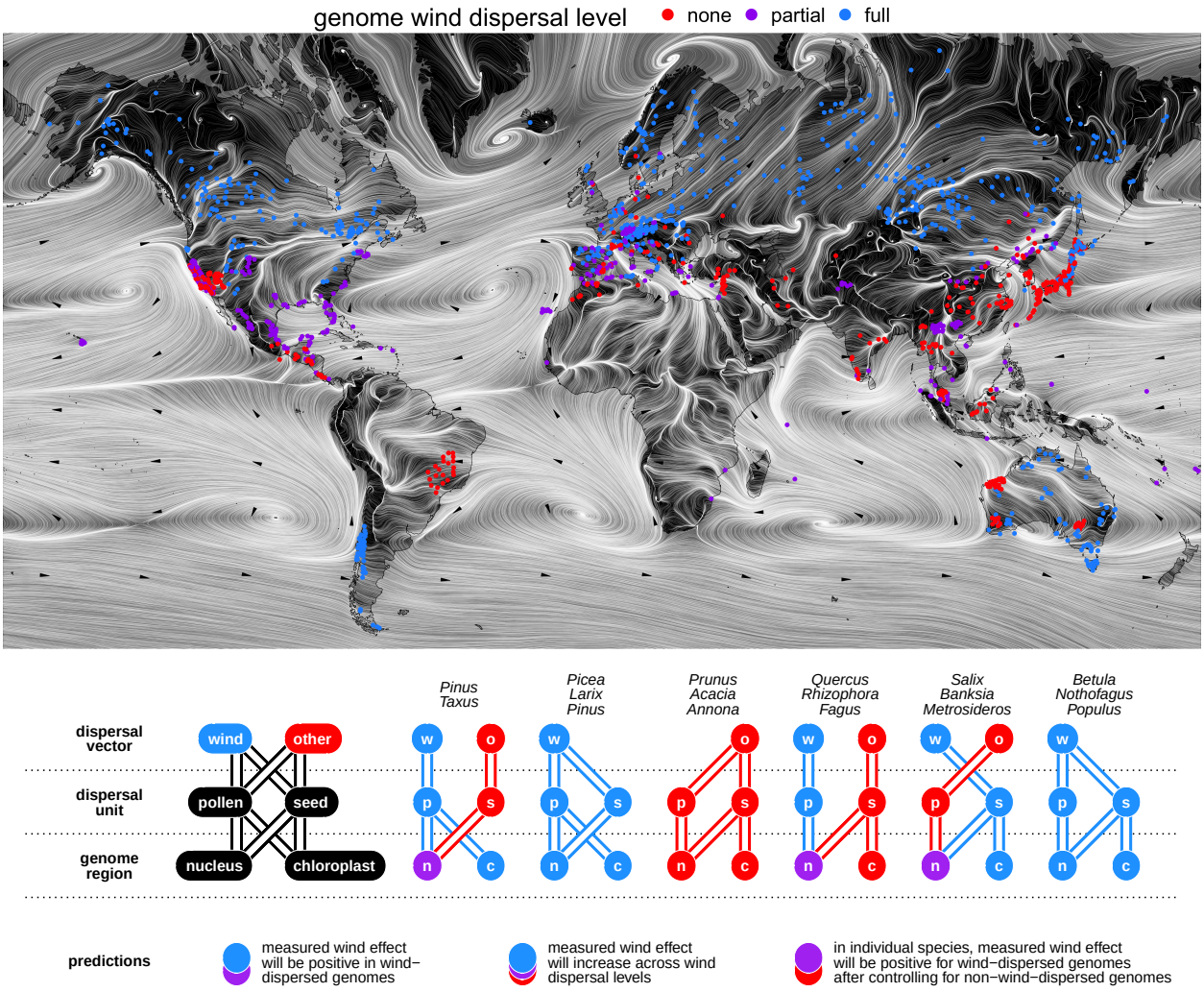

Figure 3.2: Distribution and wind dispersal ecology of the tree genetic datasets analyzed in this study. (a) Population locations (points, colored by wind dispersal level) and global prevailing wind direction (black arrows and white paths; a Mercator projection is used to avoid distorting direction). (b) Schematics of relationships between seed plant genomes and wind dispersal. The influence of wind on a particular region of the genome (nuclear or chloroplast) is determined by species-specific differences in which dispersal unit (pollen or seed) carries the DNA and which dispersal vector (wind or non-wind) transports each dispersal unit. The six distinct syndromes exhibited by species in this study are shown, with example genera listed for each (eight syndromes are theoretically possible, but animal pollination is highly unusual in gymnosperms where chloroplast DNA tends to be paternally inherited). (c) Three predictions about relationships between wind dispersal level and landscape genetic patterns, each addressed using a different combination of datasets.

While distance and environment are useful statistical controls in these models focused on wind connectivity, they are also important beyond their roles as null models. IBD and IBE are emergent patterns that reflect the balance between fundamental processes of selection, migration, mutation, and drift. They are shaped by many aspects of a species' ecology and reproductive biology (Sexton et al., 2014), and they can in turn have important effects on ecology, microevolution, and macroevolution (Givnish, 2010). Many prior studies have shown that life history traits including dispersal and pollination syndromes influence levels of IBD and IBE in plants (e.g. Sexton et al. (2014)), but most macroecological studies on this topic have been meta-analyses of published statistics rather than syntheses and reanalyses of source data. As a secondary question to the wind connectivity analyses described above, here we use the same collection of landscape genetic datasets to ask how dispersal syndrome shapes IBD and IBE. We ignore wind connectivity metrics for this question since wind connectivity is correlated with distance and masks its full effect, and focus simply on the relationships between distance, climate, and genetic differentiation. We ask how wind dispersal level as defined above shapes the degree of genetic differentiation (F_{st}) among populations of trees, and how it shapes the proportion of variation in F_{st} that is explained by distance and environment. Based on prior studies, we expect that genomes with higher wind dispersal levels will exhibit less differentiation at a given geographic or environmental distance. We also expect correlations for IBD to be stronger than for IBE, which is the typical pattern in plants (Sexton et al., 2014). What is less predictable is how these correlations, which reflect signal-to-noise ratios rather than absolute effect sizes, will differ by wind dispersal level.

In sum, our goals in this study are threefold. First, we begin with a basic quantification of wind connectivity patterns among populations of tree species, to provide a descriptive assessment of the potential for variation in wind speed and direction to shape spatial genetic patterns. Next, we use these data to test the four major hypotheses about the way wind connectivity shapes gene flow, genetic differentiation, asymmetric gene flow, and genetic diversity across tree species. Finally, we test how the classical IBD and IBE patterns differ in wind- versus animal-dispersed tree genomes. These statistical tests required that we develop a new extension of existing inference methods due to the novel structure of our dataset, which comprises pairwise data for many species—while methods for analyzing pairwise data and for analyzing hierarchal multispecies data are both widely used, we are not aware of any published method for data that combines both of these characteristics. We therefore introduce two alternative statistical tests for this purpose, each based on extending the traditional partial Mantel test to our multispecies case, and discuss differences between these approaches.

3.3 Results

We found usable data from 72 publications, representing 126 datasets, 102 tree species, and 1,956 populations from around the world, with a total of 28,297 pairwise population comparisons within datasets (figure 3.2; table S3.2). The median dataset had 11 populations.

The data included 56 fully-wind-dispersed genomes, 36 partially-wind-dispersed genomes, and 35 non-wind-dispersed genomes. There were 106 (21) nuclear (chloroplast) datasets, and 113 (14) SSR (SNP) datasets.

Measures of wind conductance among populations show that wind flow rates are highly spatially variable, and that this is a product of both strong directional asymmetry and high geographic variation wind speed (figure 3.3). While wind travel time is correlated with distance, wind flow speeds, which express variation in wind travel times after controlling for distance, varied by a factor of more than 30 across the analysis. The median pair of populations had a wind asymmetry ratio greater than 2:1, while some had ratios greater than 10:1. Pairwise mean wind diffusion speed, representing the strength of wind connectivity after factoring out directionality, varied by a factor of more than 10 over the entire analysis and by a factor of more than 4 across population pairs within the median individual dataset.

Each of the four hypotheses (flow, isolation, asymmetry, diversity) about how these wind patterns affect landscape genetics was tested against three predictions, for a total of twelve wind-genetic relationships. We used two variations of a hierarchical Mantel test (figure S3.1), which we call the "dataset null" test and "global null" test according to whether null distributions were evaluated separately for each dataset and then combined, or first combined into a single null distribution for a global summary statistic and then evaluated. The two inference methods yielded strongly correlated estimates of statistical significance across the twelve hypothesis tests ($r = 0.88$), with the global null method estimating more extreme p-values (one-sided p-values farther from 0.5) on average compared to the dataset null method (figure S3.2).

Eleven of these twelve relationships had effects in the hypothesized direction, and the majority of these were statistically significant (figure 3.4). For the "wind dispersers" prediction that wind-dispersed genomes will have positive wind-genetic correlations, we found positive relationships for all four genetic facets; all facets except flow were statistically significant under both the "global null" and "dataset null" significance tests (figure 3.4 first and second rows, respectively). For the "dispersal level comparison" prediction comparing correlations across functional groups, there was a trend toward higher and more significant correlations for all four genetic metrics; this trend was significant under the global null test for all facets except flow, and under the dataset null test for all facets except diversity. For the "genome control" comparison focused on six oak species, the median partial correlation between wind and the nuclear signal after controlling for the plastid signal was positive for all facets except diversity; this result was significant for the flow metric under the global null test, and non-significant in the remaining facets.

Patterns for flow, isolation, asymmetry, and diversity were largely independent. In the raw pairwise input data (figure S3.3a), gene flow explained 34% of variation in genetic differentiation and 29% of variation in gene flow asymmetry ratios, while all other combinations of genetic metrics had r-squared values less than 5%. In the results for each dataset, partial correlation coefficients and Mantel p-values did not correlate strongly among most genetic facets—with the exception of gene flow and gene flow asymmetry, r-squared values for all combinations of genetic facets were less than 13% (figure S3.3).

Controlling for the latitudinal trends apparent in wind dispersal syndrome (figure 3.2) did not substantially change the estimated relationship between dispersal syndrome and wind-genetic correlations. When absolute latitude was added to models predicting the effect of dispersal syndrome on correlations, the estimated effect sizes decreased only slightly for each of the landscape metrics (table S3.1), though significances did decrease as would be expected when adding a correlated predictor to a model. The latitude effects in these bivariate models were all positive but were extremely weak and not significant, indicating that distance from the equator has a negligible effect on wind-genetic correlations after controlling for dispersal syndrome.

Wind- and non-wind dispersers also differed in their degrees of genetic differentiation, IBD, and IBE, in models with only distance and environment as predictors (figure 3.5). F_{st} was substantially higher in non-wind-dispersed genomes than in fully- or partially-wind-dispersed genomes (figure 3.5c). Median IBD was significantly positive for all wind dispersal levels, and increased with wind dispersal level (figure 3.5a). Median IBE was lower than IBD, and was significantly positive only in non-wind-dispersers, declining to near zero in fully-wind-dispersed genomes (figure 3.5b).

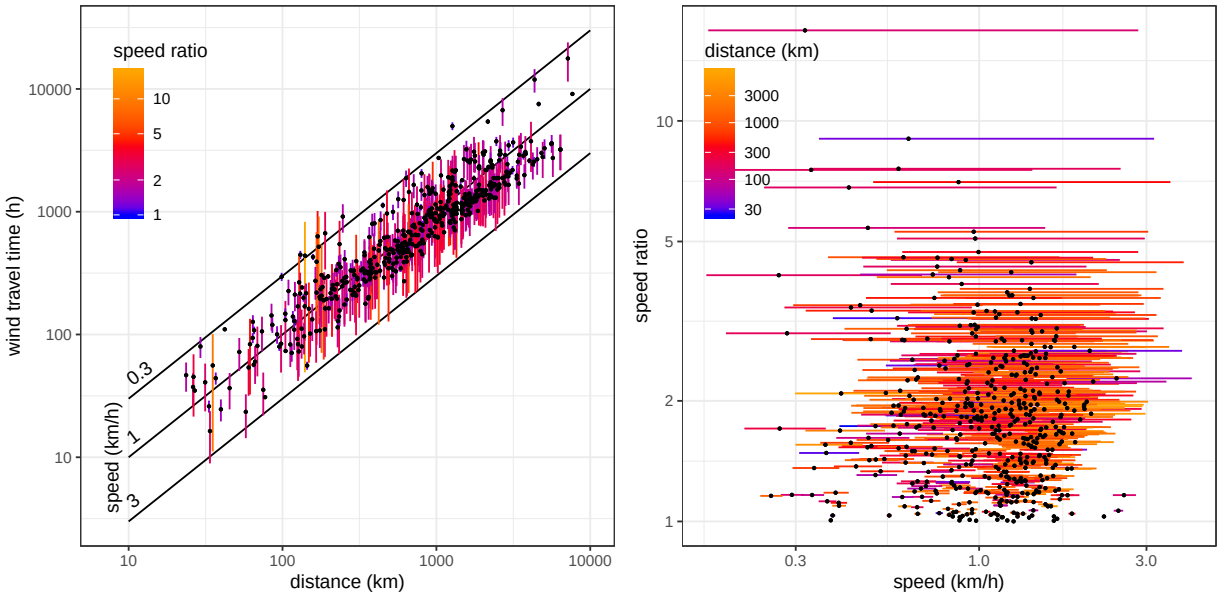

Figure 3.3: Variation in and relationships among wind connectivity metrics. The two plots show different views of the same data, representing geographic distance, wind travel time, wind speed, and wind speed ratios for 500 population pairs randomly selected across all species in the analysis. For each population pair, line segments link the wind flow metrics in the two directions, while points indicate the average wind speed or wind travel time.

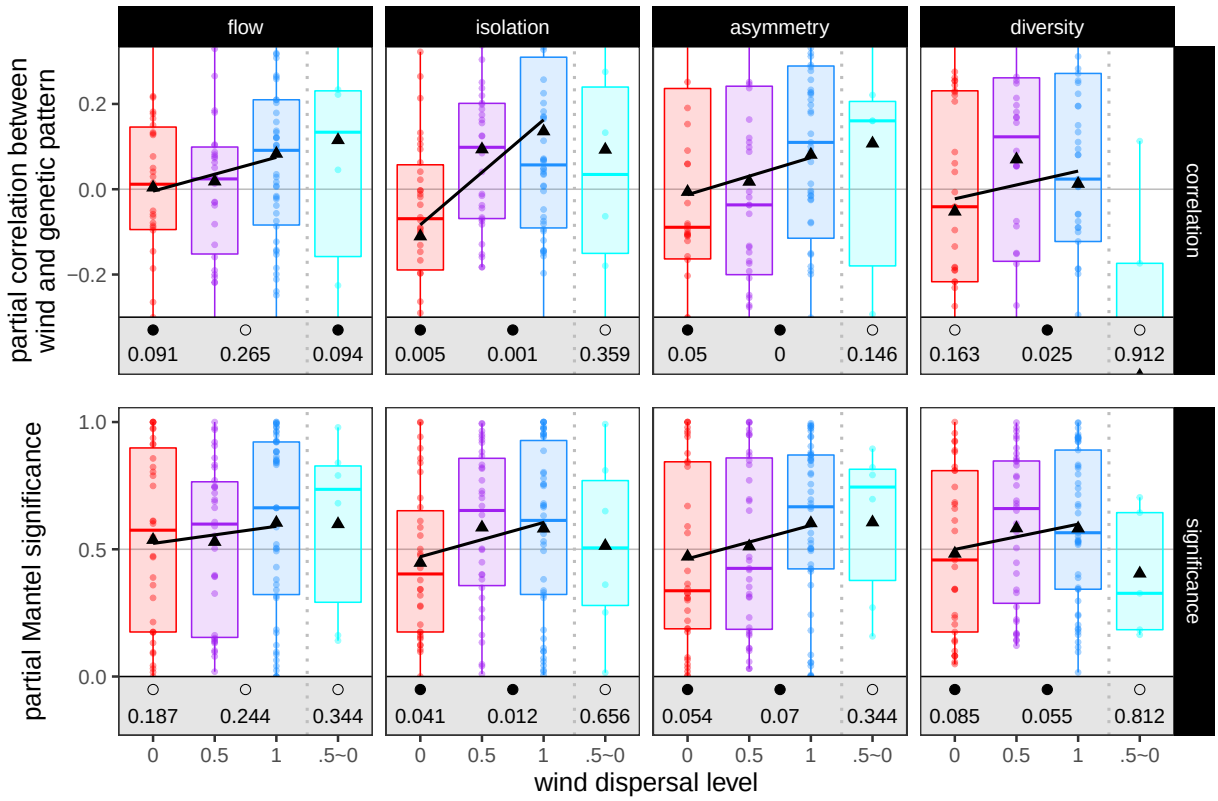

Figure 3.4: Partial correlations between wind and each of the four landscape genetic patterns: flow, connectivity, symmetry, and diversity. The first row shows distributions of partial correlation coefficients with overall significance based on the global null hypothesis test. The second row shows distributions of traditional partial Mantel p-values values with overall significance tested based on the distributions of these values; these are one-sided p-values, with the direction set so that higher p-values correspond to more positive correlation coefficients. Red, purple, and blue boxplots represent correlations for datasets with different wind dispersal levels, while cyan boxplots represent correlations for the six *Quercus* nuclear datasets that have corresponding chloroplast data available as a control for non-wind dispersal. Triangles are averages across datasets. The correlation plots hide absolute values above 0.3 to emphasize central patterns over outliers. The gray shaded regions show statistical significance for the three tests shown in figure 3.2c, with filled points significant at p ¡ 0.1.

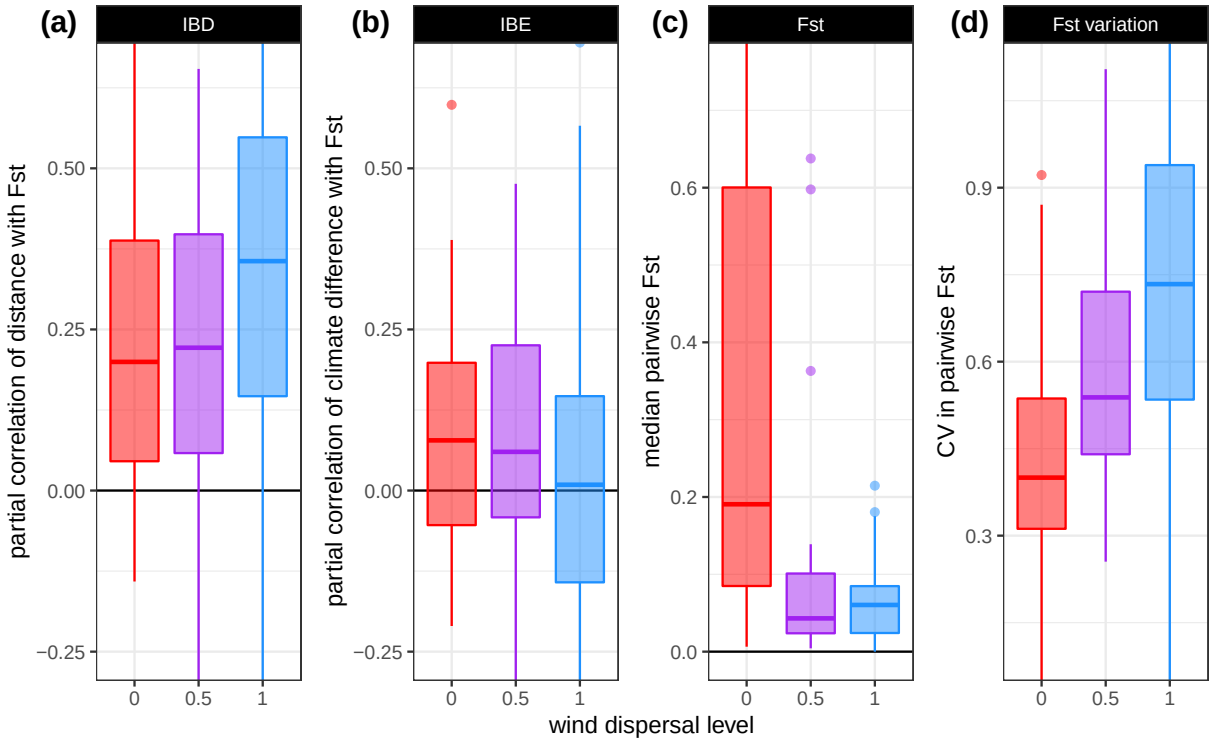

Figure 3.5: Differentiation patterns by wind dispersal level. (a, b) Partial correlations of geographic distance and climatic difference with F_{st}, in models without wind connectivity. (c) Mean pairwise F_{st}. All plots illustrate variation among datasets, with one data point per dataset per panel. Extreme outliers are omitted from plots but still used in generating boxplots.

3.4 Discussion

Isolation by wind

We found that real-world wind patterns deviate substantially from the assumption that distance alone is an adequate descriptor of wind dispersal potential. Directional wind diffusion speeds between pairs of conspecific tree populations, reflecting wind accessibility after controlling for distance, varied more than 30-fold across the world. This variation results in part from highly asymmetric wind flows along many dispersal routes: wind travel between the median pair of populations took more than twice as long in one direction as the other. It is also a product of geographic variation in wind strength: the median species in our analysis had fourfold variation among population pairs in pairwise mean wind speed after controlling for directionality. These estimates help to clarify the potential for anisotropic and spatially variable wind regimes to shape dispersal dynamics and biodiversity patterns. River and ocean currents are strongly constrained and directional, with major evolutionary implications in those systems (Cowen & Sponaugle, 2009; Morrissey & de Kerckhove, 2009; Pringle et al., 2011). While the degree of asymmetry is lower for aerial dispersal due to the temporal variability associated with weather systems and fine-scale atmospheric turbulence, our models highlight the potential for important biological effects. Asymmetric and nonstationary propagule dispersal rates that correspond to our estimated wind flow rates can have a strong influence on evolutionary outcomes.

Our results strongly suggest that these wind patterns do influence forest genetics. We found evidence that wind influences gene flow, genetic isolation, asymmetric gene flow, and genetic diversity patterns in the ways we hypothesized. For each of these distinct genetic facets, partial correlations between wind and genetics were positive in wind-dispersed genomes after controlling for distance and environment, and were higher in wind-dispersed genomes than non-wind-dispersed genomes. Results of the genome control test (*Quercus* data) also trended in the hypothesized direction, with the exception of the diversity hypothesis, but these tests were mostly inconclusive due to small sample size and high variability in effect size among species. Because we tested the influence of wind on each genetic hypothesis in three distinct ways and found general agreement across these tests, we can have higher confidence that the observed effects of wind are real. Taken together, these tests provide clear evidence for the effects of wind on landscape genetics in trees.

Importantly, our results show that wind has distinct, independent effects on genetic isolation, gene flow asymmetry, and genetic diversity (figure S3.3). Wind-genetic correlations for wind-dispersed genomes were almost entirely uncorrelated among these three hypotheses. (Results for flow, the fourth hypothesis, were correlated with asymmetry and isolation, as expected given mathematical relationships among the metrics). This confirms that these are not simply alternative measures of the same underlying pattern in the raw genetic data that were predetermined to yield similar results, but instead represent three genuinely distinct tests of the influence of wind on different facets of landscape genetics. It also implies that while all three patterns are consistently influenced by differences among the life history traits

we used to determine wind dispersal level, biogeographic or trait-based variation among species within a given wind dispersal group does not consistently shape the overall influence of wind. Aspects of the life history and biogeography of these species presumably do influence their dispersal sensitivity to wind, but any such influences appear to operate independently on these three landscape genetic metrics.

Strong latitudinal trends in wind dispersal level in our analysis (figure 3.2), which match known patterns (Regal, 1982), mean that wind influences on genetic patterns are primarily a temperate and subtropical phenomenon. They also raised the possibility that some unknown factor correlated with latitude, rather than dispersal syndrome itself, could be responsible for the observed differences in wind-genetic relationships among wind dispersal levels. But when we compared the effects of wind dispersal level on wind-genetic correlations in models with and without latitude, estimated effects were nearly identical (table S3.1). Latitude coefficients in these models were also very small and not statistically significant, indicating there were no major latitudinal trends within wind dispersal groups. We conclude that confounding latitudinal effects are unlikely to be a concern in this study.

While the effects of wind on these genetic metrics are clear and significant, they are not especially strong or consistent. Average partial correlations are low, and there is wide variability among species, with the role of wind becoming clear only when data are pooled across large numbers of taxa. While this analysis reveals that wind connectivity models are useful for understanding landscape genetic patterns at macroecological scales, our results imply that they still fall short for many individual species. On average across the four facets, partial correlations for two thirds (64–69%) of fully wind-dispersed genomes had Mantel p-values in the hypothesized direction. Given the substantial uncertainties in estimates of both wind connectivity and genetic patterns discussed above, it is perhaps unsurprising that a third of species did not follow predicted trends. While some irreducible uncertainty is inevitable due to idiosyncrasies in population genetic histories, it is clear there is room for improvement in future studies of landscape wind connectivity. Because trees tend to have high levels of standing genetic variation within vs. among populations (Hamrick et al., 1992; Petit & Hampe, 2006; Savolainen et al., 2007), sampling uncertainty can be high, and so collecting data from larger numbers of populations, individuals, and/or loci could give more power to detect subtle patterns such as wind effects. Wind connectivity models could also be refined in a number of ways. For example, our modeled wind flow pathways were unconstrained by landscape features (other than large water bodies) and were based on all wind conditions during each species' dispersal or pollination season; more realistically, gene flow may is perhaps likely to follow pathways through inhabited patches within the species range, and dispersal can be driven by specific weather conditions at specific times of day (Greene, 2005; Maurer et al., 2013; S. J. Wright et al., 2008). These factors could be accounted for given sufficient information on a focal species.

While the overall results are consistent with our core hypotheses for all four genetic facets, other aspects of the data are unexpected. For the isolation and asymmetry analyses, the majority of non-wind dispersers had significantly negative correlations between wind and genetic patterns. This is surprising, as genomes in this group would be expected to have

zero correlation with wind, and it raises the possibility of biases in the measured correlations. These results underscore the value of comparing genomes with different wind dispersal levels rather than only analyzing wind dispersers. The true historic effects of wind on gene flow are obscured by uncertainty in the wind and genetic components of our model, and we expect most of the wind and genetic uncertainty to be uncorrelated, introducing noise rather than bias in our results. However, wind speed and direction are strongly spatially structured, and so there is potential for correlation with non-wind drivers of gene flow, like postglacial range expansion and animal movement. Modeling those processes is beyond the scope of this study, but we can speculate about how they might contribute to negative correlations in non-wind dispersers, and dampen positive correlations in wind dispersers. For the asymmetry hypothesis, negative wind-genetic correlations indicate asymmetric gene flow against the prevailing wind direction. Founder effects, such as may be common in postglacial range expansions, can generate a bias in perceived migration rates, incorrectly estimating net migration from the newly founded population toward the older source population (Sundqvist et al., 2016). If prevailing winds tended to blow opposite the direction of recent range expansions, the expected genetic signal of founder effects and wind effects would be similar and the result could be confounded. In the northern temperate latitudes representing the large majority of our datasets, postglacial range expansions and prevailing meridional winds driven by Hadley cells both move in the poleward direction, and the artifacts of founder events would thus be expected to cause negative bias in the estimated effect of wind directionality on gene flow directionality. For the isolation hypothesis, negative relationships between genetic similarity and wind connectivity in non-wind-dispersed species imply that genetic exchange resulting from animal movement is higher in less windy portions of a species range, or is higher along routes perpendicular rather than parallel to prevailing winds. This latter effect could potentially occur because east-west windspeeds in most places are stronger than north-south windspeeds, whereas seasonal migration pathways of animals, as well as range expansion pathways between the LGM and present day, tend to be oriented in the north-south direction.

These results also imply that wind patterns are relevant to the conservation and management of forests vulnerable to multiple threats from global environmental change. With ongoing climate change, the rate and direction of gene flow are important for transporting adaptive alleles to both the warm and cold edges of a species range (Bontrager & Angert, 2019; Sexton et al., 2011), and the efficacy of these processes is likely to be shaped by global wind patterns (Kling & Ackerly, 2020). With widespread habitat destruction and fragmentation, isolated forest fragments will depend on long-distance wind dispersal and pollination for maintaining genetic diversity and reducing inbreeding depression (Jump & Peñuelas, 2006; Lowe et al., 2015). And with increasing concern about engineered genes leaking from commercial forestry plantations into wild tree populations, understanding how wind geography shapes gene flow will be important for risk management (DiFazio et al., 2004; Small & Antle, 2003).

Isolation by distance and environment

Dispersal syndrome affects other aspects of species' spatial genetic patterns beyond their sensitivity to wind, as illustrated by our analysis of how genetic differentiation relates to distance and environment in models without wind connectivity a predictor. Like various prior studies (Givnish (2010) and references therein), our results show that the average level of genetic differentiation between populations is much lower in wind-dispersed genomes than in non-wind-dispersed genomes, implying that wind facilitates higher rates of long-distance gene flow compared to alternative dispersal and pollination modes. Also in keeping with prior comparisons across plant species (Sexton et al., 2014), we found that distance and environment both explain significant portions of the variance in pairwise genetic differentiation, with substantially stronger IBD than IBE overall. Perhaps more interestingly, we found a clear interaction between wind dispersal level and the degrees of IBD and IBE. These results are correlations rather than regression coefficients, and so represent the effects of life history traits on the predictability of genetic differentiation rather than on the absolute level of differentiation. Wind dispersers had higher IBD and lower IBE than genomes with non-wind vectors, while partially-wind-dispersed genomes had intermediate values for both phenomena, strengthening the conclusion that the relationships are meaningful. IBE was significant for non-wind-dispersed genomes but declined to near zero in fully-wind-dispersed genomes, which were as likely to have negative climate-F_{st} correlations as positive. While the vast majority of genetic loci in our analyses were presumed to be selectively neutral and their climatic associations don't speak directly to local adaptation, it is common to find IBE in neutral markers due to linkage with loci that are under selection (Sork et al., 2010). Overall, these results imply that wind dispersal facilitates higher absolute rates of gene flow, diffuses migrants more uniformly across space, and swamps signals of local adaptation with higher rates of counter-gradient gene flow.

Our use of three discrete wind dispersal levels is a simplification of functional trait variation across species. One issue is that propagules can be dispersed by both wind and non-wind vectors, making the relative contribution of wind to dispersal patterns a gradient rather than a discrete ranking; examples include wind-dispersed pine seeds with varying levels of secondary dispersal by rodents, willows pollinated by both insects and wind, and species pollinated by insects which are themselves subsequently transported by wind. Another issue is that the efficacy of long-distance wind dispersal varies enormously even among wind-dispersed taxa, ranging from heavy winged seeds and large pollen grains that generally disperse only short distances, to cottony seeds and small pollen grains capable of traveling vast distances. On the one hand, the use of three discrete levels makes sense in the context wind-genetic correlations, which measure the predictability of gene flow rather than absolute rates of gene flow as noted above—functional variation in wind dispersal ability should relate more to absolute rates, whereas predictability may simply relate to the degree of noise contributed by non-wind dispersal vectors like animals. On the other hand, genetic patterns reflect the balance between multiple evolutionary rates, and patterns in genomes with slower rates of wind dispersal should be relatively more influenced by processes such as selection

and drift, making them less predictable from wind. It would be valuable for future work to integrate quantitative measures of wind dispersal ability into molecular macroecology analyses.

Conclusions

Our results provide insight into the ways that wind patterns shape various aspects of landscape genetic patterns across populations of wind-dispersed and wind-pollinated trees. While the marginal effects of wind are subtle after controlling for distance and climate, they are clearly detectable using the combination of time-integrated wind connectivity models, a large global multispecies genetic dataset, and extensions of existing statistical methods. This analysis offers a new category of evidence of the large-scale influences of wind on spatial genetic patterns, demonstrating that wind has distinct influences on genetic diversity, genetic differentiation, and asymmetric gene flow.

3.5 Methods

Genetic data

Our study is based on reanalysis of previously published datasets available on the Dryad data repository. We compiled a global list of 165 tree genera, entered each genus as a search term in Dryad, and reviewed the abstracts of all results for each genus. Microsatellite (SSR) and single nucleotide polymorphism (SNP) datasets from landscape genetics studies representing multiple individuals of a given species from multiple geographic locations were downloaded. Hereafter we use the term "dataset" to refer to the data of a single type (SSR or SNP) representing a single genome (nuclear or chloroplast) of a single species from a single publication; some publications contained multiple datasets, which we disaggregated for most downstream analysis. Studies focused on hybridization between species were excluded, except in cases where populations in the hybrid zone of overlap between species ranges could be identified and removed, retaining only the non-overlapping portions of species ranges for analysis.

Each dataset was individually restructured into a standardized format. Because wind connectivity cannot be computed between populations occurring in the same spatial grid cell (see below), populations from a given genetic dataset that fell within the same grid cell were merged prior to analysis by averaging the latitude and longitude of the constituent populations and pooling individual genotype data into a single population. After all filtering, cleaning, and reformatting, our final analysis was based on 126 datasets representing 1956 populations of 103 tree species, sourced from 72 original publications.

Genetic metrics

We analyzed genetic patterns in each dataset using a fully connected lattice model of populations, in which all population pairs are connected. For each dataset, we calculated genetic differentiation and directional migration (gene flow) for every population pair, and genetic diversity for every population. Diversity was measured as mean allelic richness for every population using the resampling method in the divBasic function in the R package diveRsity (Keenan et al., 2013); to convert these diversity values into the data structure of pairwise relationships between populations, we calculated genetic diversity ratios for each population pair in each direction, as the ratio of allelic richness in the destination versus the origin population. Pairwise genetic similarity was measured as 1 - F_{st}.

Migration was estimated via the divMigrate method (Sundvquist et al. 2016) implemented in the R package diveRsity (Keenan et al., 2013), which uses allele frequency differences between population pairs to estimate rates of migration in each direction. Note that these rates are relative to other pairs in the same dataset, and cannot be compared across datasets. This method was chosen for its straightforwardness and for its computational tractability given the size of our analysis, compared to computationally-intensive model-based alternatives (e.g. Beerli and Felsenstein (1999), Wilson and Rannala (2003)). We modified the divMigrate function in order to accommodate haplotype (chloroplast) data, as these data are consistent with the theoretical method but not supported in the original R package. Gene flow asymmetry was calculated for each population pair as the ratio of outbound to inbound gene flow; reciprocal values were calculated reversing outbound and inbound, for distance-based matrix analyses.

Traits

For each species, we compiled data on pollination and seed dispersal syndromes, the months of the year when pollination and seed dispersal occur, and whether chloroplast DNA is transmitted via pollen or seed. Data were sourced from TRY (Kattge et al., 2020) and BIEN (Maitner et al., 2018) using bulk multi-species queries, and holes were filled by manual searching on Google Scholar and Google. Based on these traits, each dataset was classified as non-wind dispersed, partially wind dispersed, or fully wind dispersed, according to the expected role of wind in shaping genetic patterns (figure 3.3).

Wind

We used the windscape R package (Kling, 2020b) in combination with three decades of hourly global wind data from the Climate System Forecase Reanalysis (CFSR) (Saha et al., 2010) to estimate wind connectivity among sites. In this framework, a connectivity graph is constructed in which each grid cell is connected to its eight neighbors in proportion to the frequency and strength with which wind blows in that direction, integrating over decades of hourly wind conditions. Wind conductance over non-terrestrial cells was down-weighted by

90%, to reflect the reduced likelihood of long-distance dispersal across large water bodies. The most efficient route between any two points can then be identified using a least cost path algorithm, with its "cost" quantified as the mean estimated number of hours wind would take to diffuse to that location based on the full spatiotemporal distribution of wind conditions across the landscape. We quantify wind flow as the inverse of this travel time, measured in units of h-1.

We calculated wind flow in both directions for every pair of populations in each dataset. For each population pair we used these two flow values to calculate wind flow asymmetry, i.e. the ratio of outbound to inbound wind flow, which like gene flow asymmetry are reciprocals that contain the same information. We also calculated wind connectivity, the mean of wind flows in the two directions.

Wind patterns differ seasonally in many parts of the world, and for each dataset we therefore calculated wind flow based on data only from months of the year when wind pollination and/or dispersal is thought to occur for that genome. For datasets where wind dispersal or pollination is relevant, wind data from only the relevant months was used. For non-wind-dispersed datasets, and for the small minority of datasets where pollination or dispersal phenology was unknown, wind data from all months of the year was used. This was determined for each dataset based on the combination of genome type, plastid inheritance, and seed and pollen dispersal syndromes.

Climate

Both to control for and test for IBD and IBE, we also calculated the pairwise geographic distance and the pairwise climatic difference between every pair of populations. Climatic difference was calculated based on four climate variables deemed likely to shape patterns of local adaptation in trees: maximum temperature of the warmest month, minimum temperature of the coldest month, annual actual evapotranspiration (AET, a measure of water available for plant growth), and annual climatic water deficit (CWD, a measure of dryness intensity). We used gridded 1 km global terrestrial climate data from CHELSA (Karger et al., 2017) representing mean climates from 1979–2013. We derived AET and CWD from monthly temperature and precipitation values and latitude following the methods of (T. Wang et al., 2012), and then transformed them for normality using $log(x + 1)$. The four variables were then standardized using a principal component analysis across all terrestrial grid cells outside the (ant)arctic circles, yielding four climate dimensions with equal variances. Pairwise Euclidean distances between populations were calculated in this principal component space.

Statistical models

The steps described above generated nine pairwise matrices for each dataset, including two asymmetric matrices with different values in the upper and lower triangles (gene flow, wind flow), three reciprocally-symmetrical matrices with reciprocal values in the upper and lower

triangles (gene flow ratio, genetic diversity ratio, wind flow ratio), and four symmetric matrices with identical values in the upper and lower triangles (geographic distance, climatic difference, genetic similarity, wind connectivity). Most variables were log-transformed prior to statistical analysis, both to improve the normalcy of data distributions and so that correlations would reflect fine-scale variance among nearby/similar populations as well as large-scale variance among relatively distant populations, rather than being dominated by the latter. (The one exception was genetic similarity, for which log transformation would have increased skew in the distribution).

These data were used to test the four hypotheses about how wind shapes different landscape genetic patterns. We tested the flow hypothesis as the partial correlation between wind flow and gene flow; the isolation hypothesis as the partial correlation of wind connectivity and genetic similarity; the asymmetry hypothesis as the partial correlation between wind flow ratio and gene flow ratio; and the diversity hypothesis as the partial correlation between wind flow ratio and genetic diversity ratio. All of these partial correlations were hypothesized to be positive for wind-dispersed genomes. Geographic distance and climatic difference were included as controls in the partial correlations for the flow and isolation analyses, ensuring that only residual variation not associated with these predictors was tested. (Distance and climatic difference by definition have zero correlations with log-transformed wind and genetic asymmetry ratios, so it was not necessary to include them as controls in the asymmetry and diversity analyses.)

For each of these four hypotheses we tested three predictions, for a total of twelve hypothesis tests. We refer to these as the "wind disperser", "dispersal level comparison", and "genome control" predictions. The wind disperser prediction considers only the fully or partially wind-dispersed datasets, predicting that the majority of them will have positive partial correlations between the wind and genetic metrics. The dispersal level comparison prediction considers all datasets, predicting that the partial wind-genetic correlation will increases across the three wind dispersal levels (none, partial, full). The genome comparison prediction considers only datasets from studies where partially-wind-dispersed nuclear data and non-wind-dispersed chloroplast data were collected for the same individuals and populations, which comprised six Quercus species, predicting that the majority of nuclear datasets will have positive partial wind-genetic correlations after the chloroplast genetic signal is added as a control.

All tests were conducted using partial Mantel tests, the statistical approach most widely used to test patterns in pairwise matrix data for applications such as IBD and IBE (Sexton et al., 2014). However, because we are testing global hypotheses about macroecological patterns across the entire multispecies dataset rather than hypotheses about any individual species in particular, an extension of the traditional single-species partial Mantel test is needed. We used two alternative approaches that accommodate this hierarchical data, which we call the "dataset null" and "global null" approaches, and tested each of our twelve hypotheses using both approaches. Both approaches begin by using Mantel-style permutations of the rows and columns of the genetic matrix of every dataset, to derive a null distribution of 10,000 randomized partial correlation coefficients for every dataset; they differ in how those

randomized null values are summarized to derive a final global p-value representing the significance of the overall hypothesis (figure S3.1).

For the global null approach (A in figure S3.1), we used the randomization data to calculate global summary statistics across datasets separately for each random iteration, to derive null distributions of these global test statistics that we then compared to the measured test statistic to test the overall hypothesis. Our test statistic for the wind disperser and genome control predictions was the median correlation coefficient across datasets. For the dispersal level comparison prediction, our test statistic was the Spearman rank correlation between wind dispersal level and correlation coefficient.

For the dataset null approach (B in figure S3.1), we used these randomization data to calculate one-sided p-values separately for each specific dataset, comparing each dataset's actual correlation coefficient to its null distribution following the standard practice for the partial Mantel test. These one-sided p-values contain information about both the direction and uncertainty of the relationship for each dataset. To derive final global p-values we tested whether this collection of independent p-values deviated significantly from null expectations. For the wind disperser and genome control predictions discussed above, the null expectation is that p-values above and below 0.5 are equally likely; we tested this with simple one-sided binomial tests. For the dispersal level comparison prediction, the null expectation is that p-values do not differ across the three wind dispersal levels; we used one-sided Spearman's rank correlation tests to determine whether p-values decreased as wind dispersal level increased.

Wind dispersal level is strongly geographically patterned (figure 3.2), raising the possibility that some latitude-associated phenomenon other than wind dispersal level could in fact explain any observed relationships between wind dispersal level and wind-genetic correlations. To test for this, for each of the four hypotheses, we fit a regression model predicting a dataset's partial wind-genetic correlation based on wind dispersal level, and a second based on wind dispersal level and the absolute value of the mean latitude of populations, and compared the effects of wind dispersal level between these two models. Because correlations are bounded between -1 and 1, we rescaled them to the 0–1 range and then used logistic regression. Model significance was assessed using the "global null" testing approach described above, with logistic regression coefficients as test statistics.

Finally, we conducted a separate, secondary analysis with the same data to test how IBD and IBE differ by wind dispersal level, ignoring wind connectivity metrics and focusing just on relationships between distance, climatic difference, and genetic differentiation (F_{st}). For each wind dispersal level we used the global null method described above to calculate whether median partial correlations for distance and climate were greater than zero, and whether they differed from each other. We also used the global null method to test for trends across wind dispersal levels in partial correlation coefficients for each of these two predictors, using the rank correlation as described above for the "dispersal level comparison" test.

All analysis was done in R (R Core Team, 2017).

Conclusion

Through three different views of large-scale plant spatial ecology, this dissertation research explored how the dynamics of migration and selection influence basic biodiversity patterns and vulnerability to anthropogenic climate change. This work informs various aspects of our understanding of basic ecology. At least as importantly, it also informs applied questions about biodiversity conservation and land management in the face of global environmental change.

For example, findings about spatial patterns in the importance of different climate variables to different vegetation types can help land managers assess climate change vulnerability using the climate variables most appropriate for their local landscape. Similarly, the integration of three dimensions of climate novelty aims to help guide choices among alternative climate adaptation strategies ranging from assisted migration to assisted regeneration to assisted gene flow. And the work on wind identifies landscapes and populations that may be more or less vulnerable to future climate change, which could help to guide monitoring programs and target the systems most likely to need intensive management intervention to resist the worst effects of climate change.

But much work remains to be done on these questions. Chapters 1 and 2 introduce new conceptual frameworks and explore their potential implications in large modeling studies. These analyses leverage big empirical datasets to generate a variety of novel, spatially explicit predictions about climate vulnerability patterns, but they offer no definitive answer about how well these predictions translate to real patterns of biotic response to climate change on the ground. Follow-up studies helping compare and validate these predictions and translate them into actionable forecasts for climate adaptation will be essential.

For example, chapter 1 presented a framework comparing and integrating niche novelty, temporal novelty, and spatial novelty, and showed that these three dimensions of predicted climate threat exhibit starkly different geographic and ecological patterns. By integrating these predictions with observational data on emerging ecological responses to climate change over recent decades, it should be possible to identify which of these three metrics, or which combination of metrics, best predict biotic change in which ecological contexts. In turn, combining these sorts of insights with additional macroecological data on species traits and future climate change could help to reduce the uncertainty of ecological forecasts and guide the efficient and effective application of various types of management intervention.

Similarly, chapter 2 introduced an important new question about how wind patterns may

shape vulnerability to rapid future climate change. In future work, these predictions can be tailored to best represent the ecology of particular species and landscapes, and can then be compared to observations of recent or paleoecological responses to climate change to validate and improve the wind connectivity models. Wind patterns could influence rates of biotic response to climate change throughout a species range, including by influencing rates of species turnover at trailing edges, rates of adaptive gene flow at the range center, and rates of evolution and range expansion at the leading edge. All of these phenomena should be testable given sufficient data on population trends over time, which are becoming increasingly available thanks to open data reporting and standardized biodiversity databases. There is much potential for future analyses like these to narrow the uncertainty in the wind-climate change predictions presented here, helping to guide the appropriate future use of assisted migration and assisted gene flow.

Chapter 3 provides a validation for the usefulness of these wind connectivity models in historical landscape genetics. It also complicates the above set of questions by showing that wind influences not just directional gene flow as explored in chapter 2 but also genetic diversity and genetic isolation. This raises questions about how dispersal patterns interact with patterns of habitat fragmentation, overharvesting, and other anthropogenic stressors to shape variation in vulnerability to global environmental change. Further work should explore how wind shapes these aspects of conservation genetics and their interactions with climate change.

The importance of these future research agendas notwithstanding, uncertainty is no excuse for inaction. The scientific consensus is clear on the gravity of the impending threats to biodiversity, on the increasing costs to biodiversity and humanity associated with every additional month of delayed action against juggernauts like climate change and deforestation, and on steps that could be taken now to mitigate the worst of these effects. Stemming the threats of global environmental change requires society's full attention and immediate mobilization, and there is more than enough existing ecological understanding to steer those initiatives.

References

Ackerly, D. D., Cornwell, W. K., Weiss, S. B., Flint, L. E., & Flint, A. L. (2015). A geographic mosaic of climate change impacts on terrestrial vegetation: Which areas are most at risk? *PloS One*, *10*(6), e0130629.

Ackerly, D., Loarie, S., Cornwell, W., Weiss, S., Hamilton, H., Branciforte, R., & Kraft, N. (2010). The geography of climate change: Implications for conservation biogeography. *Diversity and Distributions*, *16*(3), 476–487.

Aguilée, R., Raoul, G., Rousset, F., & Ronce, O. (2016). Pollen dispersal slows geographical range shift and accelerates ecological niche shift under climate change. *Proceedings of the National Academy of Sciences*, *113*(39), E5741–E5748.

Ahmed, S., Compton, S. G., Butlin, R. K., & Gilmartin, P. M. (2009). Wind-borne insects mediate directional pollen transfer between desert fig trees 160 kilometers apart. *Proceedings of the National Academy of Sciences*, *106*(48), 20342–20347.

Aitken, S. N., & Whitlock, M. C. (2013). Assisted gene flow to facilitate local adaptation to climate change. *Annual Review of Ecology, Evolution, and Systematics*, *44*.

Angert, A. L., Crozier, L. G., Rissler, L. J., Gilman, S. E., Tewksbury, J. J., & Chunco, A. J. (2011). Do species' traits predict recent shifts at expanding range edges? *Ecology Letters*, *14*(7), 677–689.

Ashcroft, M. B., Chisholm, L. A., & French, K. O. (2009). Climate change at the landscape scale: Predicting fine-grained spatial heterogeneity in warming and potential refugia for vegetation. *Global Change Biology*, *15*(3), 656–667.

Ashley, M. V. (2010). Plant parentage, pollination, and dispersal: How DNA microsatellites have altered the landscape. *Critical Reviews in Plant Sciences*, *29*(3), 148–161.

Austerlitz, F., Dutech, C., Smouse, P., Davis, F., & Sork, V. (2007). Estimating anisotropic pollen dispersal: A case study in Quercus lobata. *Heredity*, *99*(2), 193–204.

Aycrigg, J. L., Davidson, A., Svancara, L. K., Gergely, K. J., McKerrow, A., & Scott, J. M. (2013). Representation of ecological systems within the protected areas network of the continental United States. *PLoS One*, *8*(1), e54689.

Bahn, V., & McGill, B. J. (2013). Testing the predictive performance of distribution models. *Oikos*, *122*(3), 321–331.

Barbet-Massin, M., & Jetz, W. (2014). A 40-year, continent-wide, multispecies assessment of relevant climate predictors for species distribution modelling. *Diversity and Distributions*, *20*(11), 1285–1295.

Beerli, P., & Felsenstein, J. (1999). Maximum-likelihood estimation of migration rates and effective population numbers in two populations using a coalescent approach. *Genetics*, *152*(2), 763–773.

Beever, E. A., O'Leary, J., Mengelt, C., West, J. M., Julius, S., Green, N., Magness, D., Petes, L., Stein, B., Nicotra, A. B., Et al. (2016). Improving conservation outcomes with a new paradigm for understanding species' fundamental and realized adaptive capacity. *Conservation Letters*, *9*(2), 131–137.

Bellard, C., Bertelsmeier, C., Leadley, P., Thuiller, W., & Courchamp, F. (2012). Impacts of climate change on the future of biodiversity. *Ecology Letters*, *15*(4), 365–377.

Belote, R. T., Carroll, C., Martinuzzi, S., Michalak, J., Williams, J. W., Williamson, M. A., & Aplet, G. H. (2018). Assessing agreement among alternative climate change projections to inform conservation recommendations in the contiguous United States. *Scientific Reports*, *8*(1), 1–13.

Bontrager, M., & Angert, A. L. (2019). Gene flow improves fitness at a range edge under climate change. *Evolution Letters*, *3*(1), 55–68.

Born, C., le Roux, P. C., Spohr, C., McGEOCH, M. A., & van Vuuren, B. J. (2012). Plant dispersal in the sub-antarctic inferred from anisotropic genetic structure. *Molecular Ecology*, *21*(1), 184–194.

Bradie, J., & Leung, B. (2017). A quantitative synthesis of the importance of variables used in MaxEnt species distribution models. *Journal of Biogeography*, *44*(6), 1344–1361.

Brown, J. K., & Hovmøller, M. S. (2002). Aerial dispersal of pathogens on the global and continental scales and its impact on plant disease. *Science*, *297*(5581), 537–541.

Buckley, L. B., & Kingsolver, J. G. (2012). Functional and phylogenetic approaches to forecasting species' responses to climate change. *Annual Review of Ecology, Evolution, and Systematics*, *43*.

Bullock, J. M., & Clarke, R. T. (2000). Long distance seed dispersal by wind: Measuring and modelling the tail of the curve. *Oecologia*, *124*(4), 506–521.

Bullock, J. M., White, S. M., Prudhomme, C., Tansey, C., Perea, R., & Hooftman, D. A. (2012). Modelling spread of british wind-dispersed plants under future wind speeds in a changing climate. *Journal of Ecology*, *100*(1), 104–115.

Carroll, C., Lawler, J. J., Roberts, D. R., & Hamann, A. (2015). Biotic and climatic velocity identify contrasting areas of vulnerability to climate change. *PloS One*, *10*(10), e0140486.

Chen, I.-C., Hill, J. K., Ohlemüller, R., Roy, D. B., & Thomas, C. D. (2011). Rapid range shifts of species associated with high levels of climate warming. *Science*, *333*(6045), 1024–1026.

Clark, J. S., Fastie, C., Hurtt, G., Jackson, S. T., Johnson, C., King, G. A., Lewis, M., Lynch, J., Pacala, S., Prentice, C., Et al. (1998). Reid's paradox of rapid plant migration: Dispersal theory and interpretation of paleoecological records. *BioScience*, *48*(1), 13–24.

Comer, P., Faber-Langendoen, D., Evans, R., Gawler, S., Josse, C., Kittel, G., Menard, S., Pyne, M., Reid, M., Schulz, K., Et al. (2003). Ecological systems of the United States: A working classification of us terrestrial systems. *NatureServe, Arlington, VA*, *75*.

Comer, P., Crist, P., Reid, M., Hak, J., Hamilton, H., Braun, D., Kittel, G., Varley, I., Unnasch, B., Auer, S., Et al. (2013). A rapid ecoregional assessment of the Central Basin and Range Ecoregion. *Report, appendices, and databases provided to the Bureau of Land Management. BLM, Washington, DC, USA*.

Cowen, R. K., & Sponaugle, S. (2009). Larval dispersal and marine population connectivity. *Annual Review of Marine Science*, *1*(1), 443–466.

Daly, C., Halbleib, M., Smith, J. I., Gibson, W. P., Doggett, M. K., Taylor, G. H., Curtis, J., & Pasteris, P. P. (2008). Physiographically sensitive mapping of climatological temperature and precipitation across the conterminous United States. *International Journal of Climatology*, *28*(15), 2031–2064.

Davis, H. G., Taylor, C. M., Lambrinos, J. G., & Strong, D. R. (2004). Pollen limitation causes an allee effect in a wind-pollinated invasive grass (Spartina alterniflora). *Proceedings of the National Academy of Sciences*, *101*(38), 13804–13807.

Dawson, T. P., Jackson, S. T., House, J. I., Prentice, I. C., & Mace, G. M. (2011). Beyond predictions: Biodiversity conservation in a changing climate. *Science*, *332*(6025), 53–58.

DiFazio, S. P., Slavov, G. T., Burczyk, J., Leonardi, S., & Strauss, S. H. (2004). 23 gene flow from tree plantations and implications for transgenic risk assessment. *Forest Biotechnology for the 21st Century*, 405–422.

Dillon, M. E., Wang, G., & Huey, R. B. (2010). Global metabolic impacts of recent climate warming. *Nature*, *467*(7316), 704–706.

Dobrowski, S. Z., Abatzoglou, J., Swanson, A. K., Greenberg, J. A., Mynsberge, A. R., Holden, Z. A., & Schwartz, M. K. (2013). The climate velocity of the contiguous United States during the 20th century. *Global Change Biology*, *19*(1), 241–251.

Dobrowski, S. Z., Thorne, J. H., Greenberg, J. A., Safford, H. D., Mynsberge, A. R., Crimmins, S. M., & Swanson, A. K. (2011). Modeling plant ranges over 75 years of climate change in California, USA: Temporal transferability and species traits. *Ecological Monographs*, *81*(2), 241–257.

Dorp, D. v., Hoek, W. v. d., & Daleboudt, C. (1996). Seed dispersal capacity of six perennial grassland species measured in a wind tunnel at varying wind speed and height. *Canadian Journal of Botany*, *74*(12), 1956–1963.

Dullinger, S., Dirnböck, T., & Grabherr, G. (2003). Patterns of shrub invasion into high mountain grasslands of the Northern Calcareous Alps, Austria. *Arctic, Antarctic, and Alpine Research*, *35*(4), 434–441.

Elith, J., & Leathwick, J. R. (2009). Species distribution models: Ecological explanation and prediction across space and time. *Annual Review of Ecology, Evolution, and Systematics*, *40*, 677–697.

Etten, J. v. (2017). R package gdistance: Distances and routes on geographical grids.

Faber-Langendoen, D., Keeler-Wolf, T., Meidinger, D., Tart, D., Hoagland, B., Josse, C., Navarro, G., Ponomarenko, S., Saucier, J.-P., Weakley, A., Et al. (2014). Ecoveg: A new approach to vegetation description and classification. *Ecological Monographs*, *84*(4), 533–561.

Felicısimo, Á. M., Muñoz, J., & González-Solis, J. (2008). Ocean surface winds drive dynamics of transoceanic aerial movements. *PLoS One*, *3*(8), e2928.

Fernández-López, J., & Schliep, K. (2018). rWind: Download, edit and include wind data in ecological and evolutionary analysis. *Ecography*, *42*(4).

Garcia, R. A., Cabeza, M., Altwegg, R., & Araújo, M. B. (2016). Do projections from bioclimatic envelope models and climate change metrics match? *Global Ecology and Biogeography*, *25*(1), 65–74.

Garcia, R. A., Cabeza, M., Rahbek, C., & Araújo, M. B. (2014). Multiple dimensions of climate change and their implications for biodiversity. *Science*, *344*(6183).

Garcıa-Ramos, G., & Kirkpatrick, M. (1997). Genetic models of adaptation and gene flow in peripheral populations. *Evolution*, *51*(1), 21–28.

Gassmann, M. I., & Pérez, C. F. (2006). Trajectories associated to regional and extra-regional pollen transport in the southeast of Buenos Aires province, Mar del Plata (Argentina). *International Journal of Biometeorology*, *50*(5), 280.

Geremew, A., Woldemariam, M. G., Kefalew, A., Stiers, I., & Triest, L. (2018). Isotropic and anisotropic processes influence fine-scale spatial genetic structure of a keystone tropical plant. *AoB Plants*, *10*(1), plx076.

Gergely, K. J., & McKerrow, A. (2013). *Terrestrial ecosystems: National inventory of vegetation and land use* (tech. rep.). US Geological Survey.

Ghalambor, C. K., Huey, R. B., Martin, P. R., Tewksbury, J. J., & Wang, G. (2006). Are mountain passes higher in the tropics? Janzen's hypothesis revisited. *Integrative and Comparative Biology*, *46*(1), 5–17.

Gillespie, R. G., Baldwin, B. G., Waters, J. M., Fraser, C. I., Nikula, R., & Roderick, G. K. (2012). Long-distance dispersal: A framework for hypothesis testing. *Trends in Ecology & Evolution*, *27*(1), 47–56.

Givnish, T. J. (2010). Ecology of plant speciation. *Taxon*, *59*(5), 1326–1366.

Gornall, R. J., Hollingsworth, P. M., & Preston, C. D. (1998). Evidence for spatial structure and directional gene flow in a population of an aquatic plant, potamogeton coloratus. *Heredity*, *80*(4), 414.

Greene, D. F. (2005). The role of abscission in long-distance seed dispersal by the wind. *Ecology*, *86*(11), 3105–3110.

Grubb, P. J. (1977). The maintenance of species-richness in plant communities: The importance of the regeneration niche. *Biological Reviews*, *52*(1), 107–145.

Hamann, A., Roberts, D. R., Barber, Q. E., Carroll, C., & Nielsen, S. E. (2015). Velocity of climate change algorithms for guiding conservation and management. *Global Change Biology*, *21*(2), 997–1004.

Hampe, A. (2011). Plants on the move: The role of seed dispersal and initial population establishment for climate-driven range expansions. *Acta Oecologica*, *37*(6), 666–673.

Hamrick, J. L., Godt, M. J. W., & Sherman-Broyles, S. L. (1992). Factors influencing levels of genetic diversity in woody plant species, In *Population genetics of forest trees*. Springer.

Hensen, I., & Müller, C. (1997). Experimental and structural investigations of anemochorous dispersal. *Plant Ecology*, *133*(2), 169–180.

Hereford, J. (2009). A quantitative survey of local adaptation and fitness trade-offs. *The American Naturalist*, *173*(5), 579–588.

Heydel, F., Cunze, S., Bernhardt-Römermann, M., & Tackenberg, O. (2014). Long-distance seed dispersal by wind: Disentangling the effects of species traits, vegetation types, vertical turbulence and wind speed. *Ecological Research*, *29*(4), 641–651.

Higgins, S. I., Clark, J. S., Nathan, R., Hovestadt, T., Schurr, F., Fragoso, J., Aguiar, M. R., Ribbens, E., & Lavorel, S. (2003). Forecasting plant migration rates: Managing uncertainty for risk assessment. *Journal of Ecology*, *91*(3), 341–347.

Hijmans, R. J. (2012). Cross-validation of species distribution models: Removing spatial sorting bias and calibration with a null model. *Ecology*, *93*(3), 679–688.

Hijmans, R. J. (2019). *raster: Geographic Data Analysis and Modeling* [R package version 2.8-19]. R package version 2.8-19. https://CRAN.R-project.org/package=raster

Hijmans, R. J., Phillips, S., Leathwick, J., & Elith, J. (2017). *dismo: Species Distribution Modeling* [R package version 1.1-4]. R package version 1.1-4. https://CRAN.R-project.org/package=dismo

Hobbs, R. J., Higgs, E., Hall, C. M., Bridgewater, P., Chapin III, F. S., Ellis, E. C., Ewel, J. J., Hallett, L. M., Harris, J., Hulvey, K. B., Et al. (2014). Managing the whole landscape: Historical, hybrid, and novel ecosystems. *Frontiers in Ecology and the Environment*, *12*(10), 557–564.

Hoegh-Guldberg, O., Hughes, L., McIntyre, S., Lindenmayer, D., Parmesan, C., Possingham, H., & Thomas, C. (2008). Assisted colonization and rapid climate change. *Science*, *321*(5887), 345–346.

ipcc special report on global warming of 1.5 c. (n.d.).

Jackson, S. T., Betancourt, J. L., Booth, R. K., & Gray, S. T. (2009). Ecology and the ratchet of events: Climate variability, niche dimensions, and species distributions. *Proceedings of the National Academy of Sciences*, *106*(Supplement 2), 19685–19692.

Jackson, S. T., & Overpeck, J. T. (2000). Responses of plant populations and communities to environmental changes of the late Quaternary. *Paleobiology*, *26*(sp4), 194–220.

Jackson, S. T., & Sax, D. F. (2010). Balancing biodiversity in a changing environment: Extinction debt, immigration credit and species turnover. *Trends in Ecology & Evolution*, *25*(3), 153–160.

Janzen, D. H. (1967). Why mountain passes are higher in the tropics. *The American Naturalist*, *101*(919), 233–249.

Jump, A. S., & Peñuelas, J. (2006). Genetic effects of chronic habitat fragmentation in a wind-pollinated tree. *Proceedings of the National Academy of Sciences*, *103*(21), 8096–8100.

Karger, D. N., Conrad, O., Böhner, J., Kawohl, T., Kreft, H., Soria-Auza, R. W., Zimmermann, N. E., Linder, H. P., & Kessler, M. (2017). Climatologies at high resolution for the earth's land surface areas. *Scientific Data*, *4*, 170122.

Kattge, J., Bönisch, G., Dıaz, S., Lavorel, S., Prentice, I. C., Leadley, P., Tautenhahn, S., Werner, G. D., Aakala, T., Abedi, M., Et al. (2020). Try plant trait database—enhanced coverage and open access. *Global Change Biology*, *26*(1), 119–188.

Kawecki, T. J., & Holt, R. D. (2002). Evolutionary consequences of asymmetric dispersal rates. *The American Naturalist*, *160*(3), 333–347.

Keeley, A. T., Ackerly, D. D., Cameron, D. R., Heller, N. E., Huber, P. R., Schloss, C. A., Thorne, J. H., & Merenlender, A. M. (2018). New concepts, models, and assessments of climate-wise connectivity. *Environmental Research Letters*, *13*(7), 073002.

Keenan, K., McGinnity, P., Cross, T. F., Crozier, W. W., & Prodöhl, P. A. (2013). diveRsity: An R package for the estimation of population genetics parameters and their associated errors [R package version 1.9.90]. *Methods in Ecology and Evolution*, *4*(8), 782–788. https://doi.org/10.1111/2041-210X.12067

Klausmeyer, K. R., Shaw, M. R., MacKenzie, J. B., & Cameron, D. R. (2011). Landscape-scale indicators of biodiversity's vulnerability to climate change. *Ecosphere*, *2*(8), 1–18.

Kling, M. M. (2020a). *Matthewkling/winds-of-change: Version 1.0.0* (Version v1.0.0). Zenodo. https://doi.org/10.5281/zenodo.3860687

Kling, M. M. (2020b). *Matthewkling/windscape: Version 1.0.0* (Version v1.0.0). Zenodo. https://doi.org/10.5281/zenodo.3857730

Kling, M. M., & Ackerly, D. D. (2020). Global wind patterns and the vulnerability of wind-dispersed species to climate change. *Nautre Climate Change*.

Kling, M. M., Auer, S. L., Comer, P. J., Ackerly, D. D., & Hamilton, H. (2020). Multiple axes of ecological vulnerability to climate change. *Global Change Biology*, *26*(5), 2798–2813.

Koontz, M. J., Oldfather, M. F., Melbourne, B. A., & Hufbauer, R. A. (2018). Parsing propagule pressure: Number, not size, of introductions drives colonization success in a novel environment. *Ecology and evolution*, *8*(16), 8043–8054.

Kremer, A., Ronce, O., Robledo-Arnuncio, J. J., Guillaume, F., Bohrer, G., Nathan, R., Bridle, J. R., Gomulkiewicz, R., Klein, E. K., Ritland, K., Et al. (2012). Long-distance gene flow and adaptation of forest trees to rapid climate change. *Ecology Letters*, *15*(4), 378–392.

Kuhn, M. (2018). *caret: Classification and Regression Training* [R package version 6.0-81]. R package version 6.0-81. https://CRAN.R-project.org/package=caret

Kulkarni, S., & Huang, H.-P. (2014). Changes in surface wind speed over North America from CMIP5 model projections and implications for wind energy. *Advances in Meteorology*, *2014*.

Kuparinen, A., Katul, G., Nathan, R., & Schurr, F. M. (2009). Increases in air temperature can promote wind-driven dispersal and spread of plants. *Proceedings of the Royal Society B: Biological Sciences*, *276*(1670), 3081–3087.

Larson-Johnson, K. (2016). Field observations of Carpinus (Betulaceae) demonstrate high dispersal asymmetry and inform migration simulations with implications for times of rapid climate change. *International Journal of Plant Sciences*, *177*(5), 389–399.

Lenoir, J., Gégout, J.-C., Marquet, P., De Ruffray, P., & Brisse, H. (2008). A significant upward shift in plant species optimum elevation during the 20th century. *Science*, *320*(5884), 1768–1771.

Li, D., Wu, S., Liu, L., Zhang, Y., & Li, S. (2018). Vulnerability of the global terrestrial ecosystems to climate change. *Global Change Biology*, *24*(9), 4095–4106.

Little Jr, E. L. (1971). Atlas of United States trees, volume 1: Conifers and important hardwoods. Miscellaneous publication 1146. *US Department of Agriculture, Forest Service, Washington, DC*.

Loarie, S. R., Duffy, P. B., Hamilton, H., Asner, G. P., Field, C. B., & Ackerly, D. D. (2009). The velocity of climate change. *Nature*, *462*(7276), 1052–1055.

Lowe, A., Cavers, S., Boshier, D., Breed, M., & Hollingsworth, P. (2015). The resilience of forest fragmentation genetics—no longer a paradox—we were just looking in the wrong place. *Heredity*, *115*(2), 97–99.

Lundqvist, E., & Andersson, E. (2001). Genetic diversity in populations of plants with different breeding and dispersal strategies in a free-flowing boreal river system. *Hereditas*, *135*(1), 75–83.

Ma, J., Foltz, G. R., Soden, B. J., Huang, G., He, J., & Dong, C. (2016). Will surface winds weaken in response to global warming? *Environmental Research Letters*, *11*(12), 124012.

Maclean, I. M., Suggitt, A. J., Wilson, R. J., Duffy, J. P., & Bennie, J. J. (2017). Fine-scale climate change: Modelling spatial variation in biologically meaningful rates of warming. *Global Change Biology*, *23*(1), 256–268.

MacLean, S. A., & Beissinger, S. R. (2017). Species' traits as predictors of range shifts under contemporary climate change: A review and meta-analysis. *Global Change Biology*, *23*(10), 4094–4105.

Mahony, C. R., & Cannon, A. J. (2018). Wetter summers can intensify departures from natural variability in a warming climate. *Nature Communications*, *9*(1), 1–9.

Mahony, C. R., Cannon, A. J., Wang, T., & Aitken, S. N. (2017). A closer look at novel climates: New methods and insights at continental to landscape scales. *Global Change Biology*, *23*(9), 3934–3955.

Maitner, B. S., Boyle, B., Casler, N., Condit, R., Donoghue, J., Durán, S. M., Guaderrama, D., Hinchliff, C. E., Jørgensen, P. M., Kraft, N. J., Et al. (2018). The BIEN R package: A tool to access the Botanical Information and Ecology Network (BIEN) database. *Methods in Ecology and Evolution*, *9*(2), 373–379.

Maurer, K. D., Bohrer, G., Medvigy, D., & Wright, S. J. (2013). The timing of abscission affects dispersal distance in a wind-dispersed tropical tree. *Functional Ecology*, *27*(1), 208–218.

McVicar, T. R., Roderick, M. L., Donohue, R. J., Li, L. T., Van Niel, T. G., Thomas, A., Grieser, J., Jhajharia, D., Himri, Y., Mahowald, N. M., Et al. (2012). Global review

and synthesis of trends in observed terrestrial near-surface wind speeds: Implications for evaporation. *Journal of Hydrology*, *416*, 182–205.

Molinos, J. G., Burrows, M., & Poloczanska, E. (2017). Ocean currents modify the coupling between climate change and biogeographical shifts. *Scientific Reports*, *7*(1), 1–9.

Mora, C., Frazier, A. G., Longman, R. J., Dacks, R. S., Walton, M. M., Tong, E. J., Sanchez, J. J., Kaiser, L. R., Stender, Y. O., Anderson, J. M., Et al. (2013). The projected timing of climate departure from recent variability. *Nature*, *502*(7470), 183–187.

Morelli, T. L., Daly, C., Dobrowski, S. Z., Dulen, D. M., Ebersole, J. L., Jackson, S. T., Lundquist, J. D., Millar, C. I., Maher, S. P., Monahan, W. B., Et al. (2016). Managing climate change refugia for climate adaptation. *PLoS One*, *11*(8), e0159909.

Morrissey, M. B., & de Kerckhove, D. T. (2009). The maintenance of genetic variation due to asymmetric gene flow in dendritic metapopulations. *The American Naturalist*, *174*(6), 875–889.

Munoz, J., Felicisimo, A. M., Cabezas, F., Burgaz, A. R., & Martinez, I. (2004). Wind as a long-distance dispersal vehicle in the Southern Hemisphere. *Science*, *304*(5674), 1144–1147.

Nadeau, C. P., & Fuller, A. K. (2015). Accounting for multiple climate components when estimating climate change exposure and velocity. *Methods in Ecology and Evolution*, *6*(6), 697–705.

Nathan, R. (2006). Long-distance dispersal of plants. *Science*, *313*(5788), 786–788.

Nathan, R., Horvitz, N., He, Y., Kuparinen, A., Schurr, F. M., & Katul, G. G. (2011). Spread of North American wind-dispersed trees in future environments. *Ecology Letters*, *14*(3), 211–219.

Nathan, R., Katul, G. G., Horn, H. S., Thomas, S. M., Oren, R., Avissar, R., Pacala, S. W., & Levin, S. A. (2002). Mechanisms of long-distance dispersal of seeds by wind. *Nature*, *418*(6896), 409–413.

Nathan, R., Safriel, U. N., & Noy-Meir, I. (2001). Field validation and sensitivity analysis of a mechanistic model for tree seed dispersal by wind. *Ecology*, *82*(2), 374–388.

Nathan, R., Sapir, N., Trakhtenbrot, A., Katul, G. G., Bohrer, G., Otte, M., Avissar, R., Soons, M. B., Horn, H. S., Wikelski, M., Et al. (2005). Long-distance biological transport processes through the air: Can nature's complexity be unfolded in silico? *Diversity and Distributions*, *11*(2), 131–137.

Nolan, C., Overpeck, J. T., Allen, J. R., Anderson, P. M., Betancourt, J. L., Binney, H. A., Brewer, S., Bush, M. B., Chase, B. M., Cheddadi, R., Et al. (2018). Past and future global transformation of terrestrial ecosystems under climate change. *Science*, *361*(6405), 920–923.

Normand, S., Ricklefs, R. E., Skov, F., Bladt, J., Tackenberg, O., & Svenning, J.-C. (2011). Postglacial migration supplements climate in determining plant species ranges in Europe. *Proceedings of the Royal Society B: Biological Sciences*, *278*(1725), 3644–3653.

O'Donnell, M. S., & Ignizio, D. A. (2012). Bioclimatic predictors for supporting ecological applications in the conterminous United States. *US Geological Survey Data Series*, *691*(10).

Ordonez, A., Williams, J. W., & Svenning, J.-C. (2016). Mapping climatic mechanisms likely to favour the emergence of novel communities. *Nature Climate Change*, *6*(12), 1104–1109.

Owens, J. N. (2006). The reproductive biology of lodgepole pine: Extension note 07.

Oyler, J. W., Ballantyne, A., Jencso, K., Sweet, M., & Running, S. W. (2015). Creating a topoclimatic daily air temperature dataset for the conterminous United States using homogenized station data and remotely sensed land skin temperature. *International Journal of Climatology*, *35*(9), 2258–2279.

Oyler, J. W., Dobrowski, S. Z., Ballantyne, A. P., Klene, A. E., & Running, S. W. (2015). Artificial amplification of warming trends across the mountains of the western United States. *Geophysical Research Letters*, *42*(1), 153–161.

Pachauri, R. K., Allen, M. R., Barros, V. R., Broome, J., Cramer, W., Christ, R., Church, J. A., Clarke, L., Dahe, Q., Dasgupta, P., Et al. (2014). *Climate change 2014: Synthesis report. Contribution of Working Groups I, II and III to the fifth assessment report of the Intergovernmental Panel on Climate Change*. IPCC.

Parmesan, C., & Yohe, G. (2003). A globally coherent fingerprint of climate change impacts across natural systems. *Nature*, *421*(6918), 37–42.

Payette, S. (1993). The range limit of boreal tree species in Québec-labrador: An ecological and palaeoecological interpretation. *Review of Palaeobotany and Palynology*, *79*(1-2), 7–30.

Pazos, G. E., Greene, D. F., Katul, G., Bertiller, M. B., & Soons, M. B. (2013). Seed dispersal by wind: Towards a conceptual framework of seed abscission and its contribution to long-distance dispersal. *Journal of Ecology*, *101*(4), 889–904.

Pecl, G. T., Araújo, M. B., Bell, J. D., Blanchard, J., Bonebrake, T. C., Chen, I.-C., Clark, T. D., Colwell, R. K., Danielsen, F., Evengård, B., Et al. (2017). Biodiversity redistribution under climate change: Impacts on ecosystems and human well-being. *Science*, *355*(6332).

Petit, R. J., Duminil, J., Fineschi, S., Hampe, A., Salvini, D., & Vendramin, G. G. (2005). Comparative organization of chloroplast, mitochondrial and nuclear diversity in plant populations. *Molecular Ecology*, *14*(3), 689–701.

Petit, R. J., & Hampe, A. (2006). Some evolutionary consequences of being a tree. *Annu. Rev. Ecol. Evol. Syst.*, *37*, 187–214.

Phillips, S. J., Anderson, R. P., & Schapire, R. E. (2006). Maximum entropy modeling of species geographic distributions. *Ecological Modelling*, *190*(3-4), 231–259.

Phillips, S. J., & Dudık, M. (2008). Modeling of species distributions with MaxEnt: New extensions and a comprehensive evaluation. *Ecography*, *31*(2), 161–175.

Pringle, J. M., Blakeslee, A. M., Byers, J. E., & Roman, J. (2011). Asymmetric dispersal allows an upstream region to control population structure throughout a species' range. *Proceedings of the National Academy of Sciences*, *108*(37), 15288–15293.

Projected distributions of novel and disappearing climates by 2100 AD. (n.d.).

Pryor, S., & Barthelmie, R. (2010). Climate change impacts on wind energy: A review. *Renewable and sustainable energy reviews*, *14*(1), 430–437.

Pryor, S., & Barthelmie, R. (2011). Assessing climate change impacts on the near-term stability of the wind energy resource over the United States. *Proceedings of the National Academy of Sciences*, *108*(20), 8167–8171.

R Core Team. (2017). *R: A Language and Environment for Statistical Computing*. R Foundation for Statistical Computing. Vienna, Austria. http://www.R-project.org/

Rapacciuolo, G., Maher, S. P., Schneider, A. C., Hammond, T. T., Jabis, M. D., Walsh, R. E., Iknayan, K. J., Walden, G. K., Oldfather, M. F., Ackerly, D. D., Et al. (2014). Beyond a warming fingerprint: Individualistic biogeographic responses to heterogeneous climate change in California. *Global Change Biology*, *20*(9), 2841–2855.

Regal, P. J. (1982). Pollination by wind and animals: Ecology of geographic patterns. *Annual Review of Ecology and Systematics*, *13*(1), 497–524.

Rehfeldt, G. E., Ying, C. C., Spittlehouse, D. L., & Hamilton Jr, D. A. (1999). Genetic responses to climate in Pinus contorta: Niche breadth, climate change, and reforestation. *Ecological Monographs*, *69*(3), 375–407.

Ren, G., Liu, J., Wan, J., Li, F., Guo, Y., & Yu, D. (2018). The analysis of turbulence intensity based on wind speed data in onshore wind farms. *Renewable energy*, *123*, 756–766.

Richardson, D. M., Hellmann, J. J., McLachlan, J. S., Sax, D. F., Schwartz, M. W., Gonzalez, P., Brennan, E. J., Camacho, A., Root, T. L., Sala, O. E., Et al. (2009). Multidimensional evaluation of managed relocation. *Proceedings of the National Academy of Sciences*, *106*(24), 9721–9724.

Rollins, M. G. (2009). LANDFIRE: A nationally consistent vegetation, wildland fire, and fuel assessment. *International Journal of Wildland Fire*, *18*(3), 235–249.

Rumpf, S. B., Hülber, K., Zimmermann, N. E., & Dullinger, S. (2019). Elevational rear edges shifted at least as much as leading edges over the last century. *Global Ecology and Biogeography*, *28*(4), 533–543.

Saha, S., Moorthi, S., Pan, H.-L., Wu, X., Wang, J., Nadiga, S., Tripp, P., Kistler, R., Woollen, J., Behringer, D., Et al. (2010). The NCEP climate forecast system reanalysis. *Bulletin of the American Meteorological Society*, *91*(8), 1015–1058.

Sandel, B., Arge, L., Dalsgaard, B., Davies, R., Gaston, K., Sutherland, W., & Svenning, J.-C. (2011). The influence of Late Quaternary climate-change velocity on species endemism. *Science*, *334*(6056), 660–664.

Sandel, B., Monnet, A.-C., Govaerts, R., & Vorontsova, M. (2017). Late Quaternary climate stability and the origins and future of global grass endemism. *Annals of Botany*, *119*(2), 279–288.

Savage, D., Barbetti, M. J., MacLeod, W. J., Salam, M. U., & Renton, M. (2010). Timing of propagule release significantly alters the deposition area of resulting aerial dispersal. *Diversity and Distributions*, *16*(2), 288–299.

Savage, D., Barbetti, M. J., MacLeod, W. J., Salam, M. U., & Renton, M. (2011). Can mechanistically parameterised, anisotropic dispersal kernels provide a reliable estimate of wind-assisted dispersal? *Ecological Modelling*, *222*(10), 1673–1682.

Savage, D., Borger, C. P., & Renton, M. (2014). Orientation and speed of wind gusts causing abscission of wind-dispersed seeds influences dispersal distance. *Functional Ecology*, *28*(4), 973–981.

Savolainen, O., Pyhäjärvi, T., & Knürr, T. (2007). Gene flow and local adaptation in trees. *Annu. Rev. Ecol. Evol. Syst.*, *38*, 595–619.

Scheffers, B. R., De Meester, L., Bridge, T. C., Hoffmann, A. A., Pandolfi, J. M., Corlett, R. T., Butchart, S. H., Pearce-Kelly, P., Kovacs, K. M., Dudgeon, D., Et al. (2016). The broad footprint of climate change from genes to biomes to people. *Science*, *354*(6313).

Schippers, P., & Jongejans, E. (2005). Release thresholds strongly determine the range of seed dispersal by wind. *Ecological Modelling*, *185*(1), 93–103.

Schleussner, C.-F., Lissner, T. K., Fischer, E. M., Wohland, J., Perrette, M., Golly, A., Rogelj, J., Childers, K., Schewe, J., Frieler, K., Et al. (2016). Differential climate impacts for policy-relevant limits to global warming: The case of 1.5 C and 2 C. *Earth System Dynamics*, *7*, 327–351.

Schuetz, J. G., Mills, K. E., Allyn, A. J., Stamieszkin, K., Bris, A. L., & Pershing, A. J. (2019). Complex patterns of temperature sensitivity, not ecological traits, dictate diverse species responses to climate change. *Ecography*, *42*(1), 111–124.

Schurr, F. M., Midgley, G. F., Rebelo, A. G., Reeves, G., Poschlod, P., & Higgins, S. I. (2007). Colonization and persistence ability explain the extent to which plant species fill their potential range. *Global Ecology and Biogeography*, *16*(4), 449–459.

Sexton, J. P., Hangartner, S. B., & Hoffmann, A. A. (2014). Genetic isolation by environment or distance: Which pattern of gene flow is most common? *Evolution*, *68*(1), 1–15.

Sexton, J. P., Strauss, S. Y., & Rice, K. J. (2011). Gene flow increases fitness at the warm edge of a species' range. *Proceedings of the National Academy of Sciences*, *108*(28), 11704–11709.

Simberloff, D. (2009). The role of propagule pressure in biological invasions. *Annual Review of Ecology, Evolution, and Systematics*, *40*, 81–102.

Sinha, A., & Davidar, P. (1992). Seed dispersal ecology of a wind dispersed rain forest tree in the Western Ghats, India. *Biotropica*, 519–526.

Skarpaas, O., Auhl, R., & Shea, K. (2006). Environmental variability and the initiation of dispersal: Turbulence strongly increases seed release. *Proceedings of the Royal Society B: Biological Sciences*, *273*(1587), 751–756.

Skarpaas, O., & Shea, K. (2007). Dispersal patterns, dispersal mechanisms, and invasion wave speeds for invasive thistles. *The American Naturalist*, *170*(3), 421–430.

Small, E., & Antle, T. (2003). A preliminary study of pollen dispersal in Cannabis sativa in relation to wind direction. *Journal of Industrial Hemp*, *8*(2), 37–50.

Soons, M. B., & Bullock, J. M. (2008). Non-random seed abscission, long-distance wind dispersal and plant migration rates. *Journal of Ecology*, 581–590.

Soons, M. B., Heil, G. W., Nathan, R., & Katul, G. G. (2004). Determinants of long-distance seed dispersal by wind in grasslands. *Ecology*, *85*(11), 3056–3068.

Sork, V. L., Davis, F. W., Westfall, R., Flint, A., Ikegami, M., Wang, H., & Grivet, D. (2010). Gene movement and genetic association with regional climate gradients in California valley oak (Quercus lobata née) in the face of climate change. *Molecular Ecology*, *19*(17), 3806–3823.

Sorte, C. J. (2013). Predicting persistence in a changing climate: Flow direction and limitations to redistribution. *Oikos*, *122*(2), 161–170.

Soubeyrand, S., Enjalbert, J., Sanchez, A., & Sache, I. (2007). Anisotropy, in density and in distance, of the dispersal of yellow rust of wheat: Experiments in large field plots and estimation. *Phytopathology*, *97*(10), 1315–1324.

Stevens, G. C. (1989). The latitudinal gradient in geographical range: How so many species coexist in the tropics. *The American Naturalist*, *133*(2), 240–256.

Sundqvist, L., Keenan, K., Zackrisson, M., Prodöhl, P., & Kleinhans, D. (2016). Directional genetic differentiation and relative migration. *Ecology and Evolution*, *6*(11), 3461–3475.

Svenning, J.-C., & Skov, F. (2007). Could the tree diversity pattern in europe be generated by postglacial dispersal limitation? *Ecology letters*, *10*(6), 453–460.

Tackenberg, O., Poschlod, P., & Kahmen, S. (2003). Dandelion seed dispersal: The horizontal wind speed does not matter for long-distance dispersal—it is updraft! *Plant Biology*, *5*(05), 451–454.

Taylor, K. E., Stouffer, R. J., & Meehl, G. A. (2012). An overview of CMIP5 and the experiment design. *Bulletin of the American Meteorological Society*, *93*(4), 485–498.

Tewksbury, J. J., Huey, R. B., Deutsch, C. A., Et al. (2008). Putting the heat on tropical animals. *Science*, *320*(5881), 1296.

Thompson, S. E., & Katul, G. G. (2013). Implications of nonrandom seed abscission and global stilling for migration of wind-dispersed plant species. *Global Change Biology*, *19*(6), 1720–1735.

Thompson, S., & Katul, G. (2008). Plant propagation fronts and wind dispersal: An analytical model to upscale from seconds to decades using superstatistics. *The American Naturalist*, *171*(4), 468–479.

Thorne, J. H., Boynton, R. M., Holguin, A. J., Stewart, J. A., & Bjorkman, J. (2016). A climate change vulnerability assessment of California's terrestrial vegetation. *California Department of Fish and Wildlife, Sacramento, CA*.

Thorne, J. H., Choe, H., Stine, P. A., Chambers, J. C., Holguin, A., Kerr, A. C., & Schwartz, M. W. (2018). Climate change vulnerability assessment of forests in the Southwest USA. *Climatic Change*, *148*(3), 387–402.

Tingley, M. W., Koo, M. S., Moritz, C., Rush, A. C., & Beissinger, S. R. (2012). The push and pull of climate change causes heterogeneous shifts in avian elevational ranges. *Global Change Biology*, *18*(11), 3279–3290.

Treml, E. A., Halpin, P. N., Urban, D. L., & Pratson, L. F. (2008). Modeling population connectivity by ocean currents, a graph-theoretic approach for marine conservation. *Landscape Ecology*, *23*(1), 19–36.

Tsuda, Y., Semerikov, V., Sebastiani, F., Vendramin, G. G., & Lascoux, M. (2017). Multispecies genetic structure and hybridization in the Betula genus across Eurasia. *Molecular Ecology*, *26*(2), 589–605.

Vanschoenwinkel, B., Gielen, S., Seaman, M., & Brendonck, L. (2008). Any way the wind blows-frequent wind dispersal drives species sorting in ephemeral aquatic communities. *Oikos*, *117*(1), 125–134.

Vellend, M. (2020). *The theory of ecological communities (mpb-57)*. Princeton University Press.

von Engeln, A., & Teixeira, J. (2013). A planetary boundary layer height climatology derived from ECMWF reanalysis data. *Journal of Climate*, *26*(17), 6575–6590.

Wang, I. J., & Bradburd, G. S. (2014). Isolation by environment. *Molecular Ecology*, *23*(23), 5649–5662.

Wang, T., Hamann, A., Yanchuk, A., O'neill, G., & Aitken, S. (2006). Use of response functions in selecting lodgepole pine populations for future climates. *Global Change Biology*, *12*(12), 2404–2416.

Wang, T., Hamann, A., Spittlehouse, D. L., & Murdock, T. Q. (2012). ClimateWNA—high-resolution spatial climate data for western North America. *Journal of Applied Meteorology and Climatology*, *51*(1), 16–29.

Wang, T., O'Neill, G. A., & Aitken, S. N. (2010). Integrating environmental and genetic effects to predict responses of tree populations to climate. *Ecological applications*, *20*(1), 153–163.

Wang, Z.-F., Lian, J.-Y., Ye, W.-H., Cao, H.-L., Zhang, Q.-M., & Wang, Z.-M. (2016). Pollen and seed flow under different predominant winds in wind-pollinated and wind-dispersed species Engelhardia roxburghiana. *Tree Genetics & Genomes*, *12*(2), 19.

Wiens, J. J. (2016). Climate-related local extinctions are already widespread among plant and animal species. *PLoS Biology*, *14*(12), e2001104.

Willis, C. G., Ruhfel, B., Primack, R. B., Miller-Rushing, A. J., & Davis, C. C. (2008). Phylogenetic patterns of species loss in Thoreau's woods are driven by climate change. *Proceedings of the National Academy of Sciences*, *105*(44), 17029–17033.

Wilson, G. A., & Rannala, B. (2003). Bayesian inference of recent migration rates using multilocus genotypes. *Genetics*, *163*(3), 1177–1191.

Wolf, A., Zimmerman, N. B., Anderegg, W. R., Busby, P. E., & Christensen, J. (2016). Altitudinal shifts of the native and introduced flora of California in the context of 20th-century warming. *Global Ecology and Biogeography*, *25*(4), 418–429.

Wright, S. J., Trakhtenbrot, A., Bohrer, G., Detto, M., Katul, G. G., Horvitz, N., Muller-Landau, H. C., Jones, F. A., & Nathan, R. (2008). Understanding strategies for seed dispersal by wind under contrasting atmospheric conditions. *Proceedings of the National Academy of Sciences*, *105*(49), 19084–19089.

Wright, S. (1943). Isolation by distance. *Genetics*, *28*(2), 114.

Zeller, K. A., McGarigal, K., & Whiteley, A. R. (2012). Estimating landscape resistance to movement: A review. *Landscape Ecology*, *27*(6), 777–797.

Appendix 1: Supplementary information for chapter 1

Name	Abbreviation	Definition
Bio1	mean T	Annual Mean Temperature
Bio2	mean diurnal T range	Mean Diurnal Temperature Range (Mean of monthly (max temp - min temp))
Bio3	isothermality	Isothermality (Bio2 / Bio7)
Bio4	T seasonality	Temperature Seasonality (standard deviation)
Bio5	maxTwrmm	Max Temperature of Warmest Month
Bio6	minTcldm	Min Temperature of Coldest Month
Bio7	annual T range	Temperature Annual Range (Bio5 - Bio6)
Bio8	meanTwetq	Mean Temperature of Wettest Quarter
Bio9	meanTdryq	Mean Temperature of Driest Quarter
Bio10	meanTwrmq	Mean Temperature of Warmest Quarter
Bio11	meanTcldq	Mean Temperature of Coldest Quarter
Bio12	total P	Annual Precipitation
Bio13	Pwetm	Precipitation of Wettest Month
Bio14	Pdrym	Precipitation of Driest Month
Bio15	P seasonality	Precipitation Seasonality (coefficient of variation)
Bio16	Pwetq	Precipitation of Wettest Quarter
Bio17	Pdryq	Precipitation of Driest Quarter
Bio18	Pwrmq	Precipitation of Warmest Quarter

Table S1.1: Abbreviations and definitions for the 19 bioclimatic variables used in the analysis.

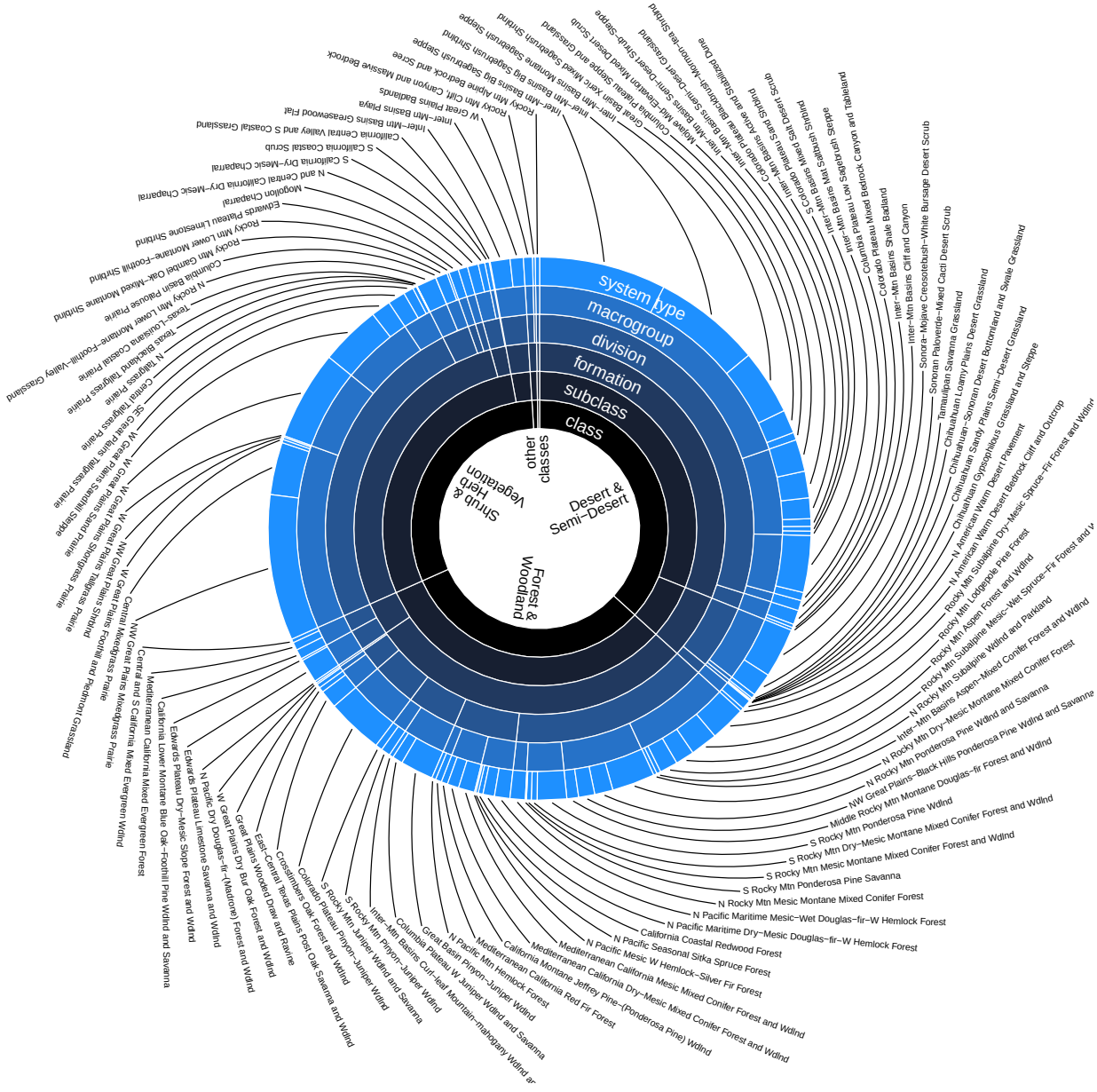

Figure S1.1: Labelled key to the six-level USNVC hierarchy. Category names are listed for the outermost layer representing the vegetation "system types" used in this analysis, and the innermost layer representing the coarsest-level vegetation "classes" referred to in the text. All slices are sized according to the land area covered by a vegetation category within our western US study area. See www.natureserveexplorer.org for detailed descriptions of each type.

Figure S1.2: Heatmap of variable importance matrix, with low ranks indicating variables more important to a given type. The top four variables (yellow-orange) were used in the novelty analyses. Data are arranged to roughly group vegetation types that are similar in the variables that shape their distributions and roughly group variables that are similar in the vegetation types whose distributions they shape.

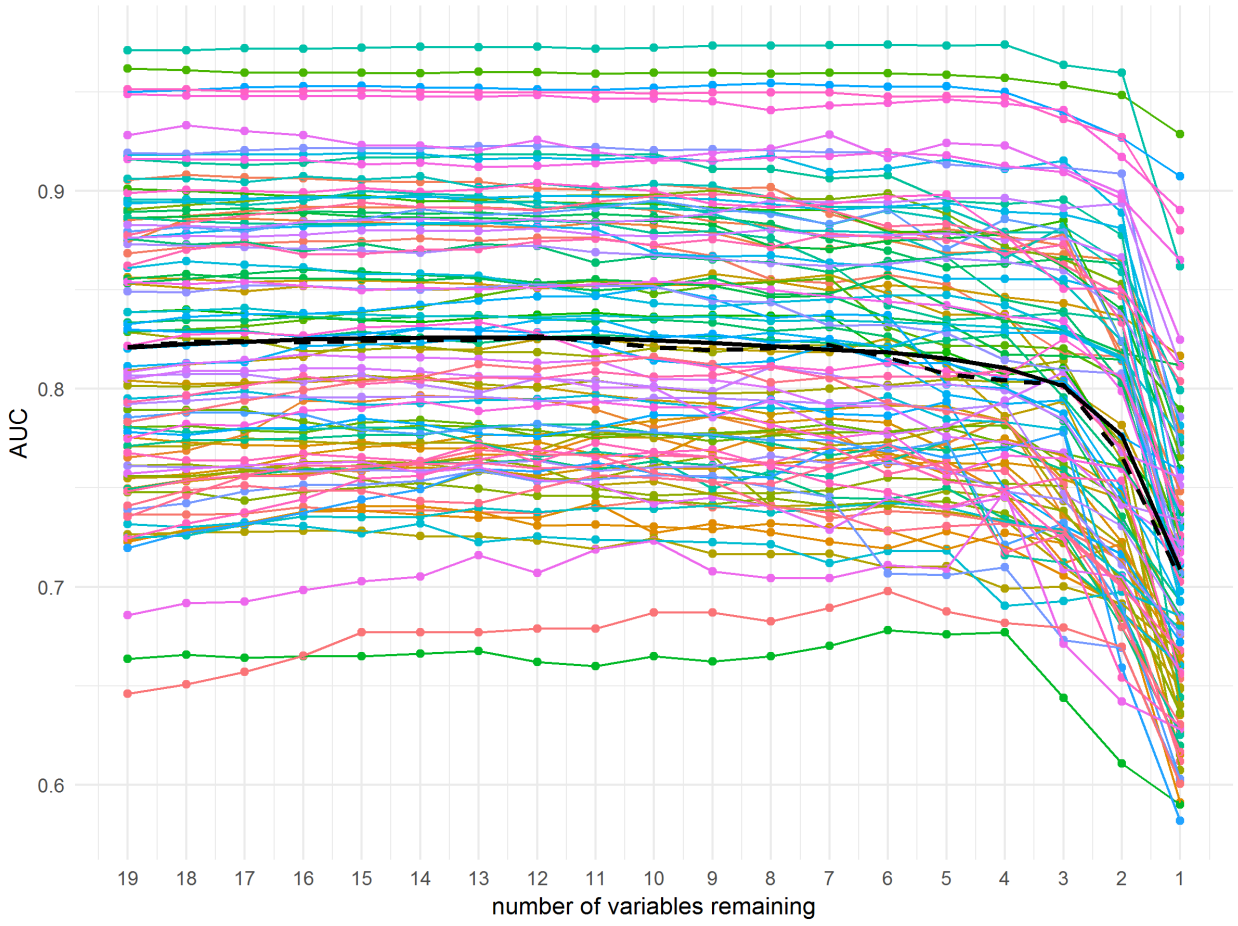

Figure S1.3: Variable selection model performance curves for each vegetation type. The recursive feature elimination algorithm used to determine relative variable importance for each type begins with all 19 bioclimatic variables and progresses left to right, iteratively removing the variable that least reduces model performance as measured by area under the receiver-operator curve (AUC) evaluated on spatially independent data. By recording the identity of the variable removed at each step, variables are ranked in order of importance for each type. The mean (solid line) and median (dashed line) AUC across all vegetation types are shown in black.

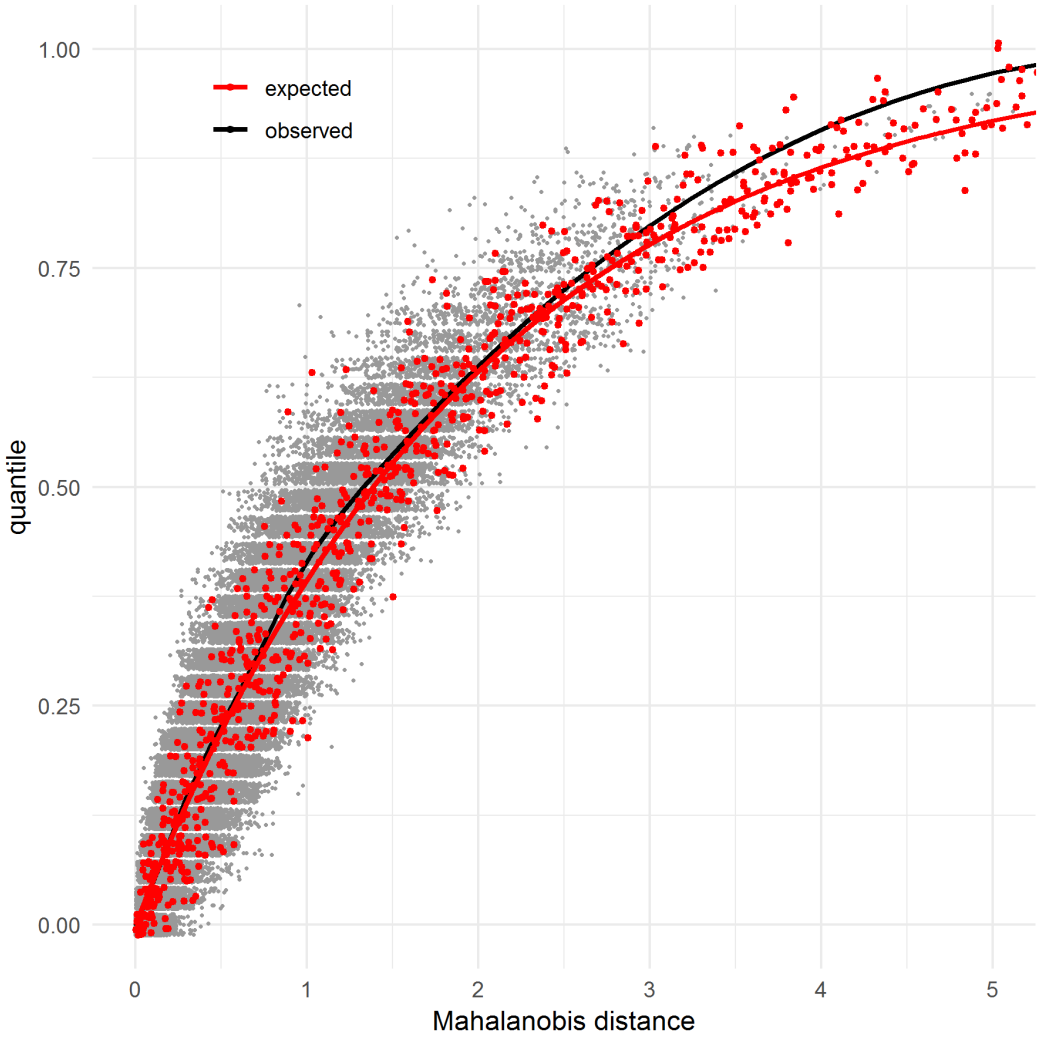

Figure S1.4: Mahalanobis distances (MD) and percentiles for empirical climate time series versus simulated multivariate normal data. X-axis values represent the MD of an individual year, while y-axis values represent the percentiles of those values with respect a 33-year time series. Gray points show a random sample of actual observed values from our analysis, summarized by the black GAM curve. Red points show the expected pattern based on multivariate normal data (draws from randomly simulated datasets each with n = 33 points), while the red curve shows the cumulative chi-squared distribution with 2 degrees of freedom. The conditional means and variances are quite similar between the observed and expected data, indicating that empirical data are sufficiently normally distributed for these statistics to be easily interpretable.

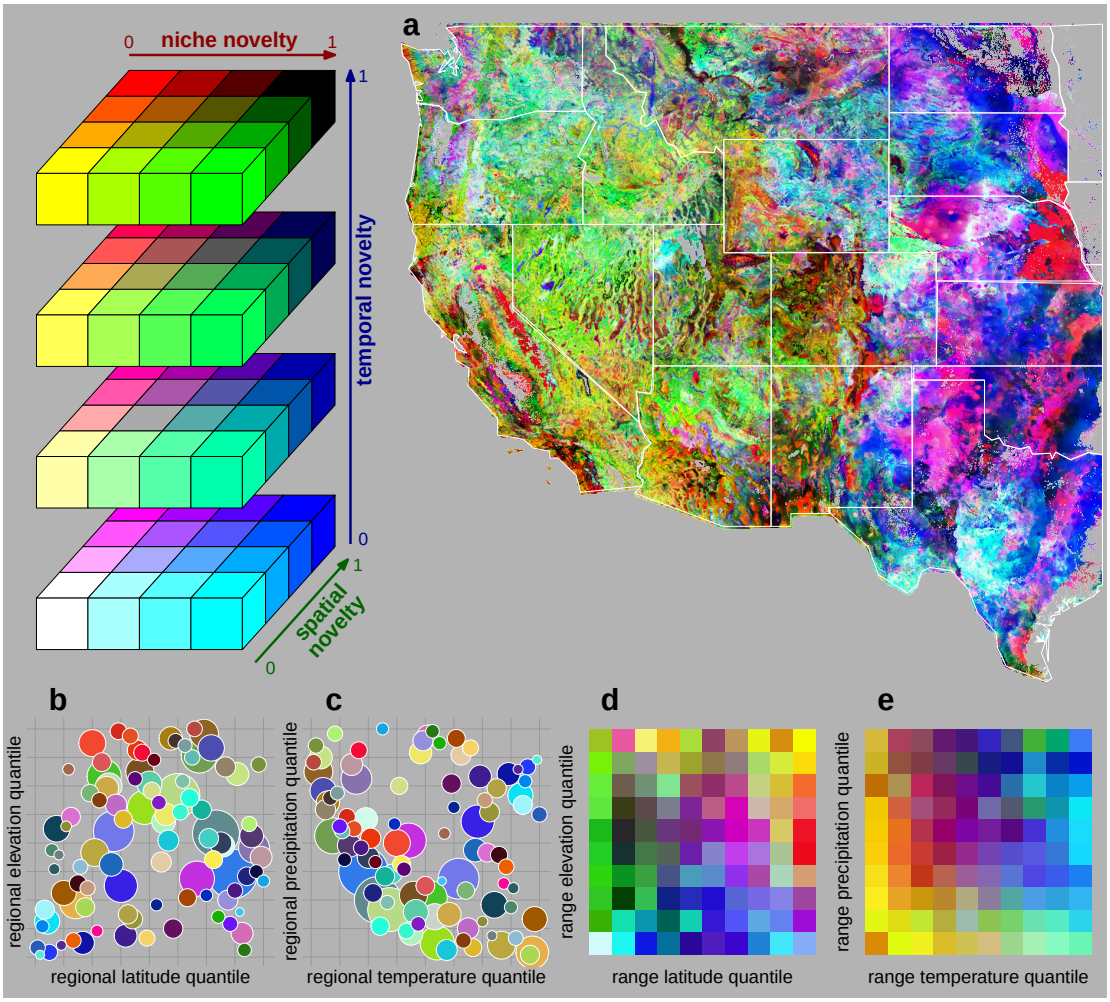

Figure S1.5: Vegetation climate change vulnerability across the western United States according to three metrics of vulnerability: niche novelty, spatial novelty, and temporal novelty. This figure presents the same results as Figure 1.4 in the main manuscript, but uses color to depict the position of sites or vegetation types in three-dimensional novelty space. Sites in white or black respectively have low or high vulnerability ranks for all three metrics, and sites in color have various combinations of high and low vulnerability across the three metrics. (a) Geographic vulnerability patterns across the western US, with grid cell values representing the mean vulnerability of local vegetation types. (b) Mean range-wide latitude, elevation, and vulnerability of each vegetation type. (c) Mean range-wide temperature, precipitation, and vulnerability of each vegetation type. (d) Vulnerability as a function of a site's position within the geographic range of a type, averaged across all types endemic to the US. (e) Vulnerability as a function of a site's position within the realized climatic niche of a type, averaged across all types endemic to the US. All vulnerability values are in quantiles relative to other values within each panel.

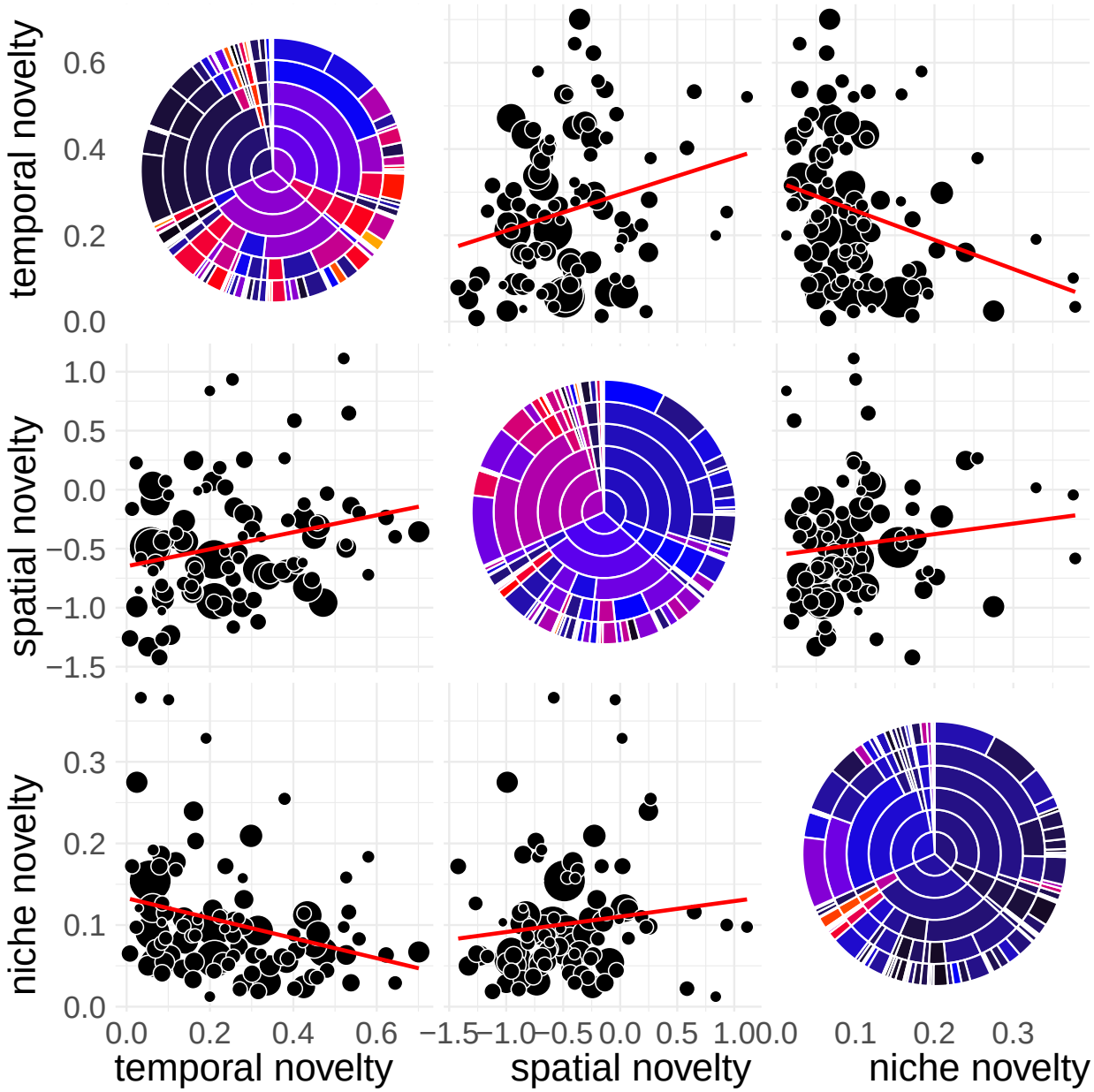

Figure S1.6: Mean distribution-wide vulnerability of the 96 vegetation types. Diagonals: exposure values across the vegetation classification (see Figure S1.1 for a labelled key). Off-diagonals: relationships between mean novelty values for the three metrics. Black-purple-yellow colors represent low-medium-high novelty.

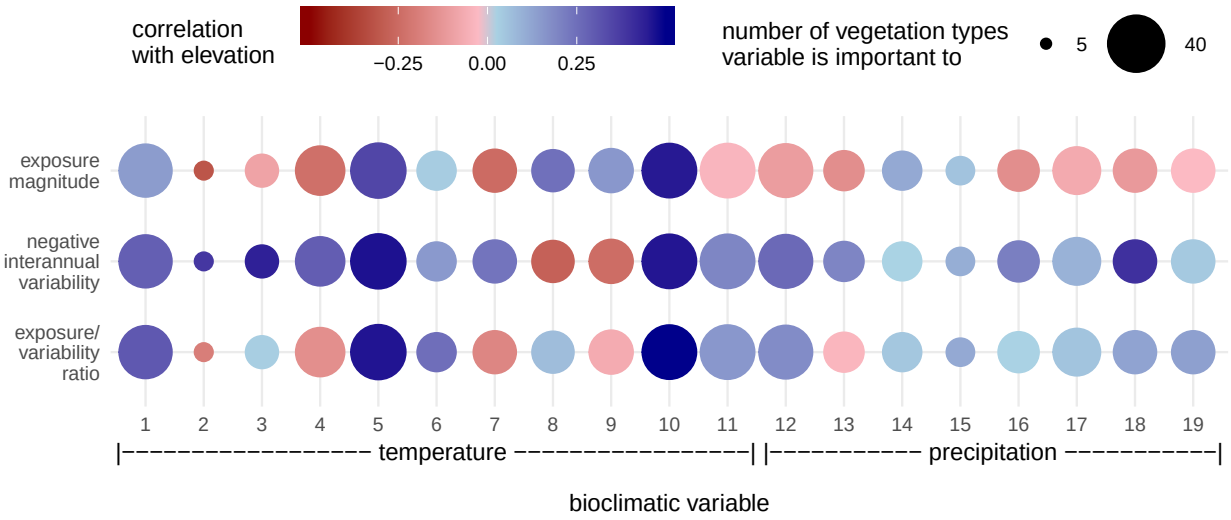

Figure S1.7: Relationships between elevation and components of univariate temporal novelty for each of the 19 bioclimatic variables. Color represents the correlation coefficient between elevation and the listed climate change statistic for a given climate variable across grid cells of the western US, while point size indicates how often the variable was among the most important to vegetation types, and thus its influence on vulnerability results. For all four statistics, higher values are associated with greater temporal novelty, and positive correlations colored in blue thus represent increasing vulnerability with elevation. *Exposure magnitude* is the absolute value of change in a given climate variable. *Negative interannual variability* is negative one times the standard deviation across years in the baseline time period, made negative so that higher values equate to higher predicted vulnerability. The *ratio of exposure to variability* for a given grid cell is the absolute z-score.

Appendix 2: Supplementary information for chapter 2

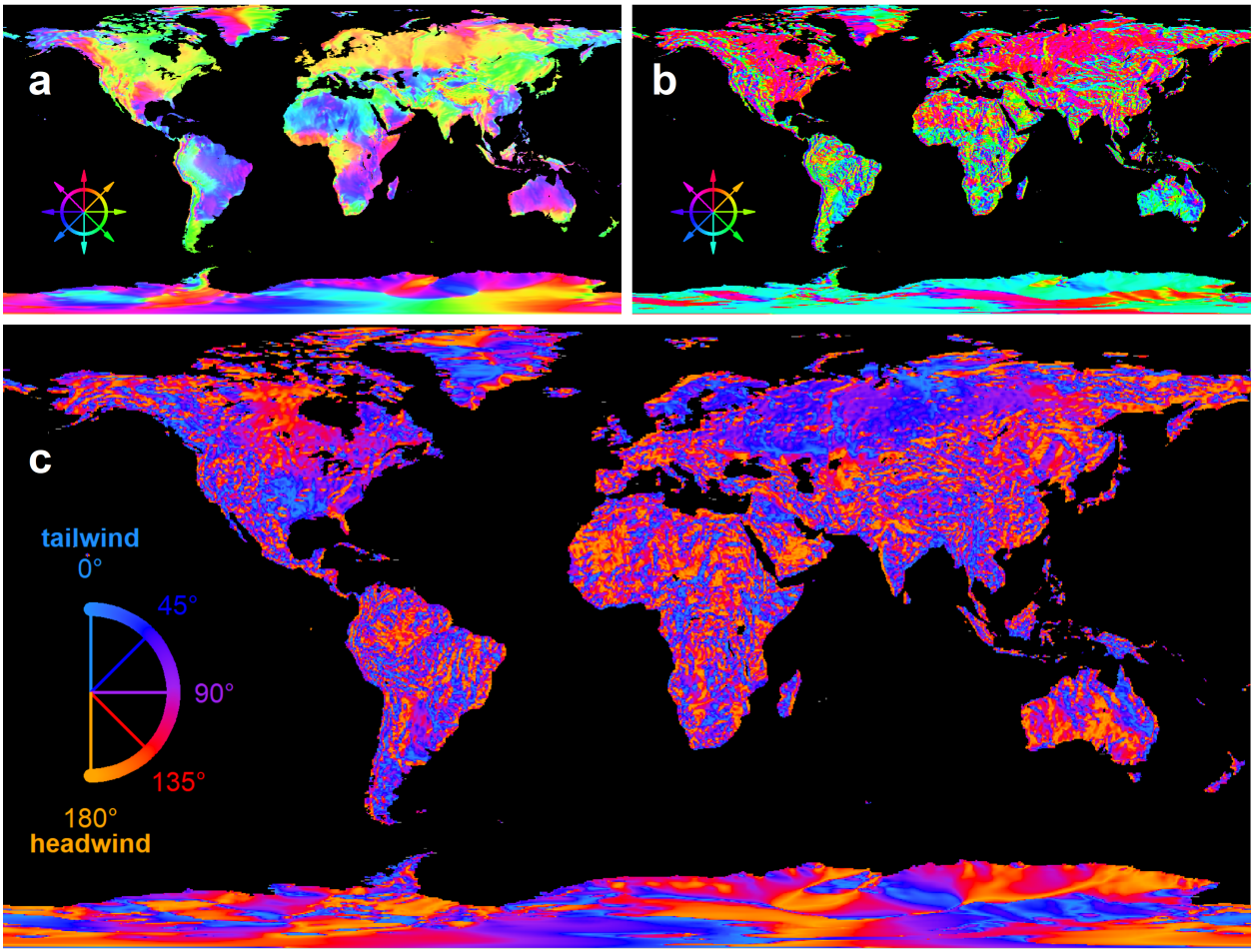

Figure S2.1: Global patterns of alignment between prevailing wind direction and temperature gradients. (a) Prevailing local wind direction, that is the bearing at which wind-dispersed organisms are expected to move on average. (b) Direction of temperature gradient descent, that is the local direction in which organisms will need to move to offset warming climate. (c) The difference between these two directions, with 0° indicating migratory tailwinds (prevailing winds blow directly down the temperature gradient) and 180° indicating migratory headwinds (prevailing winds blow directly up the temperature gradient).

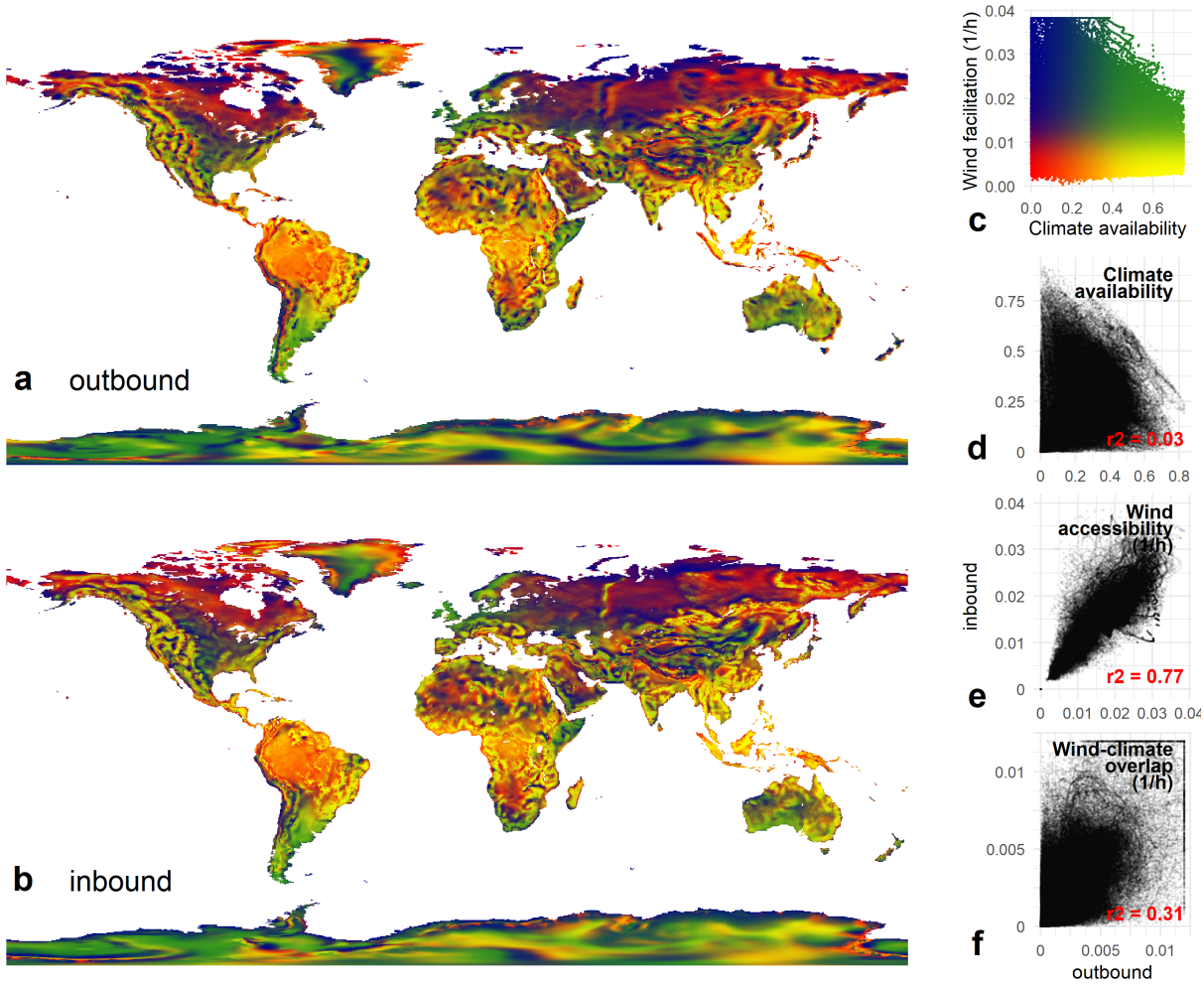

Figure S2.2: Global patterns of landscape overlap between windsheds and climate analogs. Maps show the amount of climatically analogous area versus the proportion of that area that is wind-accessible within 250 km of each focal site, in the outbound (a), and inbound (b), directions. (Panel *a* presents the same data as figure 2.4c of the main text, and is repeated here for comparison.) Color represents the bivariate relationship between these variables (c), with green and blue indicating wind facilitation and yellow and red indicating wind hindrance. Additional scatterplots (d–f) compare the amount of similar climate, the amount of wind-accessible area, and the amount of wind-climate overlap in the forward versus reverse directions. Extreme outliers are rescaled in panel *f* for visual purposes only.

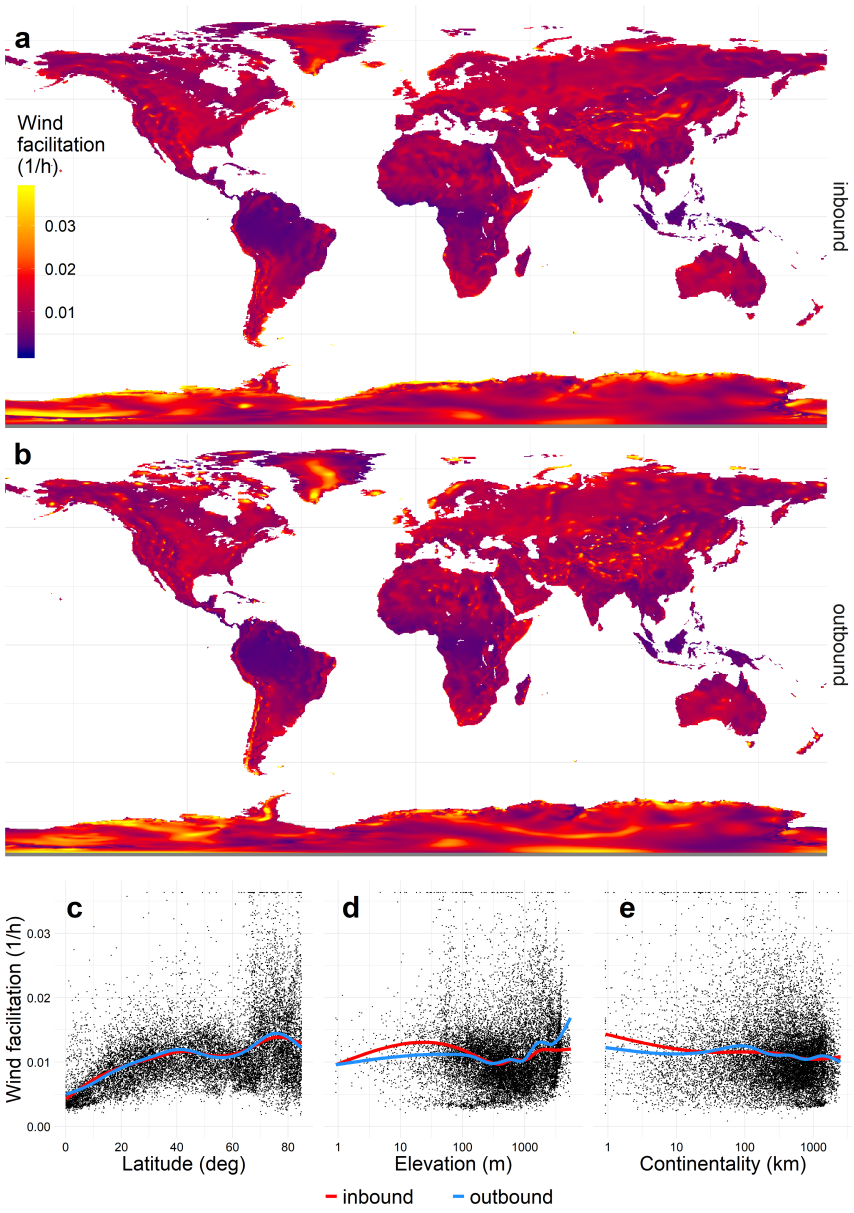

Figure S2.3: Global patterns of wind facilitation of climate change tracking. Maps show wind facilitation for the landscape within 250 km of each terrestrial grid cell, in the inbound (a), and outbound (b), directions, and with respect to major geographic gradients (c–e). In the scatterplots, latitude represents absolute latitude.

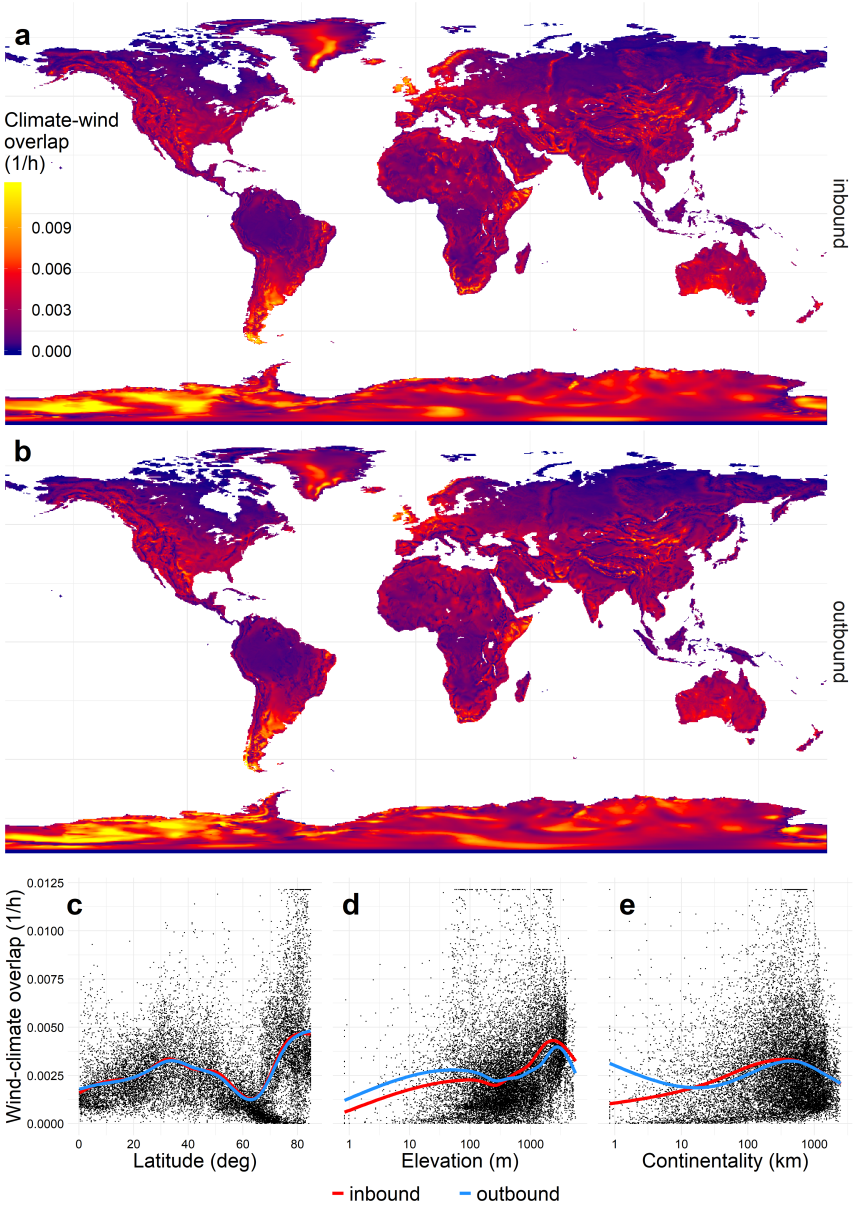

Figure S2.4: Global patterns of wind-climate overlap. Maps show overlap for the landscape within 250 km of each terrestrial grid cell, in the inbound (a), and outbound (b), directions, and with respect to major geographic gradients (c–e). In the scatterplots, latitude represents absolute latitude.

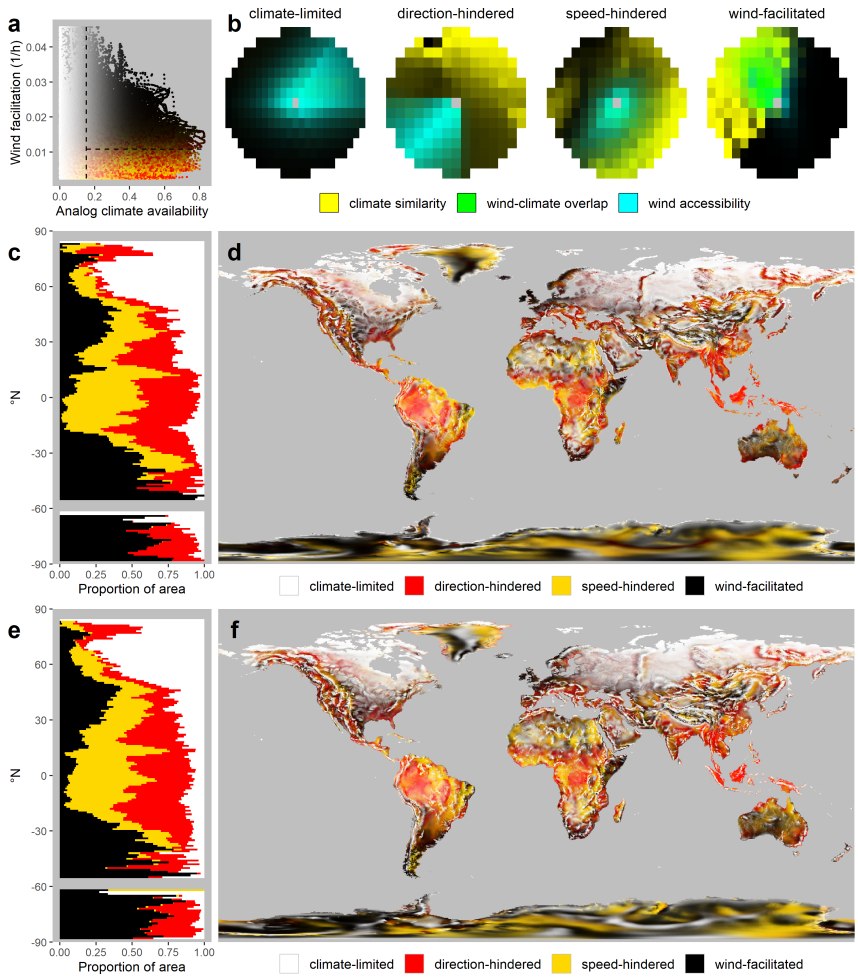

Figure S2.5: Global patterns of wind facilitation 'syndromes'. Sites can be assigned continuous rankings or discrete categories representing four alternative syndromes: wind facilitation, directional hindrance, speed hindrance, or climate limitation. (a) Sites are ranked by climate availability, wind facilitation, and directional alignment (collapsed z-axis differentiating red from yellow) to assign relative membership in each of the four syndromes. (b) Examples of each syndrome, with colors representing climate similarity, wind accessibility, and their areas of overlap across the 250-km radius landscapes surrounding each central origin cell. (c,e) Syndrome prevalence by latitude in the inbound and outbound directions, respectively; syndromes are categorized to place 25% of global land area in each category, along the dotted lines depicted in panel *a*. (d,f) Global map of syndromes in the inbound and outbound directions, respectively, with colors representing a continuous gradient among the four categories as depicted in panel *a*.

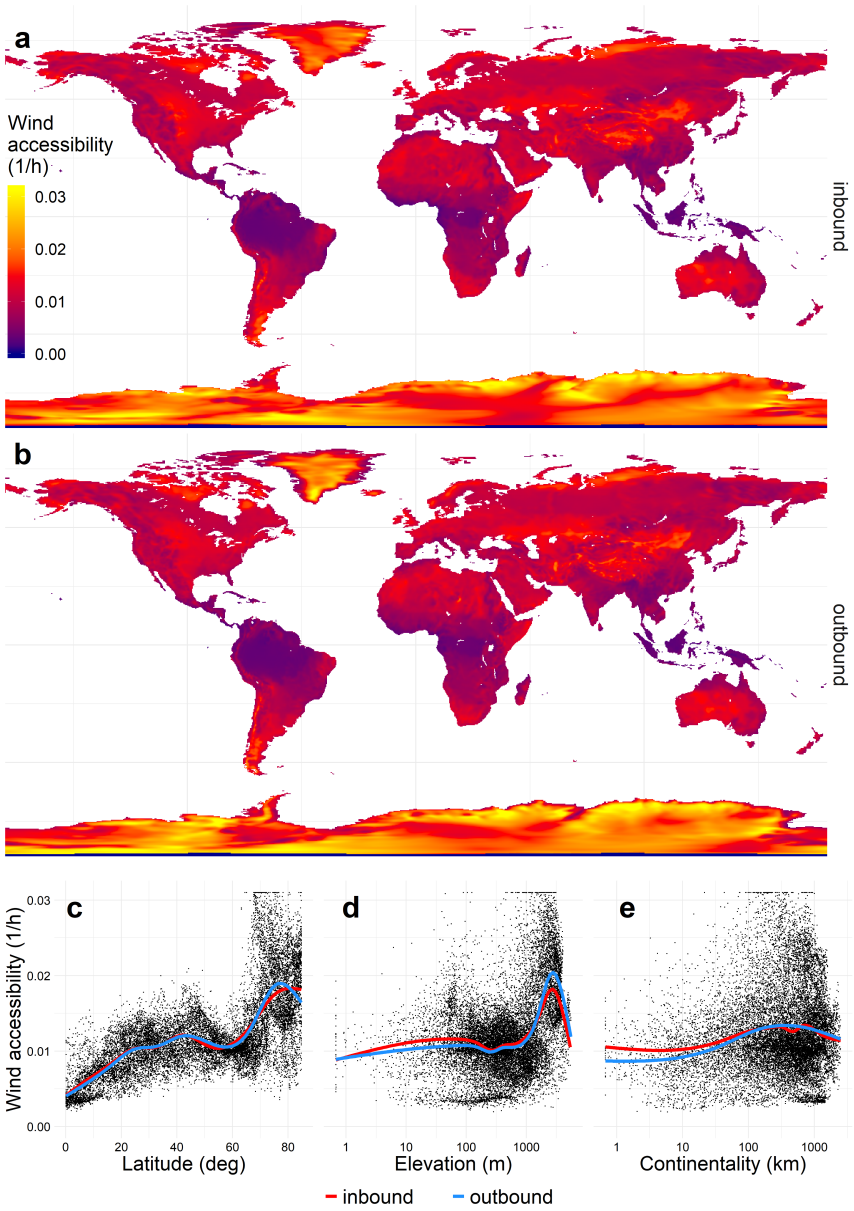

Figure S2.6: Global patterns of wind accessibility. Maps show the mean wind accessibility of landscapes within 250 km of each terrestrial grid cell, in the inbound (a), and outbound (b), directions, and with respect to major geographic gradients (c–e). In the scatterplots, latitude represents absolute latitude.

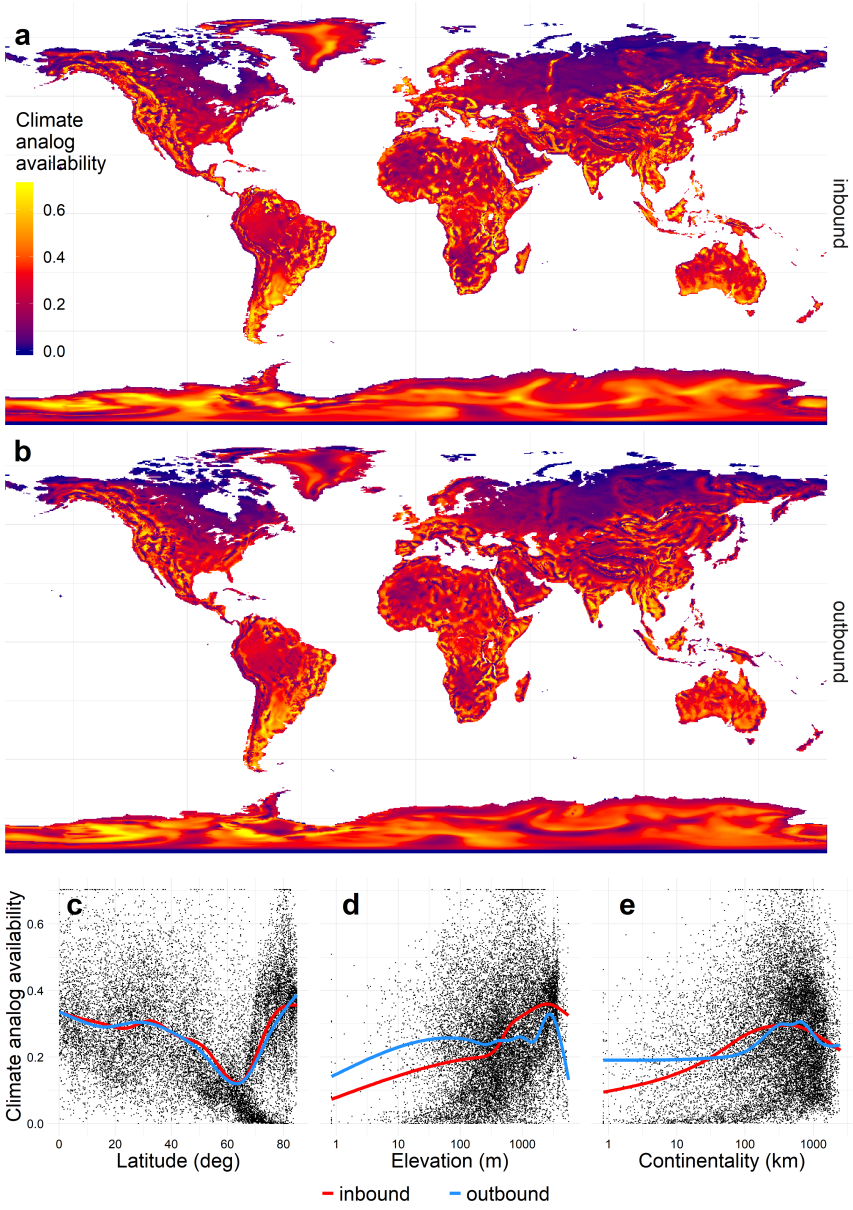

Figure S2.7: Global patterns of climate analog availability. Maps show analog availability within 250km of each terrestrial grid cell, in the inbound (a), and outbound (b), directions, and with respect to major geographic gradients (c–e). In the scatterplots, latitude represents absolute latitude.

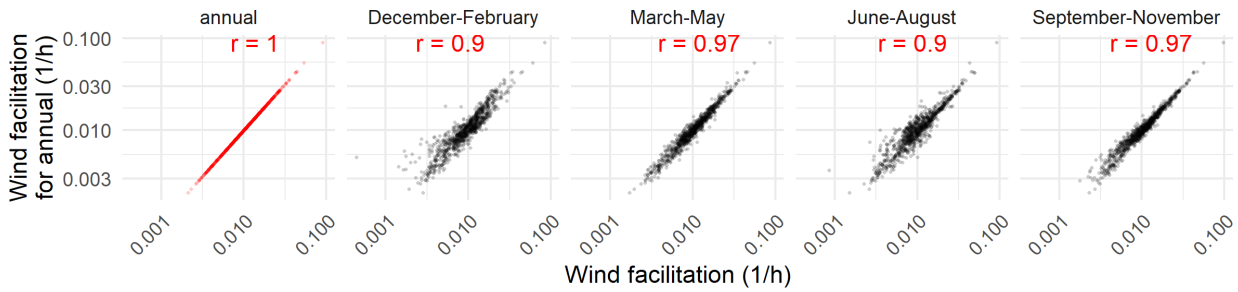

Figure S2.8: Sensitivity of global wind facilitation patterns to season of year. Our main analysis (y-axis values) used wind data from all months of the year. Here we compare these to the corresponding wind facilitation values to four seasonal versions (x-axis values) for 1000 randomly selected global grid cells. Red numbers are Pearson's correlation coefficients of log wind facilitation values.

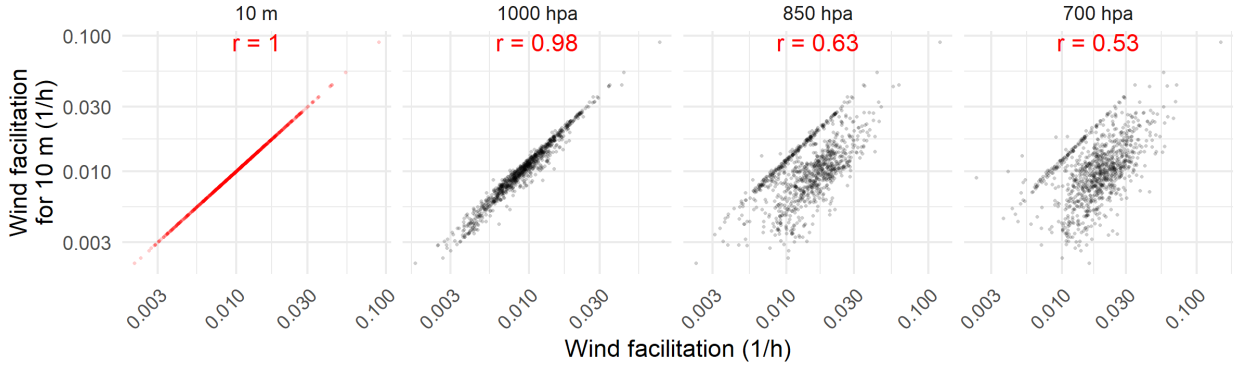

Figure S2.9: Sensitivity of global wind facilitation patterns to atmospheric height. Our main analysis (y-axis values) used wind data from 10 m aboveground. Here we compare these to the corresponding wind facilitation values for three higher layers (x-axis values) for 1000 randomly selected global grid cells. The pressure levels 1000 hpa, 850 hpa, and 700 hpa correspond to approximately 100 m, 1500 m, and 3000 m aboveground, respectively. Red numbers are Pearson's correlation coefficients of log wind facilitation values.

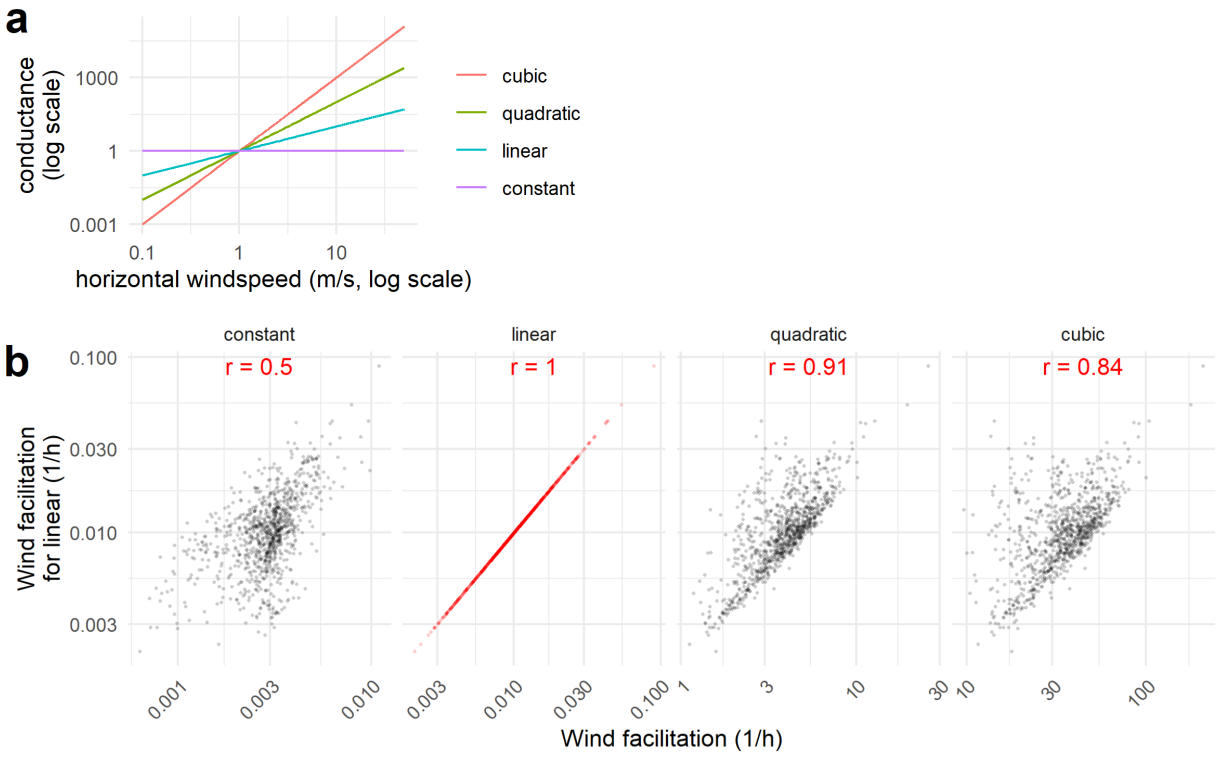

Figure S2.10: Sensitivity of wind facilitation patterns to the choice of wind conductance function, which converts instantaneous windspeeds into connectivity between neighboring grid cells. (a) Shapes of the functions compared. A linear function like the one we use in the main analysis weights conductance in proportion to wind speed, while a constant conductance function weights all windspeeds equally, effectively ignoring speed and considering only wind direction; a quadratic function based on squared windspeed is proportional to aerodynamic drag, while a cubic function of windspeed is proportional to force or energy content. Note that all of these exponential curves appear as straight lines on the log-log axes. (b) Mean landscape wind facilitation for 1000 randomly selected global grid cells for our main analysis (y-axis values) versus the corresponding values for the alternative functions (x-axis values). Red numbers are Pearson's correlation coefficients of log wind facilitation values.

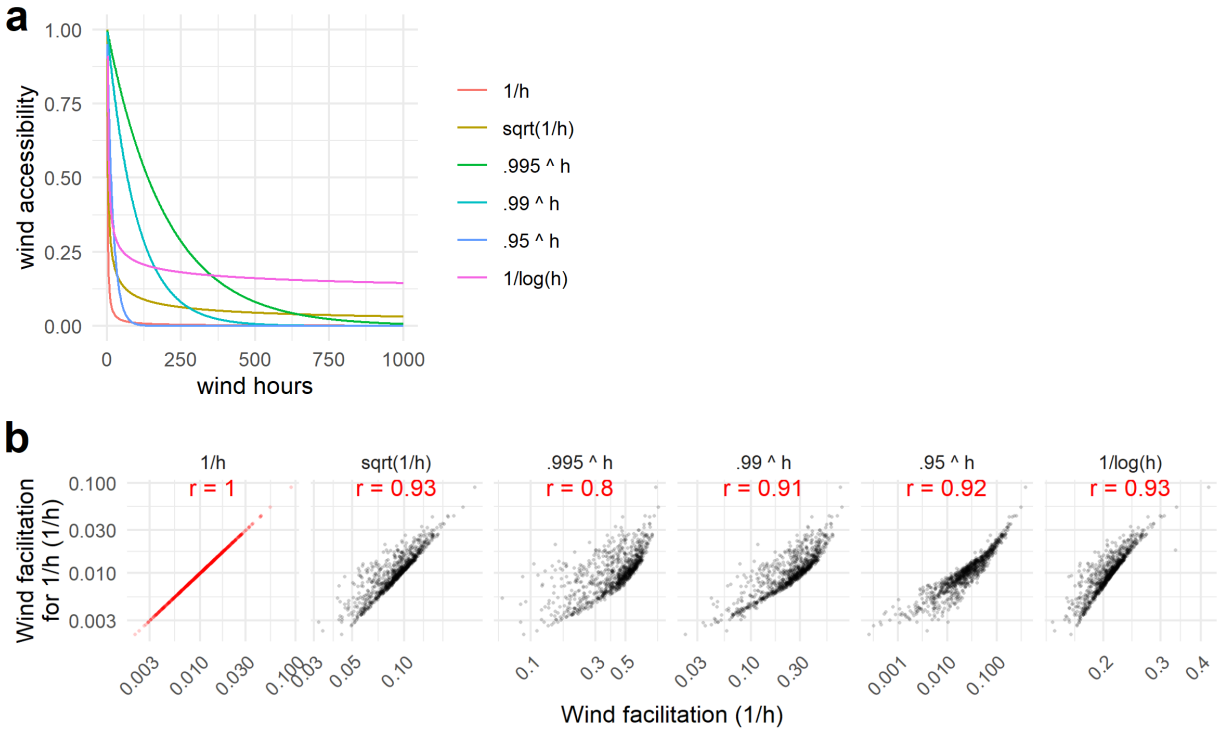

Figure S2.11: Sensitivity of global wind facilitation patterns to the choice of wind accessibility function, which converts wind-hours between two locations on a landscape into wind accessibility. (a) Shapes of the functions compared. (b) Correlations among these functions, comparing mean landscape wind facilitation for 1000 randomly selected global grid cells. (It is a coincidence that the inverse function (1/h) is the same as the units for wind facilitation (1/h).) Red numbers are Pearson's correlation coefficients of log wind facilitation values.

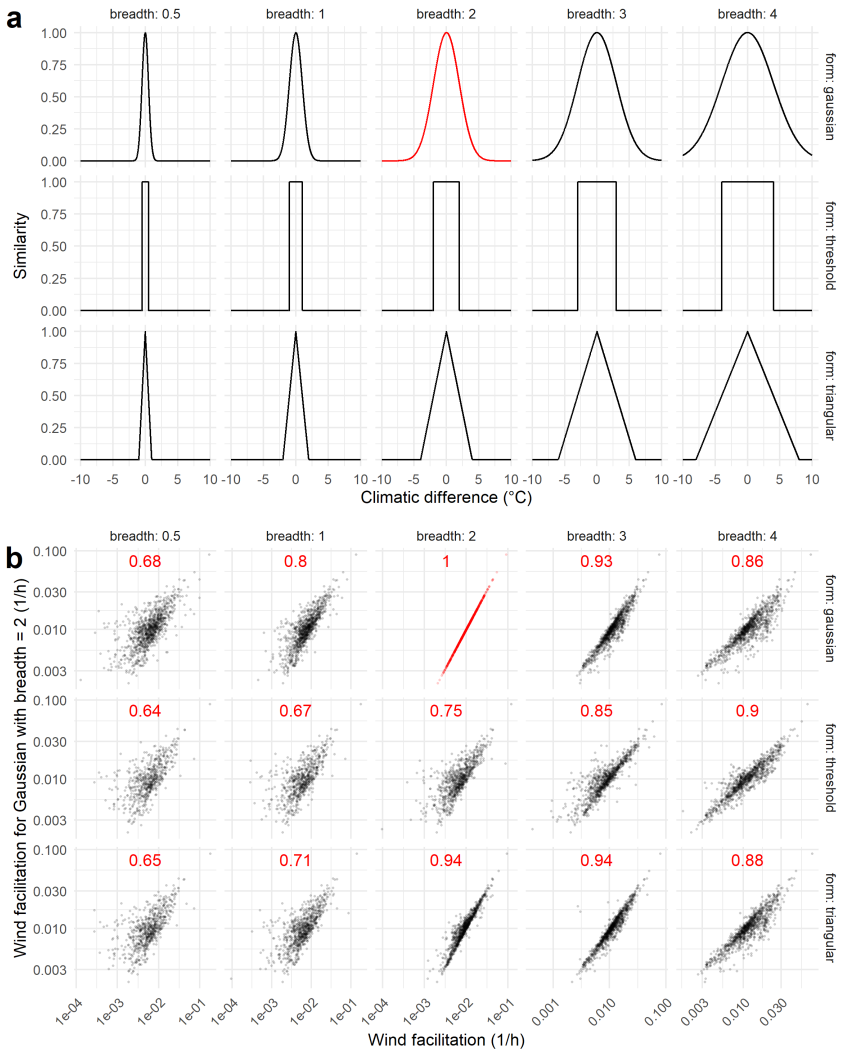

Figure S2.12: Sensitivity of global wind facilitation patterns to form and breadth of climate similarity function, which translates the difference between the temperatures of two sites (in degrees C) into a similarity index between 0 and 1. (a) The three functional forms and five breadths compared, with the version used in the main analysis in red. For the Gaussian, threshold, and triangular functions respectively, the breadth parameter represents the standard deviation of the curve, the absolute threshold difference where similarity drops to zero, and half the absolute difference where similarity drops to zero. (b) Correlations between facilitation under the main analysis (y-axis) versus the other 14 parameterizations (x-axis) for 1000 randomly selected sites globally. Red numbers are Pearson's correlation coefficients of log wind facilitation values.

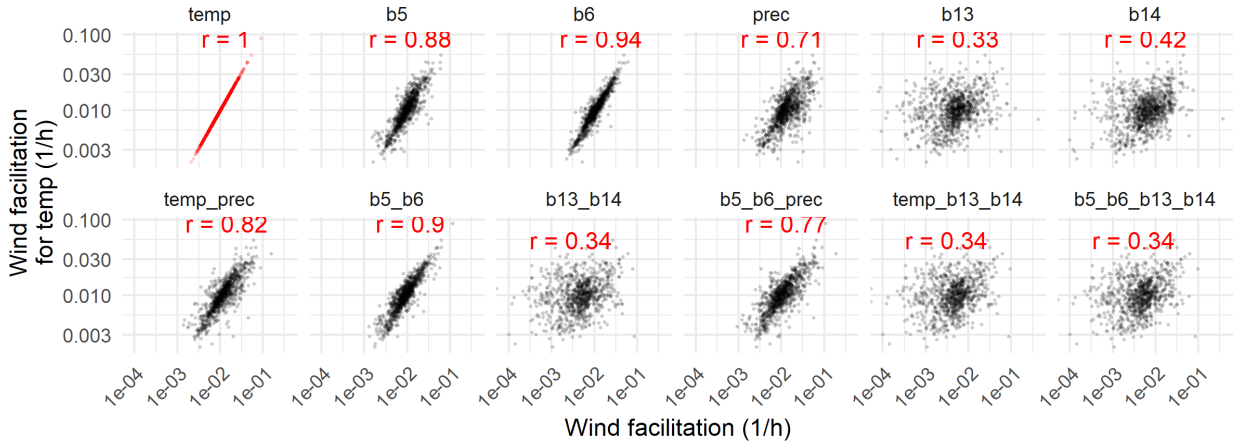

Figure S2.13: Sensitivity of wind facilitation patterns to climate variables used. Our main analysis (y-axis values) was based on mean annual temperature ("temp"). Here we compare these to the corresponding wind facilitation values for alternative climate variables (x-axis values). The first row compares the main analysis to individual climate variables, including maximum temperature of the warmest month (biovariable 5, i.e. "b5"), minimum temperature of the coldest month ("b6"), total annual precipitation ("prec"), precipitation of the wettest month ("b13"), and precipitation of the direst month ("b14"). The second row compares it to combinations of two or more of these variables, which place multivariate constraints on climate similarity by multiplying the similarity surfaces of multiple variables. Precipitation variables were log-transformed for normality and ecological relevance prior to analysis. Every climate variable uses a Gaussian climate similarity function; sigmas are set to give every variable the same ratio of sigma to the global standard deviation, based on the fixed 2 degrees C sigma value for mean annual temperature. Red numbers are Pearson's correlation coefficients of log wind facilitation values.

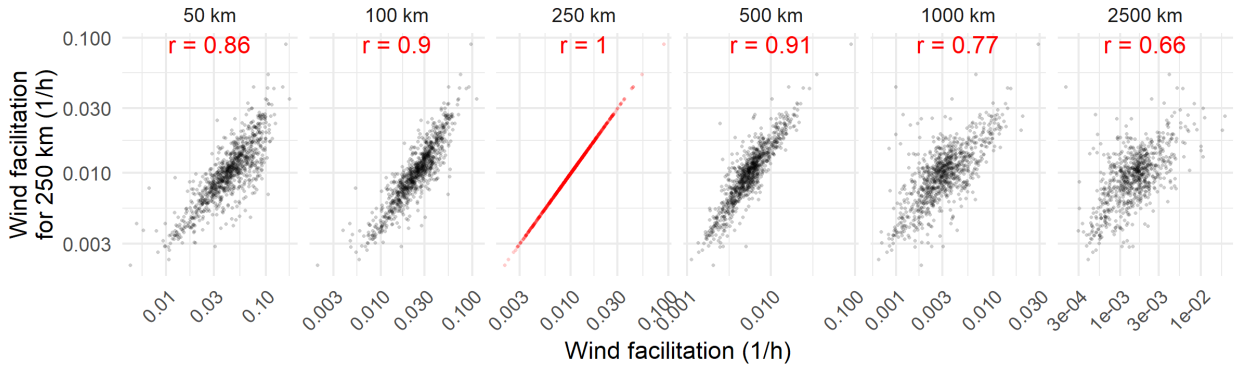

Figure S2.14: Sensitivity of wind facilitation patterns to landscape size. Our main analysis (y-axis values) considered a circular landscape with a radius of 250 km around each focal pixel. Here we compare these to the corresponding wind facilitation patterns for models using various other landscape radii (x-axis values). Red numbers are Pearson's correlation coefficients of log wind facilitation values.

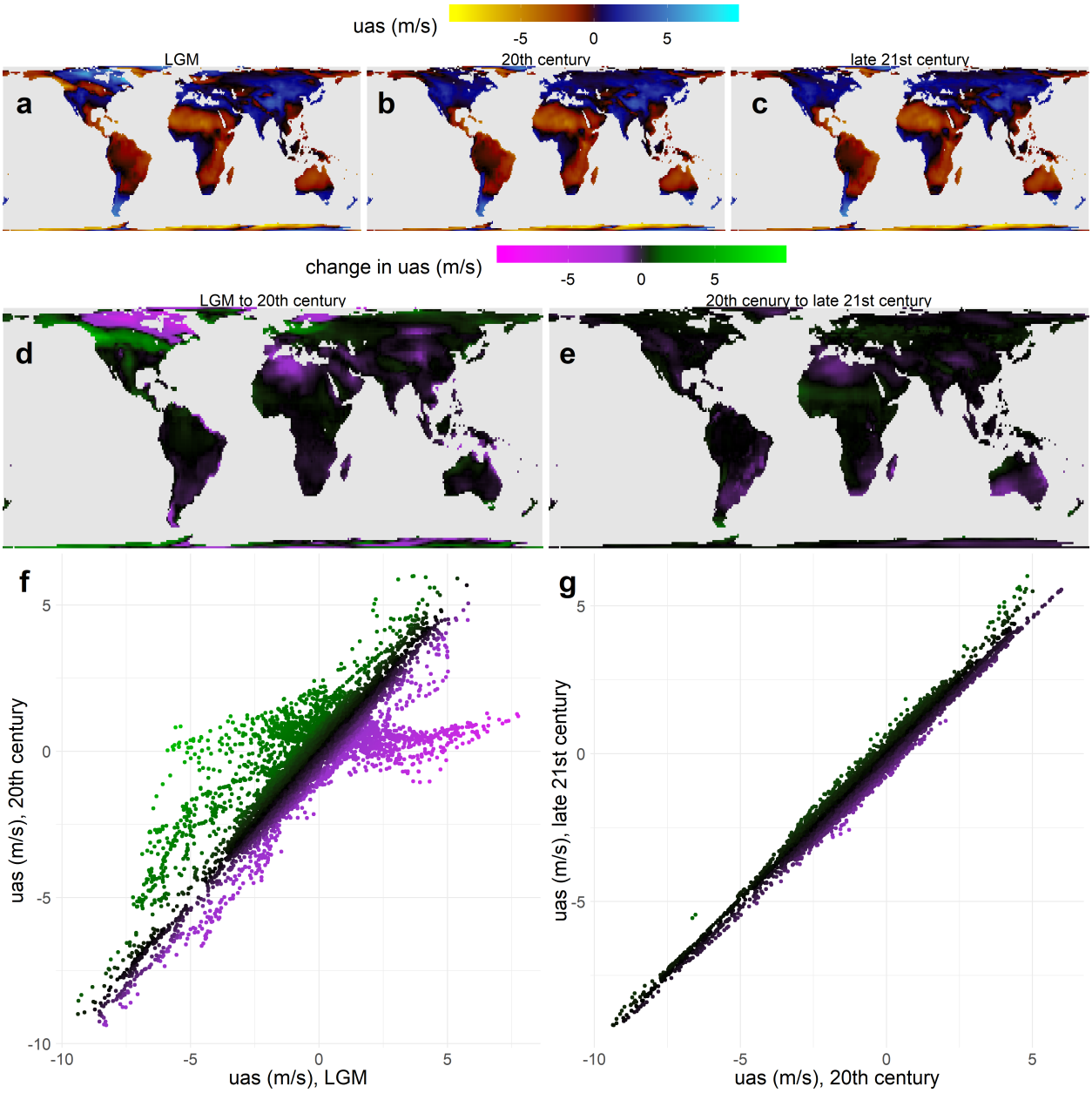

Figure S2.15: Changes in zonal windspeed ("uas") between the Last Glacial Maximum (LGM), the 20th century, and the late 21st century (RCP 8.5 emissions scenario), according to an ensemble of global circulation models. (a-c) Winds at each time period. (d-e) Differences between time periods. (f-g) Scatterplots comparing values between two time periods.

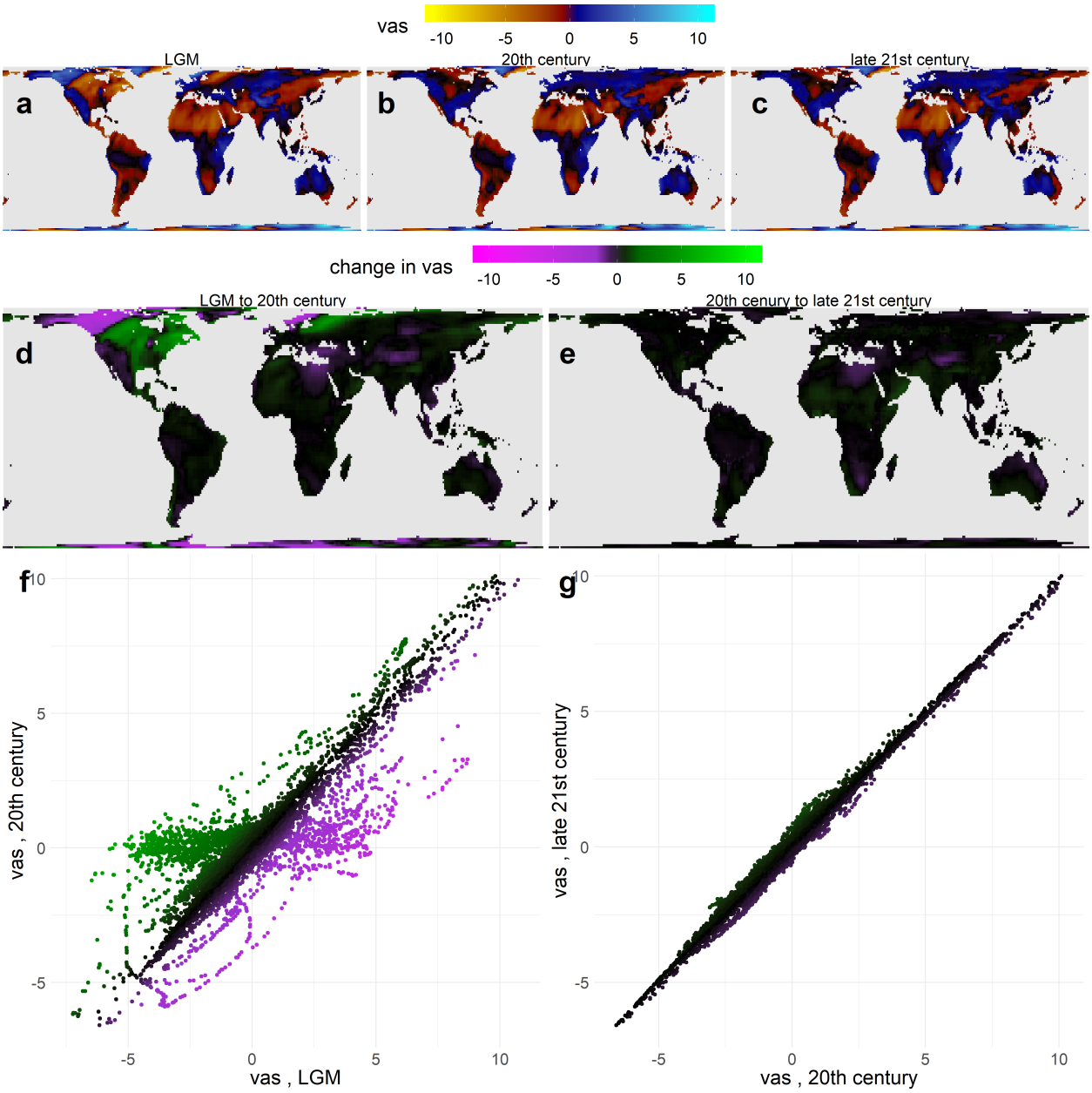

Figure S2.16: Changes in meridional windspeed ("vas") between the Last Glacial Maximum (LGM), the 20th century, and the late 21st century (RCP 8.5 emissions scenario), according to an ensemble of global circulation models. (a-c) Winds at each time period. (d-e) Differences between time periods. (f-g) Scatterplots comparing values between two time periods.

Appendix 3: Supplementary information for chapter 3

Table S3.1: Effects of including absolute latitude in logistic regression models explaining the effect of wind dispersal level (0, .5, or 1, labeled "*syndrome*" below) on the partial correlation (r) between wind and genetic metrics. Two models are reported for each of the four genetic metrics.

metric	model	term	estimate	p
flow	$r \sim syndrome$	syndrome	0.164	0.043
flow	$r \sim syndrome + latitude$	syndrome	0.162	0.096
flow	$r \sim syndrome + latitude$	latitude	0	0.504
isolation	$r \sim syndrome$	syndrome	0.477	0
isolation	$r \sim syndrome + latitude$	syndrome	0.447	0
isolation	$r \sim syndrome + latitude$	latitude	0.002	0.323
asymmetry	$r \sim syndrome$	syndrome	0.179	0.059
asymmetry	$r \sim syndrome + latitude$	syndrome	0.159	0.126
asymmetry	$r \sim syndrome + latitude$	latitude	0.001	0.417
diversity	$r \sim syndrome$	syndrome	0.109	0.206
diversity	$r \sim syndrome + latitude$	syndrome	0.03	0.378
diversity	$r \sim syndrome + latitude$	latitude	0.005	0.207

Table S3.2: Metadata for published landscape genetics data used in this analysis. The reference column provides the citation for the journal article, while the URL suffix provides the link to the data repository on Dryad—to access the data, append the listed URL suffix to the following URL: "*https://datadryad.org/stash/dataset/doi:10.5061/dryad.*". Publications associated with multiple datasets have multiple values listed one or more of the latter three columns.

Reference	**URL suffix**	**Species**	**Gen. reg.**	**Seq. type**
"Aoki, K., Tamaki, I., Nakao, K., Ueno, S., Kamijo, T., Setoguchi, H., ... & Tsumura, Y. (2019). Approximate Bayesian computation analysis of EST-associated microsatellites indicates that the broadleaved evergreen tree Castanopsis sieboldii survived the Last Glacial Maximum in multiple refugia in Japan. Heredity, 122(3), 326-340."	5sb1219	Castanopsis sieboldii	nu	SSR
"Bashalkhanov, S., Eckert, A. J., & Rajora, O. P. (2013). Genetic signatures of natural selection in response to air pollution in red spruce (P icea rubens, Pinaceae). Molecular Ecology, 22(23), 5877-5889."	10j72	Picea rubens	nu	"SSR, SNP"
"Bezemer, N., Hopper, S. D., Krauss, S. L., Phillips, R. D., & Roberts, D. G. (2019). Primary pollinator exclusion has divergent consequences for pollen dispersal and mating in different populations of a bird˙pollinated tree. Molecular Ecology, 28(22), 4883-4898."	bcc2fqz7c	Eucalyptus caesia	nu	SSR
"Bezemer, N., Krauss, S. L., Roberts, D. G., & Hopper, S. D. (2019). Conservation of old individual trees and small populations is integral to maintain species' genetic diversity of a historically fragmented woody perennial. Molecular Ecology, 28(14), 3339-3357."	bm8458m	Eucalyptus caesia	nu	SSR
"Burgarella, C., Navascus, M., Zabal˙Aguirre, M., Berganzo, E., Riba, M., Mayol, M., ... & Gonzlez˙Martnez, S. C. (2012). Recent population decline and selection shape diversity of taxol˙related genes. Molecular Ecology, 21(12), 3006-3021."	4j7q3s0t	Taxus baccata	nu	SSR

"Caseys, C., Stlting, K. N., Barbar, T., Gonzlez-Martnez, S. C., & Lexer, C. (2015). Patterns of genetic diversity and differentiation in resistance gene clusters of two hybridizing European Populus species. Tree Genetics & Genomes, 11(4), 81."	2593t	"Populus alba, Populus tremula"	nu	SSR
"Cavender˙Bares, J., Gonzlez˙Rodrguez, A., Eaton, D. A., Hipp, A. A., Beulke, A., & Manos, P. S. (2015). Phylogeny and biogeography of the American live oaks (Quercus subsection Virentes): a genomic and population genetics approach. Molecular ecology, 24(14), 3668-3687."	855pg	"Quercus virginiana, Quercus geminata, Quercus minima, Quercus fusiformis, Quercus oleoides, Quercus brandegei, Quercus sagraena"	nu	SSR
"Chhatre, V. E., & Rajora, O. P. (2014). Genetic divergence and signatures of natural selection in marginal populations of a keystone, long-lived conifer, eastern white pine (Pinus strobus) from northern Ontario. PloS one, 9(5), e97291."	6pq0n	Pinus strobus	nu	SSR
"Cisneros˙de la Cruz, D. J., Martnez˙Castillo, J., Herrera˙Silveira, J., Yez˙Espinosa, L., Ortiz˙Garca, M., Us˙Santamaria, R., & Andrade, J. L. (2018). Short˙distance barriers affect genetic variability of Rhizophora mangle L. in the Yucatan Peninsula. Ecology and Evolution, 8(22), 11083-11099."	1578ks0	Rhizophora mangle	nu	SSR
"Cornille, A., Giraud, T., Bellard, C., Tellier, A., Le Cam, B., Smulders, M. J. M., ... & Gladieux, P. (2013). Postglacial recolonization history of the European crabapple (Malus sylvestris M ill.), a wild contributor to the domesticated apple. Molecular Ecology, 22(8), 2249-2263."	sn1m7	Malus sylvestris	nu	SSR

"Cullingham, C. I., Cooke, J. E., Dang, S., Davis, C. S., Cooke, B. J., & Coltman, D. W. (2011). Mountain pine beetle host˙range expansion threatens the boreal forest. Molecular Ecology, 20(10), 2157-2171."	8677	"Pinus banksiana, Pinus contorta"	nu	SSR
"De Kort, H., Vandepitte, K., Bruun, H. H., Closset˙Kopp, D., Honnay, O., & Mergeay, J. (2014). Landscape genomics and a common garden trial reveal adaptive differentiation to temperature across Europe in the tree species Alnus glutinosa. Molecular Ecology, 23(19), 4709-4721."	rg82f	Alnus glutinosa	nu	SNP
"De La Torre, A. R., Roberts, D. R., & Aitken, S. N. (2014). Genome˙wide admixture and ecological niche modelling reveal the maintenance of species boundaries despite long history of interspecific gene flow. Molecular ecology, 23(8), 2046-2059."	7h65f	Picea engelmannii	nu	SNP
"de Lafontaine, G., Prunier, J., Grardi, S., & Bousquet, J. (2015). Tracking the progression of speciation: variable patterns of introgression across the genome provide insights on the species delimitation between progenitorderivative spruces (Picea mariana˙ P. rubens). Molecular ecology, 24(20), 5229-5247."	9kb02	"Picea mariana, Picea rubens"	nu	SNP
"Delplancke, M., Alvarez, N., Benoit, L., Espindola, A., I Joly, H., Neuenschwander, S., & Arrigo, N. (2013). Evolutionary history of almond tree domestication in the Mediterranean basin. Molecular Ecology, 22(4), 1092-1104."	g416t	Prunus dulcis	"nu, cp"	SSR
"Delplancke, M., Alvarez, N., Espndola, A., Joly, H., Benoit, L., Brouck, E., & Arrigo, N. (2012). Gene flow among wild and domesticated almond species: insights from chloroplast and nuclear markers. Evolutionary Applications, 5(4), 317-329."	5f41fq18	Prunus orientalis	"nu, cp"	SSR

"DeWoody, J., Trewin, H., & Taylor, G. (2015). Genetic and morphological differentiation in P opulus nigra L.: isolation by colonization or isolation by adaptation?. Molecular Ecology, 24(11), 2641-2655."	kq0n5	Populus nigra	nu	SSR
"Di Pierro, E. A., Mosca, E., Rocchini, D., Binelli, G., Neale, D. B., & La Porta, N. (2016). Climate-related adaptive genetic variation and population structure in natural stands of Norway spruce in the South-Eastern Alps. Tree Genetics & Genomes, 12(2), 16."	n818s	Picea abies	nu	SNP
"Duncan, C. J., Worth, J. R. P., Jordan, G. J., Jones, R. C., & Vaillancourt, R. E. (2016). Duncan, C. J., Worth, J. R. P., Jordan, G. J., Jones, R. C., & Vaillancourt, R. E. (2016). Genetic differentiation in spite of high gene flow in the dominant rainforest tree of southeastern Australia, Nothofagus cunninghamii. Heredity, 116(1), 99-106. Heredity, 116(1), 99-106."	dn175	Nothofagus cunninghamii	nu	SSR
"Evans, L. M., Allan, G. J., DiFazio, S. P., Slavov, G. T., Wilder, J. A., Floate, K. D., ... & Whitham, T. G. (2015). Geographical barriers and climate influence demographic history in narrowleaf cottonwoods. Heredity, 114(4), 387-396."	82kv2	Populus angustifolia	nu	SSR
"Fuentes-Utrilla, P., Venturas, M., Hollingsworth, P. M., Squirrell, J., Collada, C., Stone, G. N., & Gil, L. (2014). Extending glacial refugia for a European tree: genetic markers show that Iberian populations of white elm are native relicts and not introductions. Heredity, 112(2), 105-113."	2r6m4	Ulmus laevis	nu	SSR
"Garca´Verdugo, C., Forrest, A. D., Fay, M. F., & Vargas, P. (2010). The relevance of gene flow in metapopulation dynamics of an oceanic island endemic, Olea europaea subsp. guanchica. Evolution: International Journal of Organic Evolution, 64(12), 3525-3536."	1767	Olea europaea	nu	SSR

"Goicoechea, P. G., Petit, R. J., & Kremer, A. (2012). Detecting the footprints of divergent selection in oaks with linked markers. Heredity, 109(6), 361-371."	099s2	"Quercus robur, Quercus petraea"	nu	SSR
"Graignic, N., Tremblay, F., & Bergeron, Y. (2016). Genetic consequences of selection cutting on sugar maple (Acer saccharum Marshall). Evolutionary Applications, 9(6), 777-790."	37354	Acer saccharum	nu	SSR
"Graignic, N., Tremblay, F., & Bergeron, Y. (2018). Influence of northern limit range on genetic diversity and structure in a widespread North American tree, sugar maple (Acer saccharum Marshall). Ecology and Evolution, 8(5), 2766-2780."	36634	Acer saccharum	nu	SSR
"Gramlich, S., Sagmeister, P., Dullinger, S., Hadacek, F., & Hrandl, E. (2016). Evolution in situ: hybrid origin and establishment of willows (Salix L.) on alpine glacier forefields. Heredity, 116(6), 531-541."	dn53j	"Salix purpurea, Salix helvetica"	nu	SSR
"Gugger, P. F., Ikegami, M., & Sork, V. L. (2013). Influence of late Q uaternary climate change on present patterns of genetic variation in valley oak, Quercus lobata Ne. Molecular Ecology, 22(13), 3598-3612."	g645d	Quercus lobata	"nu, cp"	SSR
"Hansen, O. K., Changtragoon, S., Ponoy, B., Kjr, E. D., Finkeldey, R., Nielsen, K. B., & Graudal, L. (2015). Genetic resources of teak (Tectona grandis Linn. f.)Ñstrong genetic structure among natural populations. Tree Genetics & Genomes, 11(1), 802."	4mg2r	Tectona grandis	nu	SSR
"Haselhorst, M. S., & Buerkle, C. A. (2013). Population genetic structure of Picea engelmannii, P. glauca and their previously unrecognized hybrids in the central Rocky Mountains. Tree Genetics & Genomes, 9(3), 669-681."	c5c1q	"Picea engelmannii, Picea glauca"	nu	SSR
"Jennings, T. N., Knaus, B. J., Kolpak, S., & Cronn, R. (2011). Microsatellite primers for the Pacific Northwest endemic conifer Chamaecyparis lawsoniana (Cupressaceae). American Journal of Botany, 98(11), e323-e325."	bq002	Chamaecyparis lawsoniana	nu	SSR

"Jiang, X. L., An, M., Zheng, S. S., Deng, M., & Su, Z. H. (2018). Geographical isolation and environmental heterogeneity contribute to the spatial genetic patterns of Quercus kerrii (Fagaceae). Heredity, 120(3), 219-233."	0r20b	Quercus kerrii	nu	SSR
"Jolivet, C., Rogge, M., & Degen, B. (2013). Molecular and quantitative signatures of biparental inbreeding depression in the self-incompatible tree species Prunus avium. Heredity, 110(5), 439-448."	p1g31	Prunus avium	nu	SSR
"Keller, S. R., Olson, M. S., Silim, S., Schroeder, W., & Tiffin, P. (2010). Genomic diversity, population structure, and migration following rapid range expansion in the Balsam Poplar, Populus balsamifera. Molecular Ecology, 19(6), 1212-1226."	1164	Populus balsamifera	nu	SNP
"Kennedy, J. P., Pil, M. W., Proffitt, C. E., Boeger, W. A., Stanford, A. M., & Devlin, D. J. (2016). Postglacial expansion pathways of red mangrove, Rhizophora mangle, in the Caribbean Basin and Florida. American Journal of Botany, 103(2), 260-276."	609k3	Rhizophora mangle	nu	SSR
"Latutrie, M., Bergeron, Y., & Tremblay, F. (2016). Fine-scale assessment of genetic diversity of trembling aspen in northwestern North America. BMC Evolutionary Biology, 16(1), 231."	6q5g3	Populus tremuloides	nu	SSR
"Lepais, O., Muller, S. D., Saad-Limam, S. B., Benslama, M., Rhazi, L., Belouahem-Abed, D., ... & Bacles, C. F. E. (2013). High genetic diversity and distinctiveness of rear-edge climate relicts maintained by ancient tetraploidisation for Alnus glutinosa. PLoS One, 8(9), e75029."	3801d	Alnus glutinosa	nu	SSR
"Lesser, M. R., Parchman, T. L., & Jackson, S. T. (2013). Development of genetic diversity, differentiation and structure over 500 years in four ponderosa pine populations. Molecular Ecology, 22(10), 2640-2652."	pc683	Pinus ponderosa	nu	SSR

"Levy, E., Byrne, M., Coates, D. J., Macdonald, B. M., McArthur, S., & Van Leeuwen, S. (2016). Contrasting influences of geographic range and distribution of populations on patterns of genetic diversity in two sympatric Pilbara Acacias. PLoS One, 11(10), e0163995."	5cm32	"Acacia ancistrocarpa, Acacia atkinsiana"	nu	SSR
"Liu, M., Zhang, J., Chen, Y., Compton, S. G., & Chen, X. Y. (2013). Contrasting genetic responses to population fragmentation in a coevolving fig and fig wasp across a mainlandisland archipelago. Molecular Ecology, 22(17), 4384-4396."	hp6tb	Ficus pumila	nu	SSR
"Lumibao, C. Y., & McLachlan, J. S. (2014). Habitat differences influence genetic impacts of human land use on the American Beech (Fagus grandifolia). Journal of Heredity, 105(6), 887-899."	c1q38	Fagus grandifolia	nu	SSR
"Martnez˙Lpez, V., Garca, C., Zapata, V., Robledano, F., & De la Ra, P. (2020). Intercontinental long˙distance seed dispersal across the Mediterranean Basin explains population genetic structure of a bird˙dispersed shrub. Molecular Ecology, 29(8), 1408-1420."	stqjq2c0q	Pistacia lentiscus	nu	SSR
"Menon, M., Bagley, J. C., Friedline, C. J., Whipple, A. V., Schoettle, A. W., Leal˙Senz, A., ... & Sniezko, R. A. (2018). The role of hybridization during ecological divergence of southwestern white pine (Pinus strobiformis) and limber pine (P. flexilis). Molecular Ecology, 27(5), 1245-1260."	f6r55	"Pinus strobiformis, Pinus flexilis"	nu	SNP
"Mosca, E. L. E. N. A., Eckert, A. J., Di Pierro, E. A., Rocchini, D., La Porta, N., Belletti, P., & Neale, D. B. (2012). The geographical and environmental determinants of genetic diversity for four alpine conifers of the European Alps. Molecular Ecology, 21(22), 5530-5545."	tm33d	"Abies alba, Larix decidua, Pinus cembra"	nu	SNP

"Ng, C. H., Lee, S. L., Tnah, L. H., Ng, K. K., Lee, C. T., Diway, B., & Khoo, E. (2019). Genetic diversity and demographic history of an upper hill Dipterocarp (Shorea platyclados): Implications for conservation. Journal of Heredity, 110(7), 844-856."	85cg1d3	Shorea platyclados	nu	SSR
"Ortego, J., Noguerales, V., Gugger, P. F., & Sork, V. L. (2015). Evolutionary and demographic history of the Californian scrub white oak species complex: an integrative approach. Molecular Ecology, 24(24), 6188-6208."	52504	"Quercus berberidifolia, Quercus durata, Quercus corneliusmulleri, Quercus john-tuckeri, Quercus pacifica"	"cp, nu"	SSR
"Ortego, J., Riordan, E. C., Gugger, P. F., & Sork, V. L. (2012). Influence of environmental heterogeneity on genetic diversity and structure in an endemic southern Californian oak. Molecular Ecology, 21(13), 3210-3223."	rd645561	Quercus engelmannii	nu	SSR
"Piotti, A., Leonardi, S., Buiteveld, J., Geburek, T., Gerber, S., Kramer, K., ... & Vendramin, G. G. (2012). Comparison of pollen gene flow among four European beech (Fagus sylvatica L.) populations characterized by different management regimes. Heredity, 108(3), 322-331."	6kt34	Fagus sylvatica	nu	SSR
"Polezhaeva, M. A., Lascoux, M., & Semerikov, V. L. (2010). Cytoplasmic DNA variation and biogeography of Larix Mill. in Northeast Asia. Molecular Ecology, 19(6), 1239-1252."	1191	"Larix kurilensis, Larix cajanderi, Larix gmelinii, Larix kamtschatica, Larix olgensis"	cp	SSR

"Poudel, R. C., Mller, M., Li, D. Z., Shah, A., & Gao, L. M. (2014). Genetic diversity, demographical history and conservation aspects of the endangered yew tree Taxus contorta (syn. Taxus fuana) in Pakistan. Tree Genetics & Genomes, 10(3), 653-665."	3gq01	Taxus contorta	nu	SSR
"Rellstab, C., Zoller, S., Walthert, L., Lesur, I., Pluess, A. R., Graf, R., ... & Gugerli, F. (2016). Signatures of local adaptation in candidate genes of oaks (Quercus spp.) with respect to present and future climatic conditions. Molecular Ecology, 25(23), 5907-5924."	15512	"Quercus robur, Quercus pubescens, Quercus petraea"	nu	SSR
"Ribeiro, P. C., Souza, M. L., Muller, L. A., Ellis, V. A., Heuertz, M., Lemos˙Filho, J. P., & Lovato, M. B. (2016). Climatic drivers of leaf traits and genetic divergence in the tree Annona crassiflora: a broad spatial survey in the Brazilian savannas. Global Change Biology, 22(11), 3789-3803."	n7dv6	Annona crassiflora	nu	SSR
"Roberts, D. G., Forrest, C. N., Denham, A. J., & Ayre, D. J. (2016). Varying levels of clonality and ploidy create barriers to gene flow and challenges for conservation of an Australian aridzone ecosystem engineer, Acacia loderi. Biological Journal of the Linnean Society, 118(2), 330-343."	3tv33	Acacia loderi	nu	SSR
"Rodrguez-Correa, H., Oyama, K., Quesada, M., Fuchs, E. J., & Gonzlez-Rodrguez, A. (2018). Contrasting patterns of population history and seed-mediated gene flow in two endemic Costa Rican oak species. Journal of Heredity, 109(5), 530-542."	d4t7rc3	"Quercus costaricensis, Quercus bumeliodes"	cp	SSR
"Rodrguez-Correa, H., Oyama, K., Quesada, M., Fuchs, E. J., Quezada, M., Ferrufino, L., ... & Gonzlez-Rodrguez, A. (2017). Complex phylogeographic patterns indicate Central American origin of two widespread Mesoamerican Quercus (Fagaceae) species. Tree Genetics & Genomes, 13(3), 62."	v5g0p	"Quercus insignis, Quercus sapotifolia"	cp	SSR

"Sakaguchi, S., Bowman, D. M., Prior, L. D., Crisp, M. D., Linde, C. C., Tsumura, Y., & Isagi, Y. (2013). Climate, not Aboriginal landscape burning, controlled the historical demography and distribution of fire-sensitive conifer populations across Australia. Proceedings of the Royal Society B: Biological Sciences, 280(1773), 20132182."	6j777	"Callitris columellaris, Callitris glaucophylla, Callitris gracilis, Callitris intratropica, Callitris verrucosa"	nu	SSR
"Sakaguchi, S., QIU, Y. X., LIU, Y. H., QI, X. S., KIM, S. H., Han, J., ... & Isagi, Y. (2012). Climate oscillation during the Quaternary associated with landscape heterogeneity promoted allopatric lineage divergence of a temperate tree Kalopanax septemlobus (Araliaceae) in East Asia. Molecular Ecology, 21(15), 3823-3838."	91mk9	Kalopanax septemlobus	nu	SSR
"Semerikov, V. L., Semerikova, S. A., Polezhaeva, M. A., Kosintsev, P. A., & Lascoux, M. (2013). Southern montane populations did not contribute to the recolonization of W est S iberian P lain by S iberian larch (L arix sibirica): a range˙wide analysis of cytoplasmic markers. Molecular Ecology, 22(19), 4958-4971."	jq712	Larix sibirica	cp	SSR
"Shuri, K., Saika, K., Junko, K., Michiharu, K., Nagamitsu, T., Iwata, H., ... & Mukai, Y. (2012). Impact of negative frequency-dependent selection on mating pattern and genetic structure: a comparative analysis of the S-locus and nuclear SSR loci in Prunus lannesiana var. speciosa. Heredity, 109(3), 188-198."	7c425	Prunus lannesian	nu	SSR
"Soliani, C., Tsuda, Y., Bagnoli, F., Gallo, L. A., Vendramin, G. G., & Marchelli, P. (2015). Halfway encounters: Meeting points of colonization routes among the southern beeches Nothofagus pumilio and N. antarctica. Molecular phylogenetics and Evolution, 85, 197-207."	r5303	"Nothofagus pumilio, Nothofagus antarctica"	nu	SSR

"Stacy, E. A., Johansen, J. B., Sakishima, T., Price, D. K., & Pillon, Y. (2014). Incipient radiation within the dominant Hawaiian tree Metrosideros polymorpha. Heredity, 113(4), 334-342."	267kc	Metrosideros polymorpha	nu	SSR
"Tamaki, I., Kawashima, N., Setsuko, S., Itaya, A., & Tomaru, N. (2018). Morphological and genetic divergence between two lineages of Magnolia salicifolia (Magnoliaceae) in Japan. Biological Journal of the Linnean Society, 125(3), 475-490."	fq18cd1	Magnolia salicifolia	"nu, cp"	"SSR, SNP"
"Thompson, K. M., Culley, T. M., Zumberger, A. M., & Lentz, D. L. (2015). Genetic variation and structure in the neotropical tree, Manilkara zapota (L) P. Royen (Sapotaceae) used by the ancient Maya. Tree Genetics & Genomes, 11(3), 40."	244b8	Manilkara zapota	nu	SSR
"Tsuda, Y., Chen, J., Stocks, M., Kllman, T., S¿nsteb¿, J. H., Parducci, L., ... & Vliranta, M. (2016). The extent and meaning of hybridization and introgression between Siberian spruce (Picea obovata) and Norway spruce (Picea abies): cryptic refugia as stepping stones to the west?. Molecular Ecology, 25(12), 2773-2789."	6bf38	"Picea abies, Picea obovata"	nu	SSR
"Tsuda, Y., Nakao, K., Ide, Y., & Tsumura, Y. (2015). The population demography of B etula maximowicziana, a cool˙temperate tree species in J apan, in relation to the last glacial period: its admixture˙like genetic structure is the result of simple population splitting not admixing. Molecular Ecology, 24(7), 1403-1418."	dj17c	Betula maximowicziana	nu	SSR

"Tsuda, Y., Semerikov, V., Sebastiani, F., Vendramin, G. G., & Lascoux, M. (2017). Multispecies genetic structure and hybridization in the Betula genus across Eurasia. Molecular Ecology, 26(2), 589-605."	h0h3t	"Betula nana, Betula pubsescens, Betula ermanii, Betula pendula, Betula platyphylla, Betula maximowicziana"	nu	SSR
"Utomo, S., Uchiyama, K., Ueno, S., Matsumoto, A., Indrioko, S., NaÕiem, M., & Tsumura, Y. (2018). Effects of Pleistocene climate change on genetic structure and diversity of Shorea macrophylla in Kalimantan Rainforest. Tree Genetics & Genomes, 14(4), 44."	92j7j53	Shorea macrophylla	nu	SSR
"Vergara, R., Gitzendanner, M. A., Soltis, D. E., & Soltis, P. S. (2014). Population genetic structure, genetic diversity, and natural history of the South American species of Nothofagus subgenus Lophozonia (Nothofagaceae) inferred from nuclear microsatellite data. Ecology and Evolution, 4(12), 2450-2471."	h3d26	"Nothofagus obliqua, Nothofagus alpina, Nothofagus glauca"	nu	SSR
"Wagner, S., Gerber, S., & Petit, R. J. (2012). Two highly informative dinucleotide SSR multiplexes for the conifer Larix decidua (European larch). Molecular Ecology Resources, 12(4), 717-725."	08507r35	Larix decidua	nu	SSR
"Wagner, S., Liepelt, S., Gerber, S., & Petit, R. J. (2015). Within-range translocations and their consequences in European larch. PloS One, 10(5), e0127516."	h25hj	Larix decidua	nu	SSR
"Wee, A. K., Takayama, K., Chua, J. L., Asakawa, T., Meenakshisundaram, S. H., Adjie, B., ... & Salmo, S. G. (2015). Genetic differentiation and phylogeography of partially sympatric species complex Rhizophora mucronata Lam. and R. stylosa Griff. using SSR markers. BMC Evolutionary Biology, 15(1), 57."	42711	"Rhizophora mucronata, Rhizophora stylosa"	nu	SSR

"Yoder, J. B., Smith, C. I., Rowley, D. J., Flatz, R., Godsoe, W., Drummond, C., & Pellmyr, O. (2013). Effects of gene flow on phenotype matching between two varieties of Joshua tree (Yucca brevifolia; Agavaceae) and their pollinators. Journal of Evolutionary Biology, 26(6), 1220-1233."	369q9	Yucca brevifolia	nu	SSR
"Zeng, Y. F., Liao, W. J., Petit, R. J., & Zhag, D. Y. (2011). Geographic variation in the structure of oak hybrid zones provides insights into the dynamics of speciation. Molecular Ecology, 20(23), 4995-5011."	mb4mv6pm"	"Quercus liaotungensis, Quercus mongolica"	"nu, cp"	SSR

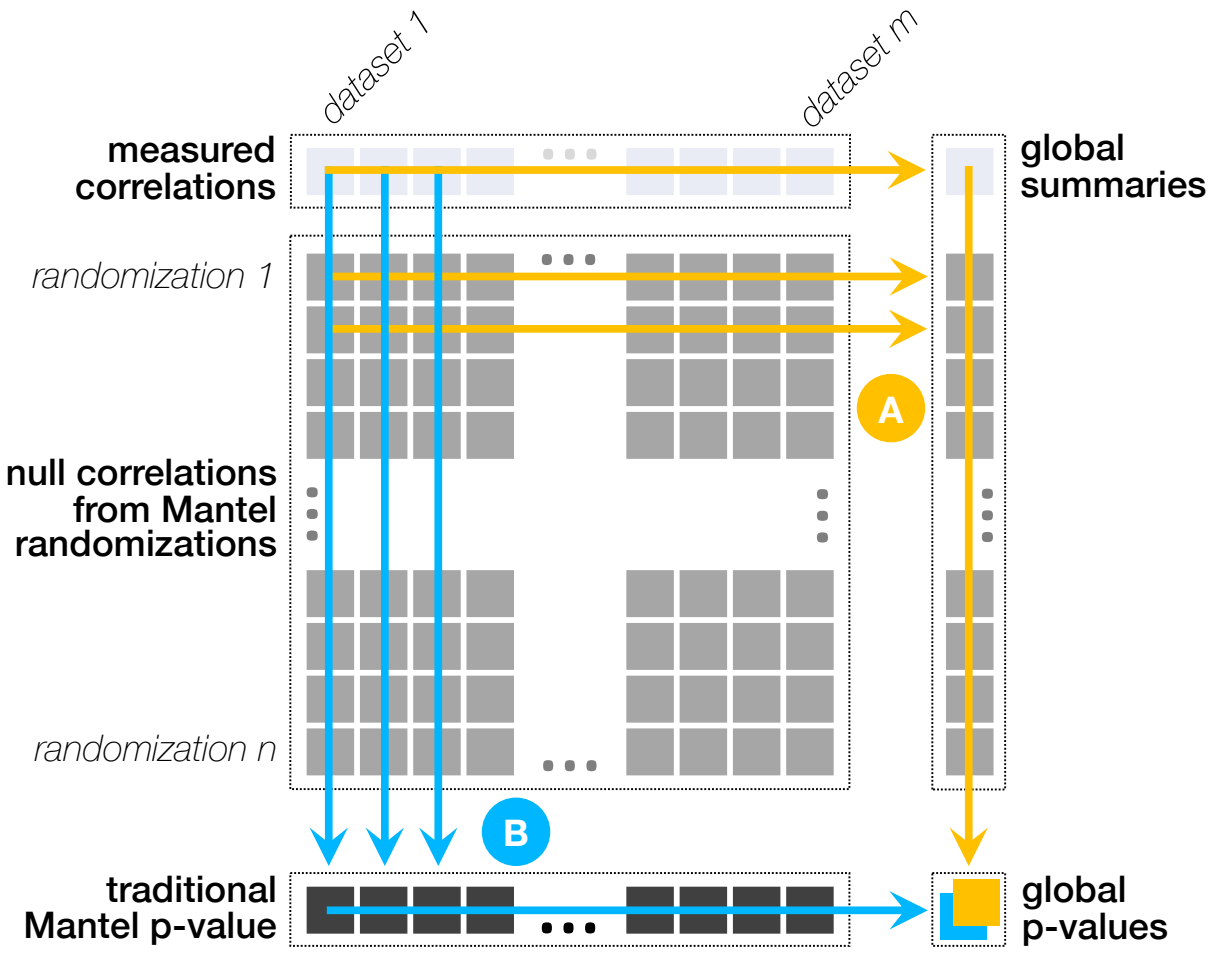

Figure S3.1: Schematic of two alternative approaches for calculating a global p-value from multispecies Mantel randomization data. Both approaches begin by using a Mantel-style randomization to calculate a large number of null partial correlation values for each dataset, but take different routes to deriving a final global p-value from these randomizations. The "global null" approach (A) first summarizes across the correlations for each randomization, deriving a separate global-level test statistic for each random iteration, and then compares the observed global test statistic to this null distribution to calculate a global p-value. The "dataset null" approach (B) instead first summarizes down the null values to derive a separate, traditional Mantel p-value for each dataset, and then uses a secondary test to summarize across these p-values to calculate a global p-value.

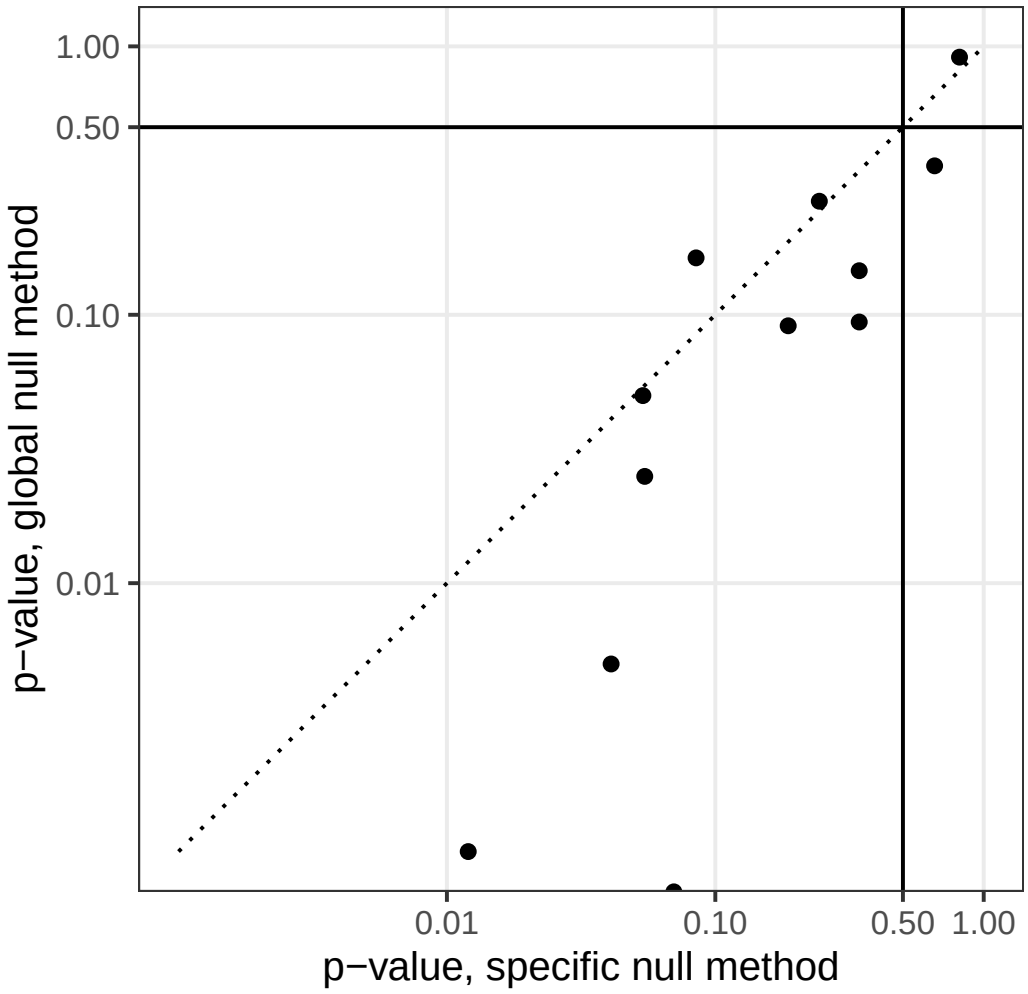

Figure S3.2: Comparison of significance estimated by the global null versus specific null methods, across the 12 hypothesis tests. r = 0.88.

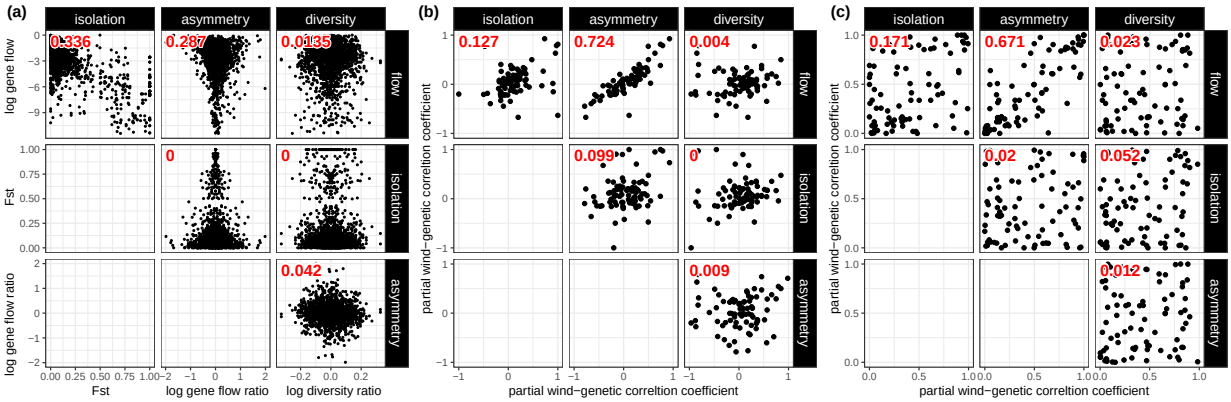

Figure S3.3: Relationships among the four landscape genetic facets, for wind-dispersed genomes. R-squared values are listed in red. (a) Correlations among pairwise genetic metrics in input data; plots show values for 1000 random population pairs across all datasets, while the listed r^2 values are the median of separate correlations was calculated for each dataset. (b) Correlations among partial wind-genetic correlation coefficients. (c) Correlations among Mantel p-values.